EXCHANGE OF CADMIUM AND LEAD ON SODIUM CLINOPTILOLITE ZEOLITE

A THESIS SUBMITTED TO
THE GRADUATE SCHOOL OF NATURAL AND APPLIED SCIENCES
OF
MIDDLE EAST TECHNICAL UNIVERSITY

BY

HAKAN MURAT İŞLER

IN PARTIAL FULFILLMENT OF THE REQUIREMENTS
FOR
THE DEGREE OF MASTER OF SCIENCE
IN
CHEMICAL ENGINEERING

MAY 2010

Approval of the thesis:

EXCHANGE OF CADMIUM AND LEAD ON SODIUM CLINOPTILOLITE ZEOLITE

submitted by **HAKAN MURAT İŞLER** in partial fulfillment of the requirements for the degree of **Master of Science in Chemical Engineering Department, Middle East Technical University** by,

Prof. Dr. Canan Özgen
Dean, Graduate School of **Natural and Applied Sciences** _____

Prof. Dr. Gürkan Karakaş
Head of Department, **Chemical Engineering** _____

Prof. Dr. Hayrettin Yücel
Supervisor, **Chemical Engineering Dept., METU** _____

Examining Committee Members:

Assoc. Prof. Dr. Naime A. Sezgi
Chemical Engineering Dept., METU _____

Prof. Dr. Hayrettin Yücel
Chemical Engineering Dept., METU _____

Assoc. Prof. Dr. İpek İmamoğlu
Environmental Engineering Dept., METU _____

Dr. Cevdet Öztin
Chemical Engineering Dept., METU _____

Assoc. Prof. Dr. Halil Kalıpçılar
Chemical Engineering Dept., METU _____

Date: May 03, 2010

I hereby declare that all information in this document has been obtained and presented in accordance with academic rules and ethical conduct. I also declare that, as required by these rules and conduct, I have fully cited and referenced all material and results that are not original to this work.

Name, Last name: Hakan Murat İŞLER

Signature:

ABSTRACT

EXCHANGE OF CADMIUM AND LEAD ON SODIUM CLINOPTILOLITE ZEOLITE

İŞLER, Hakan Murat

M.Sc., Department of Chemical Engineering

Supervisor: Prof. Dr. Hayrettin Yücel

May 2010, 114 pages

Heavy metal ions, such as cadmium and lead, should be removed from wastewaters to prevent bioaccumulation. Among many other separation processes, one of the alternatives is ion exchange involving a low cost packing material, clinoptilolite. Clinoptilolite is a natural zeolite and contains exchangeable cations such as Na^{+}, K^{+}, Mg^{2+}, and Ca^{2+} in its structure.

Aim of this study is to determine binary and multicomponent ion exchange behaviors of sodium enriched form of Gördes clinoptilolite for lead and cadmium ions. For this purpose, Pb^{+2} – Na^{+}, Cd^{+2} – Na^{+} binary and Pb^{+2} – Cd^{+2} – Na^{+} ternary systems were investigated in column operations for concentrations between 0.005 to 0.02 N and flow rates between 5 to 20 mL/min at 25 ˚C.

For determination of optimum particle size, 5/6, 8/10, 14/18, 20/30, 35/60, and 70/140 ASTM E-11 standard mesh ranges were tested and the optimum particle size, under the experimental conditions was found as 35/60.

Furthermore, although the clinoptilolite has a theoretical ion exchange capacity of 2.14 meq/g based on its aluminum content, under experimental conditions maximum exchange level was determined as 1.08 meq/g.

For binary and ternary experiments, it is observed that the clinoptilolite has affinity for both Pb^{2+} and Cd^{2+} ions. However, clinoptilolite has greater affinity to Pb^{2+} than Cd^{2+} ion. Therefore, selectivity sequence was determined as $Pb^{2+}>Cd^{2+}>Na^{+}$.

Additionally, for column studies, flow rates less than 10 mL/min and influent concentrations up to 0.01 N, sodium enriched form of Gördes clinoptilolite holds great potential to remove Pb^{2+} and Cd^{2+} ions from wastewaters.

Keywords: Clinoptilolite, Ion exchange, Lead removal, Cadmium removal

ÖZ

KADMİYUM VE KURŞUNUN SODYUM KLİNOPTİLOLİT ZEOLİT ÜZERİNDE DEĞİŞİMİ

İŞLER, Hakan Murat

Yüksek Lisans, Kimya Mühendisliği Bölümü

Tez Danışmanı: Prof. Dr. Hayrettin Yücel

Mayıs 2010, 114 sayfa

Kadmiyum ve kurşun gibi ağır metal iyonları biyolojik birikimi önlemek için atık sulardan uzaklaştırılmalıdır. Bir çok ayırma prosesi seçeneği arasından seçeneklerden birisi de düşük maliyetli yatak malzemesi klinoptilolit zeolit içeren iyon değiştirmedir. Klinoptilolit, doğal zeolittir ve yapısında Na^{+}, K^{+}, Mg^{2+} ve Ca^{2+} gibi değiştirilebilir katyonlar bulundurur.

Bu çalışmanın amacı, sodyumla zenginleştirilmiş Gördes klinoptilolitinin, kurşun ve kadmiyum iyonları için ikili ve çok bileşenli iyon değiştirme davranışının belirlenmesidir. Bu amaç için, $Pb^{+2} – Na^{+}$, $Cd^{+2} – Na^{+}$ ikili ve $Pb^{+2} – Cd^{+2} – Na^{+}$ üçlü sistemleri, 25 °C'de, 0,005 ila 0,02 N konsantrasyon ve 5 ila 20 mL/dk debi aralıklarında, kolon operasyonlarıyla incelenmiştir.

En uygun parça boyutunun belirlenmesi için, 5/6, 8/10, 14/18, 20/30, 35/60 ve 70/140 ASTM E-11 US standard mesh aralıkları denenmiş ve uygulanan

deneysel koşullar altında, en elverişli parça boyutu 35/60 aralığı olarak bulunmuştur.

Ayrıca, sodyumla zenginleştirilmiş klinoptilolitin alüminyum içeriğine göre teorik ion değiştirme kapasitesi 2,14 meq/g olmasına rağmen, uygulanan deneysel koşullar altında azami değişim seviyesi 1,08 meq/g olarak belirlenmiştir.

İkili ve üçlü deneyler için, sodyumla zenginleştirilmiş klinoptilolitin Pb^{2+} and Cd^{2+} iyonlarının ikisine birden ilgisi olduğu gözlenmiştir. Fakat, klinoptilolit, Pb^{2+} iyonuna Cd^{2+} iyonundan daha çok ilgi göstermektedir. Dolayısıyla, klinoptilolitin seçicilik sıralaması $Pb^{2+}>Cd^{2+}>Na^{+}$ olarak belirlenmiştir.

Buna ek olarak, 10 mL/dk'dan düşük debi ve 0,01 N'ye kadar olan içeri akan iyon derişimlerinde, sodyum bakımından zenginleştirilmiş formdaki Gördes tipi klinoptilolit, atık sularda bulunan Pb^{2+} ve Cd^{2+} iyonlarının gideriminde büyük potansiyele sahiptir.

Anahtar Kelimeler: Klinoptilolit, İyon değişimi, Kurşun giderimi, Kadmiyum giderimi

To My Family

ACKNOWLEDGEMENTS

I would like to express my deepest gratitude to my thesis supervisor Prof. Dr. Hayrettin Yücel for his guidance, valuable advice, criticism, and encouragements throughout this study. I would like to say it has been a great pleasure for me to know him and study with him.

My greatest gratitude is extended to Kerime Güney in instrumental analysis laboratory for her endless helps, helpful suggestions, motivation, and for chemical analysis.

I would like to express my deepest thanks to my sweetheart İlay Gözde Ekmekçi whose encouragement and enthusiasm helped me in my difficult days.

I also wish to thank my friends Wissam Abdullah, Murat Erdoğan, Ahmet Naiboğlu, Saltuk Pirgalıoğlu, and Duygu Yılmazer for their help and friendship.

Last but not least, my great indebtedness goes to my parents Rukiye İşler and Eyüp İşler, my brother Süleyman Fatih İşler for their undying love, continuous support, endless patience, and encouragement. I would not able to succeed without them.

TABLE OF CONTENTS

LIST OF TABLES

TABLES

LIST OF FIGURES

FIGURES

LIST OF SYMBOLS

a_s : Cross-sectional Area

A, B : Type of Cations

A_s : Fraction of Exchanging Cation in Solution

A_z : Fraction of Exchanging Cation in Zeolite

BV : Bed Volume

C : Ion Concentration in Effluent

C_0 : Ion Concentration in Influent

h_T : Height of Packed Bed

meq : Milliequivalent

M : Molarity

MTZ: Mass Transfer Zone

N : Normality

Q_B : Breakthrough Capacity of Clinoptilolite

Q_T : Total Capacity of Clinoptilolite

s : Solution

V_B : Effluent Volume Breakthrough

V_T : Effluent Volume up to Exhaustion

z : Zeolite

Z : Charge of Cation

Greek Letters

ρ_b : Packed Bed Density

η_c : Column Efficiency

CHAPTER 1

INTRODUCTION

Heavy metals are toxic chemicals and disposal of them is a problematic issue. As a result of industrial applications their amounts in aquatic environment increase day by day and contaminate nature. Heavy metals are not biodegradable and tend to bioaccumulate in living organisms (Petrus et al., 2003).

Removal of heavy metal ions from wastewater is achieved using active carbon adsorption, coagulation, precipitation, ion exchange, reverse osmosis processes. Due to simple application procedures and relatively mild operation conditions, the sorption processes are the most preferred one among these methods, although the regeneration conditions and cost of sorption materials are the limiting factors. Hence, looking for low cost sorbents in order to replace expensive synthetic ion exchange resins is important (Petrus et al., 2003).

Ion exchange process is favorable when a sorption material has high selectivity for the metal ion which is wanted to be removed and competing ion concentrations is low. At some conditions, special type of resins will be manufactured for removal of particular heavy metal ions which have very high selectivity. After that, the metal will be recovered and utilized in different industrial areas. In most cases however, metal ions are not valuable enough for the use of special exchangers and due to their chemical character separation of them from other metal ions are not easily achieved. In these cases, since natural zeolites have selectivity for certain heavy metal ions, they may be used for removal of mixed heavy metal ions which provide an economical benefit.

Natural zeolites are the most important inorganic cation exchangers that exhibit high selectivity and ion exchange capacity. These are naturally occurring aluminosilicate materials. Many different types of natural zeolites have already been identified. Among these clinoptilolite is the most abundant one. The clinoptilolite may be found in many parts of the world with sufficiently high purity (Petrus et al., 2003).

Turkey also has many sources for natural zeolites, especially clinoptilolite. One of the major clinoptilolite deposits in Turkey is located in Manisa, Gördes (DPT, 1996). Therefore, investigation of usage of Gördes type clinoptilolite for wastewater treatment is beneficial.

Since clinoptilolite has favorable ion exchange selectivity for the specific heavy metal cations, it has been studied for potential use in the treatment of industrial wastewaters. However, most theoretical and experimental studies of ion exchange equilibria on clinoptilolite have been focused on ion exchange reactions which involve only two cations (binary exchange) and little attention has been paid to simultaneous multicomponent ion exchange equilibrium.

The aim of this study is to determine the binary and multicomponent ion exchange behavior of Na formed Gördes type clinoptilolite for lead, cadmium, and sodium ions. For this purpose, Pb^{2+} – Na^{+} and Cd^{2+} – Na^{+} binary and Pb^{2+} – Cd^{2+} – Na^{+} ternary systems were investigated in column systems with concentration of metal ions between 0.005 N and 0.02 N constant total normality and flow rate between 5 mL/min and 20 mL/min at 25°C ambient temperature. More specially, the objectives of the study were:

- To investigate the main parameters affecting lead and cadmium removal and determination of maximum exchange level (MEL) of sodium form of Gördes clinoptilolite depending on experimental conditions.

- To determine the effect of loading flow rate on the breakthrough capacity on Pb^{2+} – Na^{+} and Cd^{2+} – Na^{+} binary, and Pb^{2+} – Cd^{2+} – Na^{+} ternary systems.

- To determine optimum particle size of clinoptilolite for removal of lead and cadmium under experimental conditions.

- To examine the effect of initial heavy metal concentration on breakthrough capacity on Pb^{2+} – Na^{+} and Cd^{2+} – Na^{+} binary and Pb^{2+} – Cd^{2+} – Na^{+} ternary systems.

- To observe and determine simultaneous multicomponent lead and cadmium removal properties of sodium form of Gördes clinoptilolite under certain experimental conditions, i.e., flow rates between 5 mL/min and 20 mL/min and influent ion concentrations between 0.005 N and 0.02 N.

- To determine the selectivity sequence of Na form of Gördes type clinoptilolite for Pb^{2+} – Cd^{2+} – Na^{+} ternary system.

CHAPTER 2

BACKGROUND INFORMATION

2.1 Heavy Metals

Technological improvement and industrialization have resulted in rapid increase, particularly in concentrations of heavy metals in the living environment. Wastewaters produced as a result of industrial applications polluted with the heavy metals, such as mining activities, tanneries, metal plating operations, and crude oil refining. These metal ions are highly toxic pollutants since they do not metabolizable and tend to bioaccumulate in living organisms, which cause a number of disorders and illnesses (Inglezakis et al., 2003). Therefore, wastewaters containing heavy metals are required to be treated prior to discharge into environment.

Heavy metal removal from wastewaters is a difficult task for the correct management of waste disposal. Among different treatment processes, ion exchange has many advantages compared to other processes. The main advantages may be listed as simplicity, safety of operation, and recovery potential of both the sorbent and precious heavy metals. Activated carbon is considered to be a particularly competitive and effective sorbent for the removal of heavy metals, however; the use of activated carbon may not be suitable due to high costs associated with production and regeneration of spent carbon (Panday et al., 1985). Therefore, investigation of low cost sorbents such as; peat, clay, lignin, chitosan, fly ash and zeolites in removal of heavy metals has arisen as a popular issue in recent years (Bailey et al., 1999).

2.2 The Zeolites

2.2.1 Definition of Zeolites

The word zeolite is of Greek origin. It means “boiling stone”, in respect to the visible water loss when they are heated. This property illustrates the ease of water loss when zeolites are heated. This property is known as “intumescence” property of zeolites.

A zeolite is an aluminosilicate, whose framework structure of $(Si,Al)O_4$ tetrahedra contains pores filled with water molecules and exchangeable cations. They are mainly aluminosilicate minerals having crystal structure. The skeletal structure of the zeolite contains voids occupied by exchangeable ions and water molecules which have a considerable freedom of movement leads to ion exchange and reversible dehydration; this accounts for the well known desiccant properties of zeolites.

Zeolites were indentified as a new type of mineral in year 1756 by the Swedish mineralogist A. F. Cronstedt (Schlenker et al., 1993). There are over 200 different synthetic zeolite types and 50 natural ones.

Zeolites are formed mainly over the earth’s surface and the sea bottom (Sand et al., 1978). However, with a few notable exceptions, they are exceedingly rare. Until 1960s, the zeolite minerals were supposed to formed mainly in cavities of basaltic and volcanic rocks. Since that time, with the help of X–ray diffraction method, many zeolite minerals occured by the natural alteration of volcanic ash in alkaline environments over long periods of time have been identified.

Over fifty known natural zeolites, chabazite, erionite, mordenite, and clinoptilolite occur in sufficient quantity and purity which allow their use as commercial products.

Generally, a zeolite ore is mined and the zeolite then processed by crushing, drying, powdering, and screening. Depending on the industrial area that they are used, it may then be chemically transformed by ion exchange and acid extraction.

2.2.2 Crystal Structure

Zeolites have a framework structure arising from $[SiO_4]^{4-}$ and $[AlO_4]^{5-}$ tetrahedra. Tetrahedron is the primary building block of zeolite framework and it is shown in Figure 2.1. The center of the tetrahedron is occupied by a silicon or aluminum atom, with four atoms of oxygen at the vertices.

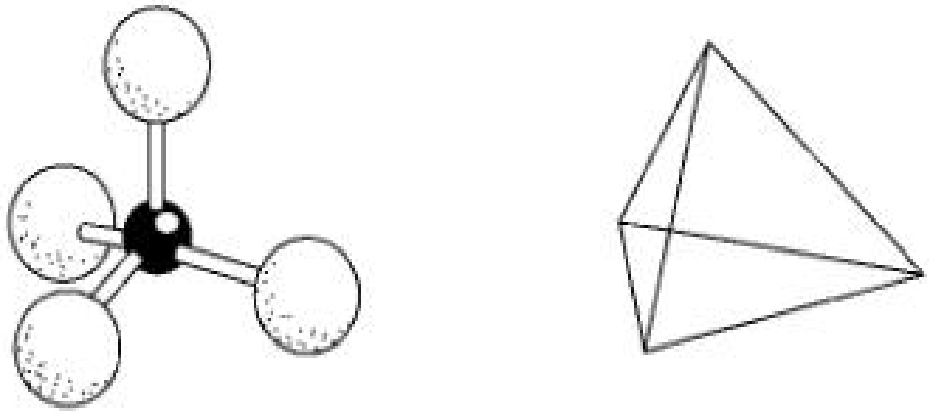

Figure 2.1 Demonstrations of $[SiO_4]^{4-}$ and $[AlO_4]^{5-}$ by means of ball and stick model and solid tetrahedron

Each oxygen atom is shared between two tetrahedra. In this way, the tetrahedra form a continuous framework. Substitution of Si^{4+} and Al^{3+} defines the negative charge of the framework; this negative charge is balanced by

monovalent or divalent cations located together with water molecules in structural channels.

Cations which reside in the channels are substituted easily, for this reason they are termed exchangeable cations unlike silica and alumina which are not exchanged under ordinary conditions; the others are termed framework cations.

The idealized unit cell formula of the zeolites is;

$$M_{x/n}\,[(AlO_2)_x\,(SiO_2)_y].wH_2O \qquad (2.1)$$

and oxide formula is;

$$M_{2/n}O.Al_2O_3.xSiO_2.yH_2O \qquad (2.2)$$

where, M is cation of valance, n is cation charge, y/x = 1 to 6, w/x = 1 to 4, and (x + y) is the total number of tetrahedra in the unit cell. The composition of the tetrahedral framework is generally given in square brackets (Breck 1974; Tsitsishvili et al. 1992).

The Si/Al ratio in natural zeolites ranges within the limits of 1 to 6. The lower limit is determined by Lowenstein's rule, which states that an AlO_4 tetrahedron can not associate with another AlO_4 tetrahedron by a common oxygen atom; at Si/Al = 1, the silicon and aluminum tetrahedra alternate to form the ordered framework. Ordered locations of Si and Al, is also possible at other Si/Al ratios. The upper limit of the Si/Al ratio in the natural zeolites, such as clinoptilolite, mordenite, and ferrierite, reaches to 5 to 6.

In synthetic zeolites the silicon can be substituted by germanium and aluminum can be substituted by gallium, iron, chromium, boron etc., but in natural specimens only Be and Fe is observed in tetrahedral sites, in addition to Si and Al (Tsitsishvili, 1992).

2.2.3 The Aluminosilicate Framework

As stated above, all zeolites have 3-D structures constructed by joining together $[SiO_4]^{4-}$ and $[AlO_4]^{5-}$ coordination polyhedra. The most conserved and stable component is the aluminosilicate framework and it defines the structure type. The topological structure of the framework, the numbers and distribution of charges and stacking faults are basically formed at the crystal growth stage and define a series of technologically important properties of zeolites. Framework topology forms the basis of contemporary classification of the zeolites.

The Si/Al distribution can be estimated confidently, by the distance between the tetrahedron center and the oxygen atom. In ordered structures one can distinguish two groups of distances, for silicate tetrahedra it is close to 0.162 nm and for aluminate tetrahedra it is close to 0.174 nm.

A remarkable characteristic zeolite property arising from their molecules framework structure is the assemblages of tetrahedral such as creating their porous structure which happens to form regular arrays of apertures. These apertures have such a size that, they selectively take up some molecules into their porous structure, while rejecting others on the basis of their larger effective molecular dimensions. For sorption and catalysis, the dimensions and locations of these channels, through which the molecules diffuse into inter crystalline free volume, are very important. This property is known as “molecular sieving”.

2.2.4 Exchangeable Cations and Water Molecules in Zeolite Structure

All zeolites have 3-D framework structures constructed by joining together $[SiO_4]^{4-}$ and $[A1O_4]^{5-}$ coordination polyhedra. The negative charge is balanced by ions found in the interstices of zeolites; they are generally alkaline or alkaline earth cations, such as Na^+, K^+, Ca^{2+}, Mg^{2+} or Sr^{2+}.

The channels and voids in zeolite framework are filled with exchangeable cations and water molecules. Ease of water removal and ion exchange creates an impression of disordered location of cations and water molecules in their structure. Determination of zeolite structures show that, most of the water molecules and cations occupy rather definite sites in the lattice structure (Tsitsishvili, 1992).

In the structure, exchangeable cations are surrounded by water molecules and oxygen atoms. Distances to the nearest neighbors are very different and cations lie at the centers of irregular polyhedra. Cation-oxygen atom and cation-water molecule distances mainly depend on the size of the cation and cover wide ranges as compared with tetrahedral interactions. Magnesium ions are coordinated only by water molecules, but potassium and barium ions are surrounded generally by oxygen atoms of the lattice.

Coordination of Ca^{2+} and Na^+ ions depend strongly on the cavity geometry.

The characteristic property for zeolites containing large cavities is the presence of large complexes of water molecules in voids and bonding between framework ions and exchangeable ions by means of aqueous bridges. Water molecules can also serve as bridges between exchangeable cations. The most typical case involves a cation bound to the channel wall on one side and to a water molecule on the other. Structural refinements show that each cation

occupies its own specific site in natural or exchanged form. Most of the time, the decisive factor is not the charge but the size of the cation.

2.2.5 Classification of Zeolites

Zeolites can be classified into groups considering common features of the aluminosilicate framework structures. The most important properties of zeolites which are structure related can be determined as follows:

- High degree of hydration and behavior as zeolitic water
- Low density and void volume after dehydration
- Exhibition of high stability of the crystal structure during dehydration
- Cation exchange properties
- Various physical properties (e.g. electrical conductivity)
- Uniform molecular-sized channels in the dehydrated crystals
- Adsorption of gases and vapors
- Catalytic properties

The classification includes mainly seven groups; for each group, zeolites have a common subunit structure which is a specific array of $(Al,Si)O_4$ tetrahedra (Breck, 1974). The groups and some examples for each group can be summarized as follows:

- Group 1: Analcime, Philipsite
- Group 2: Erionite, Offreite
- Group 3: Zeolite A
- Group 4: Faujasite, Chabazite
- Group 5: Natrolite, Mesolite
- Group 6: Mordenite, Ferrierite
- Group 7: Heulandite, Clinoptilolite

The members of Group 7, heulandite and clinoptilolite, are the most abundant zeolites in nature. In many countries, huge occurrences of clinoptilolite are mined and its interesting properties are investigated and clinoptilolite finds itself a wide variety of application areas.

2.2.6 Structure of Heulandite and Clinoptilolite

The chemical composition of the heulandite and clinoptilolite series is characterized according to their remarkable changes in the Si/Al ratio and depending on composition of exchangeable cations in their structure. Main components in the clinoptilolite structure are represented in Figure 2.2.

It is observed that all structural determinations of heulandite and clinoptilolite justify the structural scheme offered by Merkle & Slaughter (1968). In this structural scheme $(Si,Al)O_4$ tetrahedra are bound in layers in Figure 2.3. These layers are in turn bound by oxygen atoms in the symmetry plane and they form a 3-D framework as shown in Figure 2.4.

Framework units are joined in a layer like array which cause the characteristic perfect cleavage of the mineral. The channel system is 2-D, including 8 to 10 membered channels, parallel [001] and 8-tetrahedra channels along [100], termed by Koyama et al. (1977) as A, B, and C channels respectively as seen in Figure 2.2.

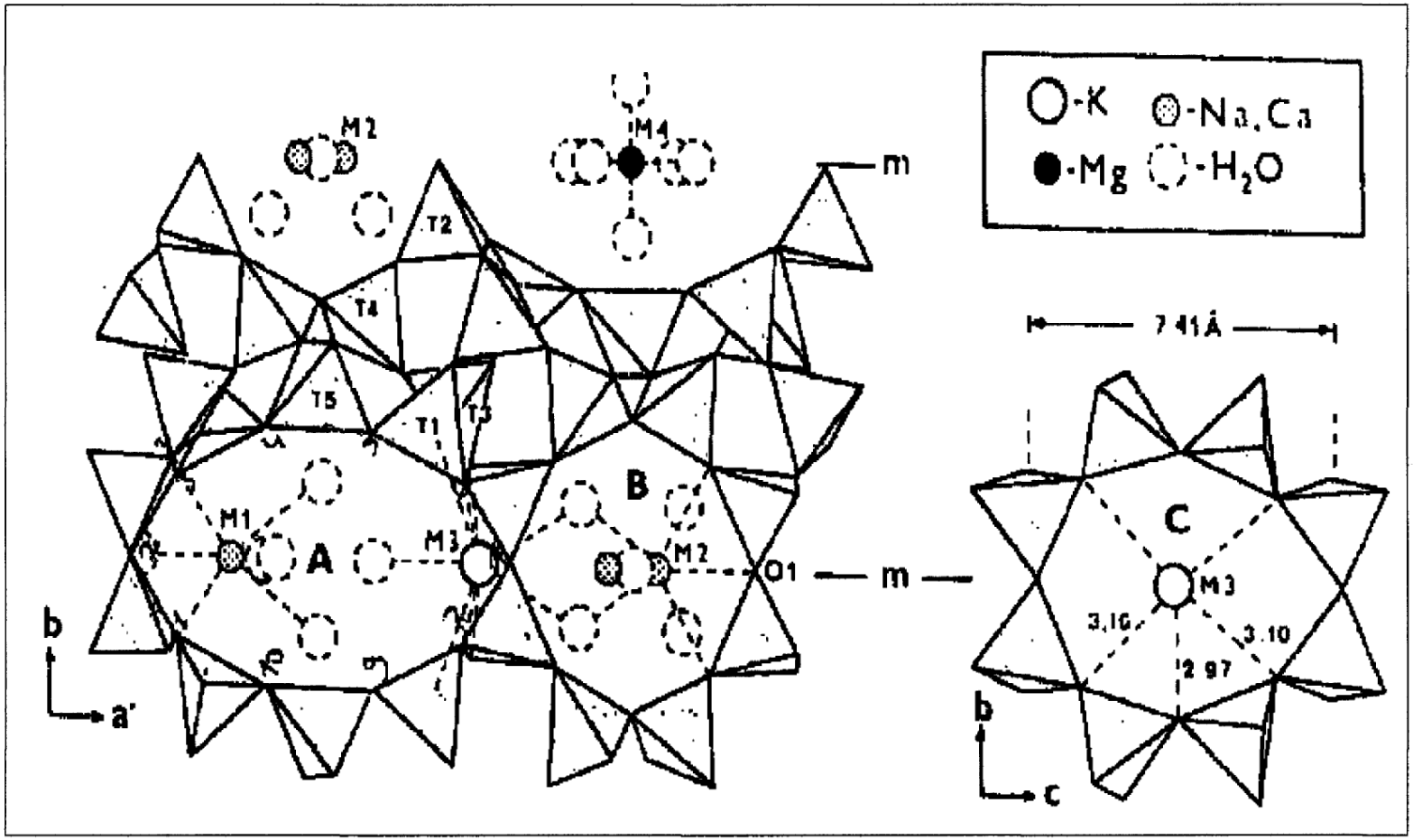

Figure 2.2 Main Components in the Clinoptilolite Structucture (Koyama, 1977)

Calcium and sodium ions both occupy two sites (Ml and M2) in channels A and B of heulandite and clinoptilolite. In addition, in clinoptilolite structure, there are two sites, M3 occupied by potassium and M4 occupied by magnesium ions.

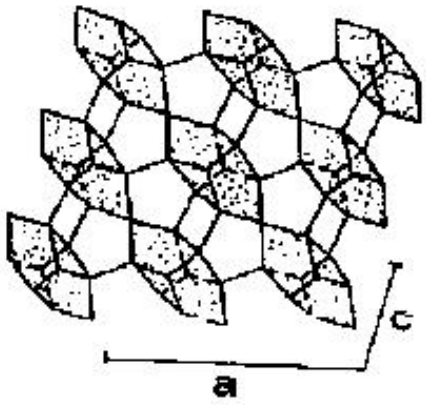

Figure 2.3 Arrangement of the 4-4-1 Units in the Framework Structure of Heulandite (Merkle and Slaughter, 1968)

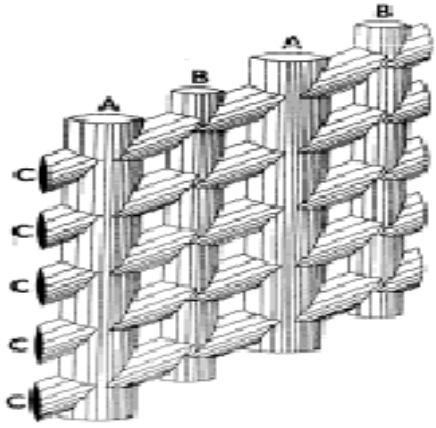

Figure 2.4 System of Channels in the ac Plane in Heulandite Structure (Koyama and Takeuchi, 1977)

2.2.7 Occurrence of Natural Zeolites

The rock forming zeolites are primarily found as products of the alteration of glasses of volcanic or impact origin. Fine grained volcanic glass is the basic source of natural zeolites due to their ion exchange capacities, chemical compositions and large surface areas (Tsitsishvili, 1992).

Huge zeolite occurrences are found in belts of recent volcanism, frequently in rocks of Cretaceous, Paleogenic and Neogenic age (Sand et al., 1978). Clinoptilolite, mordenite, chabazite, erionite, philipsite, laumontite, analcime, and ferrierite form large deposites. Six of them are used in industrial applications whereas analcime and laumontite are not utilized in industry yet.

The most important occurrences of clinoptilolite are formed in lake or marin basins. Zeolitization is the result of burial diagenesis or hydrothermal metamorphism at shallow depths. Due to mechanical strength, heat insulating and decorative properties, clinoptilolite tuffs have been used for ancient times.

Clinoptilolite tuffs consist of 70 – 90% of clinoptilolite together with authigenic species like montmorillonite, celadonite, chlorite, low cristobalite, and mordenite, also with the high temperature minerals quartz, plagioclase, biotite, and potassium feldspar.

2.2.8 Applications of Zeolites

Properties such as structural chemistry, availability, cost determines the industrial use of zeolites. Applications and uses of zeolites have attracted much attention and considerable progress has been made in utilization of zeolites in many industrial and agricultural areas in many countries.

The major industrial applications which make use of zeolites can be summarized as follows (DPT, 1996):

- Treatment of nuclear effluents
- Waste water treatment
- Use of zeolites in gas purification
- Zeolites as catalysts
- Adsorbent applications

2.3 Zeolites in Turkey

The majority of the investigated zeolite occurrences are located in Japan, USA, Russia, Eastern and Southern Europe. On the other hand, Turkey has also large occurrences of sedimentary zeolite, especially in central and western Anatolia regions. The zeolitic tuffs are associated with clay minerals, borates, carbonates, and soda minerals akin to many other parts of the world. They are also found in close association with lignite-bearing lacustrine rocks (Ören and Kaya, 2006).

Table 2.1 Zeolite Deposits and Types Detected so far in Turkey (DPT, 1996)

Type of Zeolite	Deposits
Analcime	Ayaş, Bahçelik, Beypazarı, Çandır, Çayırhan, Gölpazarı, Göynük, Hasayaz, Kalecik, Mihalıççık, Mülk, Nallıhan, Oğlakçı, Polatlı, Şabanözü
Clinoptilolite	Bigadiç, Doğantepe, Hisarcık, Gördes, Saphane, Urla, Yoncaağaç
Chabazite	Tuzköy

Western Anatolia is rich in clinoptilolite deposits. Manisa-Gördes and Balıkesir-Bigadiç regions are the most notable clinoptilolite deposits in Turkey, having nearly 20 million tons and 500 million tons of reserves, respectively (DPT, 1996). The total estimated amount of zeolite occurrences (Table 2.1) is about 50 billion tons, even though there is no comprehensive investigation on zeolite deposits for the other regions of Turkey (DPT, 1996).

2.4 Ion Exchange Properties of Clinoptilolite

Zeolite structures have unique features that lead to unusual types of cation selectivity and sieving. Therefore, cation selectivities in zeolites do not follow the typical rules which are evidenced by other inorganic and organic exchangers.

Substitution of trivalent Al for quadrivalent Si in the silicate tetrahedral of clinoptilolite structures create fixed, negatively charge sites throughout the structure. To maintain electrical neutrality the negative charges are neutralized by the presence of an equivalent number of mobile cations and these mobile cations are loosely bonded in the crystal structure and they are free to exchange with cations in the solution. The cation exchange occurs when ions from solution replace counter ions within the crystal structure.

The unusual selectivity of clinoptilolite that makes it attractive for ion exchange applications is caused by structure related ion sieve properties. Many different mechanisms exist which are responsible for the cation sieve properties exhibited by natural zeolites. One of them is the positive exclusion of certain cations due to the inability of these larger cations to enter the zeolite lattice in considerable amounts. An example of this mechanism is the sieve effect shown by analcite for Cs. The second mechanism for a cation sieve effect is the inability of the negative charge distribution on the zeolite structure to accommodate a given cation (Mumpton, 1960).

2.5 Ion Exchange Theory

The ion exchange process can be represented by the equation 2.3 as follows;

$$Z_A B_{(z)}^{Z_B^+} + Z_B A_{(s)}^{Z_A^+} \Leftrightarrow Z_A B_{(s)}^{Z_B^+} + Z_B A_{(z)}^{Z_A^+} \qquad (2.3)$$

Where, Z_A and Z_B are charges of the exchanging cations A and B, subscripts "z" and "s" refer to the zeolite and solution, respectively. The equivalent fractions of the exchanging cation in the solution and zeolite are defined by:

$$A_s = \frac{\text{Normality of exchanging cation A}}{\text{Total Normality}} \qquad (2.4)$$

$$A_z = \frac{\text{Number of equivalents of exchanging cation A}}{\text{total equivalents of cations in the zeolite}} \qquad (2.5)$$

Also, $A_s + B_s = 1$ and $A_z + B_z = 1$ (Bhatia, 1990)

2.6 Ion Exchange Isotherms

Ion exchange isotherm is a measure of the preference of the zeolite displays for one ion over another ion at equilibrium. The isotherm is constructed by plotting the equivalent fraction of the incoming cation present within the solution phase, A_s, versus the equivalent fraction of the same cation in the zeolite, A_z, at equilibrium and constant temperature.

The isotherms are classified in four types (Townsend, 1991). Example of isotherms of the first type is shown in Figure 2.5.a and represents relatively simple systems in which the exchanger is either unselective (case 1) for the

incoming ion or selective (case 2). For isotherms of the second type (Figure 2.5.b) the plot is sigmoid, indicating a change in selectivity as a function of A_z. Isotherms of the third type (Figure 2.5.c) are characterized by a plateau, and within this plateau region non-reversibility of the isotherm may be seen (hysteresis loop). Finally, isotherms of the fourth type are seen often with zeolites (Figure 2.5.d), in which a clear limit to exchange is observed which is lower than the theoretical exchange capacity of the material.

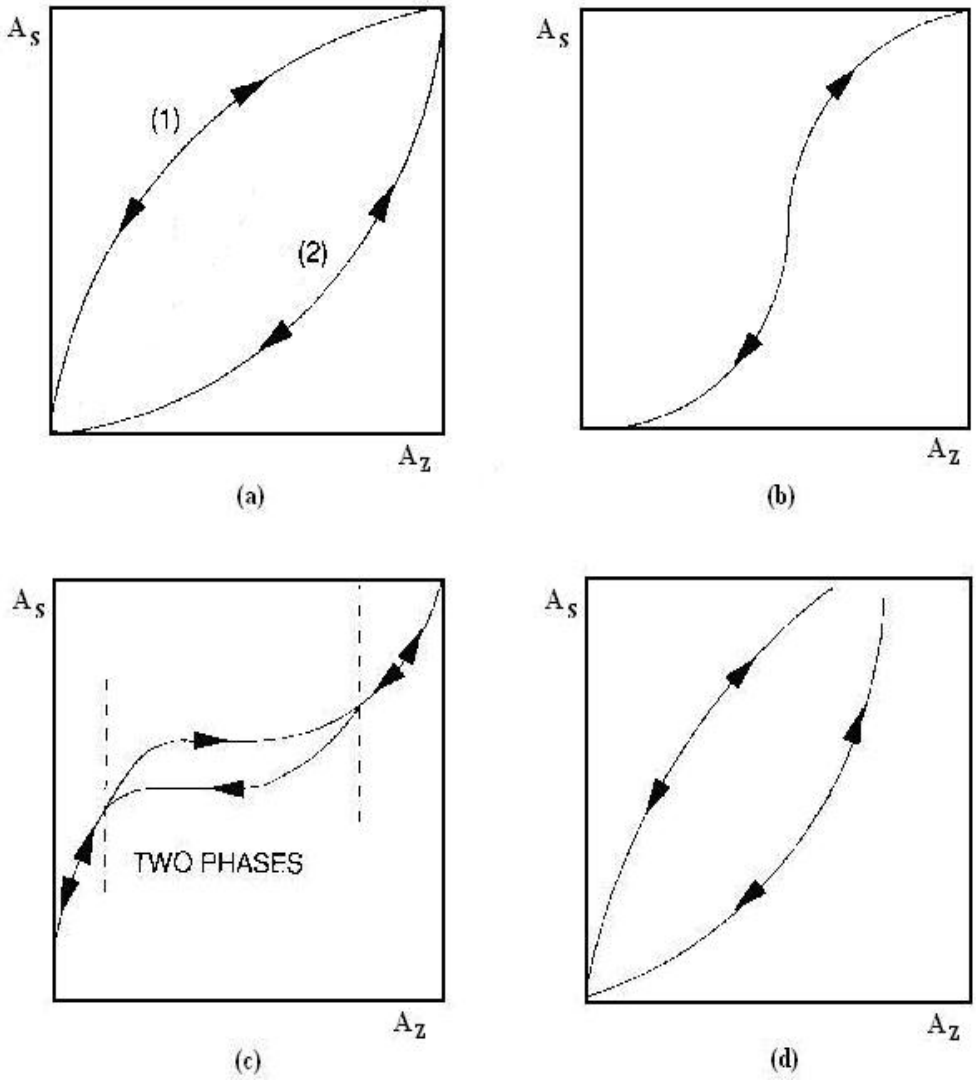

Figure 2.5 Arrangement of isotherms described by Townsend (1991): (a) first type, (b) second type, (c) third type, and (d) fourth type

2.7 Ion Exchange in Column Operations

Ion exchange operation is usually carried out in columns. Ion exchange process can be used for replacement, removal and separation of ions and non-electrolytes. The simplest column operation is the replacement of counter ion in feed by another counter ion which is initially in the ion exchanger. The counter ion from the feed is removed by ion exchange process and it is absent in the effluent until breakthrough occurs.

Considering a simple ion exchange process in column, let us assume an influent solution containing ion B^+ which will be replaced with ion A^+. When the solution is fed to the column, interaction between solution and exchanger bed begins. Firstly, upper layer of bed exchange all its exchangeable ions. As process continued, since the upper layers of the bed completely exchange its ions (A^+) with ion B^+ and turned into B form, they lost their ion exchange properties. The zone in which the ion exchange occurs is thus displaced downwards. The exchange zone reaches the bottom of the bed at the instant when the effluent cation concentration reaches about 5% of its influent value ($C/C_0 = 0.05$). This point may be called as the breakthrough point.

As the column operations continues, the concentration of the ion B^+ in the effluent increases up to 98% of its influent value ($C/C_0 = 0.98$). This point may be called as exhaustion point. Practically, the exchange process finishes at exhaustion point. The schematic demonstration of ion exchange process in column operation is shown in Figure 2.6.

If the concentration of the exchangeable ion in the effluent of packed bed ion exchange column is plotted as a function of volume of total treated solution up to that point, characteristic sigmoid shaped breakthrough curves may be obtained as seen in Figure 2.7.

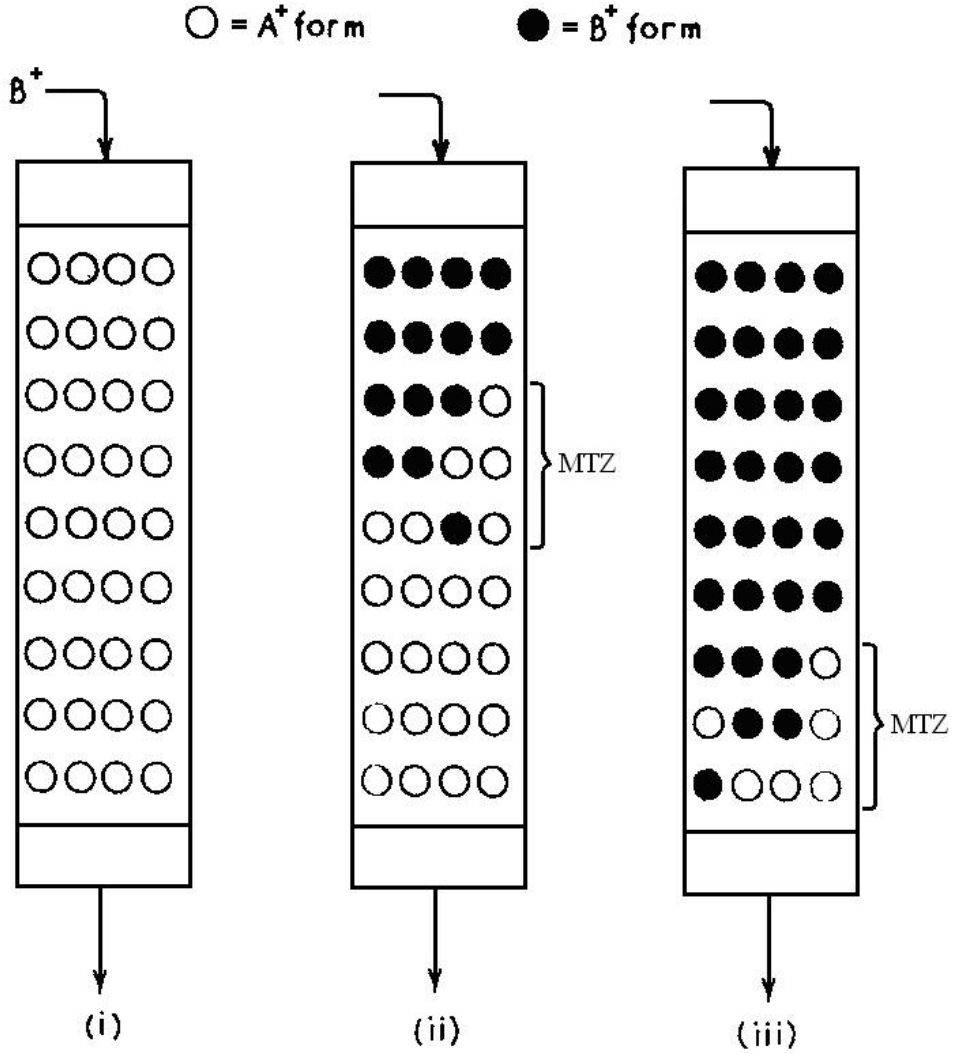

Figure 2.6 Schematic Representation of Exchange Column Showing the Ion Exchange Operation (Güray, 1997)

(MTZ: Mass Transfer Zone)

(i): A^+ Form of Zeolite Column Placed in Service

(ii): Zeolite Column Showing Typical Cation Distribution Prior to Breakthrough

(iii): Zeolite Column Showing Cation Distribution at the Onset of Breakthrough

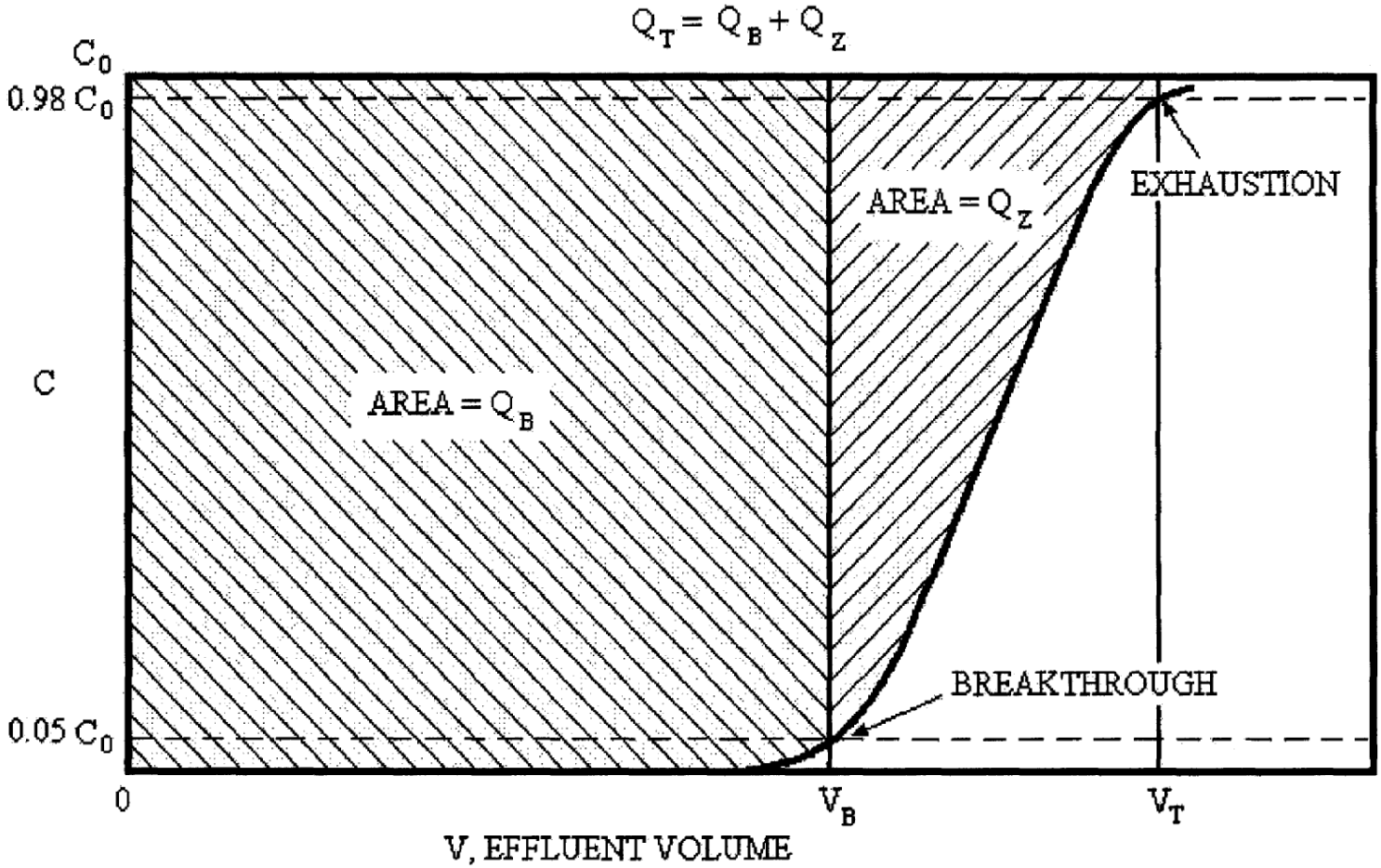

Figure 2.7 Idealized Effluent Concentration vs. Effluent Volume for Ion Exchange Column

2.8 Calculation of Breakthrough Capacity

Breakthrough curves are obtained by plotting the effluent concentration of the exchangeable cations as a function of the volume of effluent solution collected. These curves are quite useful to calculate the dynamic parameters affecting the ion exchange process.

The breakthrough curves are also suitable to determine the exchange capacity of the packed bed. For any fixed bed operating at constant flow rate, it is clear that the total exchange capacity of the bed can be calculated by integration of the area above the breakthrough up to exhaustion, according to the equation 2.6;

$$Q_T = \frac{\int_0^{V_T} (C_0 - C) dV}{\rho_b h_T a_s} \tag{2.6}$$

where, Q_T is the total capacity of clinoptilolite for the type of influent ion, and ρ_b is packed bed density.

In the same way, the breakthrough capacity of the clinoptilolite can be calculated from the relation:

$$Q_B = \frac{\int_0^{V_B} (C_0 - C) dV}{\rho_b h_T a_s} \tag{2.7}$$

The column efficiency is the fraction of the exchange capacity defined as;

$$\eta_c = \frac{Q_B}{Q_T} \tag{2.8}$$

CHAPTER 3

LITERATURE SURVEY

3.1 Ion Exchange Studies on Pb^{2+} – Na^{+} and Cd^{2+} – Na^{+} Binary Systems

Semmens and Seyfarth (1978) worked on ion exchange properties of near homoionic form of sodium clinoptilolite. Furthermore, they studied removal of heavy metals like lead and cadmium on clinoptilolite at 28°C and solution total normality near 0.30 N. Results showed that, sodium formed clinoptilolite has high selectivity and exchange levels (expressed as the percentage of the theoretical exchange capacity) for both cations; 100% for lead and 85% for cadmium, respectively. Results revealed that, near homoionic form of sodium clinoptilolite has affinity for both Pb^{2+} and Cd^{2+} ions.

Blanchard et al. (1983) examined removal of heavy metals from wastewaters by means of natural zeolites. They used sodium form of clinoptilolite and found the selectivity sequence as $Pb^{2+}>NH_4^{+}>Cu^{2+}$, $Cd^{2+}>Zn^{2+}$, and $Co^{2+}>Ni^{2+}>Hg^{2+}$.

O'Connor et al. (1985) studied the ion exchange properties for lead ions of synthetic faujasite zeolites with varying framework silica to alumina ratios. Ion exchange isotherms for all systems were demonstrated at 25°C. Stoichiometric behavior was observed in all cases. The results proved that the more siliceous the zeolite, the lower selectivity for lead.

Loizidou and Townsend (1987) studied Pb^{2+} – Na^{+} binary system by using mordenite, ferrierite, and clinoptilolite at 25 °C and 0.1 N total normality. The results showed that affinity of clinoptilolite for lead ion is higher than ferrierite and mordenite.

El Akrami (1991) examined effects of particle size, flow rate, and influent ion composition and concentration on ion exchange properties of Bigadiç clinoptilolite. During study, effects of influent composition, flow rate, particle size, and cation concentration were investigated. For this purpose, particle sizes were taken as 6/16, 16/30, and 30/50 mesh. Flow rates were taken between 22 and 78 BV/h. The optimum ion exchange conditions were found as follows: 30/50 mesh in particle size and about 30 BV/h loading flow rate. He also found that, breakthrough capacity varied depending on the influent NH_4^{+} ion concentration.

Malliou et al. (1992) studied lead and cadmium removal by clinoptilolite. Experimental parameters were particle size and temperature. Results demonstrated that the clinoptilolite selectivity was higher for lead ion than cadmium ion. Moreover, particle size did not affect metal uptake level at lower temperatures. However, at slightly higher temperatures (50°C) particle size was important for metal uptake. At equilibrium, effective capacity of zeolite was nearly 1.4 meq/g for lead and 1.1 meq/g for cadmium.

Haralambous et al. (1992) showed that pretreatment of clinoptilolite improves the zeolite's ion exchange properties, and also determined that the structure of clinoptilolite remains unchanged during the loading and regeneration cycles. The theoretical exchange capacity (TEC) of clinoptilolite was determined as 2.27 meq/g by chemical analysis and maximum exchange level (MEL) found as 1.09 meq/g.

Malliou et al. (1994) examined uptake of lead and cadmium ions by clinoptilolite. Results showed that, removal of Pb^{2+} increased by decreasing the particle size. Also, they observed the uptake level of Pb^{2+} and Cd^{2+} ions increase at higher temperatures.

Güray (1997) investigated lead removal from waters by using Bigadiç type clinoptilolite. Fixed bed column operations were performed in respect to feed composition, particle size, and flow rate and breakthrough curves were obtained. Results showed that pretreatment of natural zeolites improve their breakthrough performance. Moreover, optimum conditions determined as influent lead concentration 311 mg/L and particle size 50/60 mesh. Under these conditions, breakthrough capacity was determined as 0.94 meq/g which corresponds to 63% of theoretical exchange capacity.

Curkovic et al. (1997) studied lead and cadmium removal from wastewaters by using batch method. Both natural and pretreatment zeolites were examined during experiments. They proved that the natural zeolites include exchangeable ions such as Na^{+}, K^{+} and Ca^{2+}. They treated as-received type zeolite with 2 M NaCl solution at 22 and 70°C. It was shown that, pretreatment enhanced both exchange capacity and ion removal efficiency. For lead concentration less than 2.5 mmol/L, removal efficiency was about 90% depending on the treatment of zeolite samples while at the same concentration of cadmium; removal efficiency was varying from 45 to 70%. Moreover, the metal uptake was increased with increasing temperature during the ion exchange process.

Ouki and Kavannagh (1999) made research on clinoptilolite and chabazite regarding their selectivity and efficiency for heavy metal removal from effluents, Cd^{2+}, Cu^{2+}, Co^{2+}, Cr^{3+}, Pb^{2+}, and Zn^{2+}. Effects of ion concentration, pH and presence of competing ions were examined and ion removal performance was determined. The study showed that clinoptilolite and chabazite showed different selectivity sequences for all the metal ions except Pb^{2+} for which both zeolites

showed exceptionally well. Moreover, metal removal efficiencies exceeding 99% was achieved by both clinoptilolite and chabazite, optimum pH range was reported between 4 and 5. Also, selectivity sequence was determined as $Pb^{2+}>Cu^{2+}>Cd^{2+}>Zn^{2+}>Cr^{3+}>Co^{2+}$.

Faghihian et al. (1999) examined the use of Iranian type clinoptilolite and its pretreated, sodium form, for removal of radioactive cesium and strontium from nuclear wastewater and Ba^{2+}, Cd^{2+}, Ni^{2+}, and Pb^{2+} from municipal wastewater at 25°C and 0.1 N total normality. Results denoted that selectivity sequence was $Pb^{2+}>Cd^{2+}>Ba^{2+}>Sr^{2+}>Cs^{+}>Ni^{2+}$ and $Pb^{2+}>Ba^{2+}>Cd^{2+}>Sr^{2+}>Cs^{+}>Ni^{2+}$ for natural and pretreated clinoptilolite, respectively. Also, they concluded that, either natural or sodium form is recommended for removal of Cs^{+}, Ni^{2+}, Sr^{2+}, and Ba^{2+}, from radioactive or municipal wastewater, as the affinity of the mineral for these cations is relatively high.

Singh et al. (2000) worked on the sorption properties of natural and synthetic zeolites for cadmium ion removal from contaminated soils, to reduce the uptake of Cd^{2+} by field of crops at 20°C constant temperature. Results showed that, the cadmium sorption increased with decreasing particle size and sorption of cadmium reached maximum at pH between 4.5 and 6. Moreover, results also proved that, both natural and synthetic zeolites had high selectivity for Cd^{2+} ion and cadmium sorption was relatively high for synthetic zeolites.

Langella et al. (2000) examined ion exchange property of Sardinian type clinoptilolite zeolite. They obtained Cd^{2+}-Na^{+}, Cu^{2+}-Na^{+}, NH_4^{+}-Na^{+}, Pb^{2+}-Na^{+}, and Zn^{2+}-Na^{+} ion exchange isotherms at 25°C and 0.1 N total normality and the selectivity sequence was determined as $NH_4^{+}>Pb^{2+}>Na^{+}>Cd^{2+}>Cu^{2+}=Zn^{2+}$. The result indicated that clinoptilolite has higher affinity for NH_4^{+} and Pb^{2+} and lower affinity for Cd^{2+}, Cu^{2+}, and Zn^{2+}.

Cincotti et al. (2001) studied Sardinian type clinoptilolite at 25°C and 0.1 M to evaluate its adsorption for the ions Cd^{2+}, Cu^{2+}, NH_4^+, Pb^{2+}, and Zn^{2+}. Natural clinoptilolite was pretreated to get nearly homoionic sodium form. Results showed that the sodium form had better ion exchange capacity than as received type of clinoptilolite for all ions investigated. Furthermore, the selectivity of natural Sardinian type zeolite was determined as $Pb^{2+}>NH_4^+>Cd^{2+}>Cu^{2+}>Zn^{2+}$ and they concluded that Sardinian natural clinoptilolite is a potential adsorbent, especially for lead removal.

Panayotova and Velikov (2002) examined kinetics of heavy metal ions removal by use of natural Bulgarian type clinoptilolite. They investigated that lead ions are strongly bound to zeolite and immobilization of the other heavy metal ions (Cd^{2+}, Cu^{2+}, Ni^{2+}, and Zn^{2+}) is relatively weaker. They also stated that Pb^{2+} uptake was not influenced by the presence of Ca^{2+} and Mg^{2+} ions whereas lower uptakes were attained for Zn^{2+}, Cu^{2+}, Ni^{2+}, and Cd^{2+} in the presence of Ca^{2+}. Also, the selectivity sequence was obtained as $Pb^{2+}>Cd^{2+}>Cu^{2+}>Zn^{2+}>Ni^{2+}$.

Ponizovsky and Tsadilas (2003) examined lead sorption by alfisol (soil) and clinoptilolite at 25°C, 0.1 N total normality, and pH range 3 – 5 to find the relationship between the amounts of lead retained and ions displaced from the soil into the solution. Results showed that lead sorption by clinoptilolite was not influenced by pH and was accompanied by the increase of Ca^{2+}, Na^+, and K^+ contents in solution, whereas amounts of displaced H^+ were negligible. Research indicated that lead retention both by alfisol and clinoptilolite can be viewed as the result of ion exchange reaction with strong (soil) or very strong (zeolite) specific binding of lead. Application of zeolite in some instances may appear the most efficient treatment method for lead contaminated soils due to its high ability to retain lead in a wide range of pH.

Inglezakis et al. (2004) studied on as received and pretreated sodium form of Greek clinoptilolite. Ion exchange properties of both zeolites investigated by

using Cu^{2+}, Cr^{3+}, Fe^{3+}, and Pb^{2+} ions. Kinetic studies were performed at 0.01 N and 27°C. Equilibrium experiments showed that pretreated clinoptilolite is beneficial for metal uptake all, except Cr^{3+}, which is shown to have the same equilibrium behavior in both types of zeolite. Kinetic studies demonstrated that diffusion coefficients were not always improved in sodium rich form of clinoptilolite.

Çulfaz and Yağız (2004) studied ion exchange property of sodium form of Bigadiç type clinoptilolite to remove Pb^{2+} and Cd^{2+} at 25°C and 0.1 N total normality. According to the equilibrium studies, the selectivity sequence was obtained as $Pb^{2+}>Na^{+}>Cd^{2+}$. Therefore, they stated that the clinoptilolite can be used for the treatment of wastewaters containing lead, but not cadmium.

Bektaş and Kara (2004) investigated the removal of lead ions from aqueous solution by using Bigadiç type clinoptilolite. Experimental conditions were chosen as 0.1 N total normality, temperature range 25 – 50°C, and pH range 2 – 7. The effects of the initial metal ion concentration, agitation speed, temperature, and pH on the lead removal efficiency were investigated. Results demonstrated that the uptake rates of lead for all concentrations were rapid at initial stages and then increased gradually until the equilibrium is reached.

Medvidovic and Trgo (2006) examined removal of lead ions from aqueous solutions using Serbia and Montenegro type clinoptilolite at isothermal conditions, i.e. 25°C. Experiments were made by using fixed bed column and experimental parameters were initial concentrations and influent flow rates. They pointed out the highest column performance for the zeolite at particle size range between 0.6-0.8 mm, at the initial concentration of 215.5 mg/L and the flow rate of 2 mL/min.

Gedik (2006) worked on Bigadiç and Gördes type clinoptilolite to determine cadmium removal property, effect of pretreatment, and regeneration property.

Results showed that Gördes clinoptilolite was better than Bigadiç clinoptilolite for removal of cadmium. The ion exchange capacity of both zeolites after conditioning represents about 4 and 3 times increase for Gördes and Bigadiç samples, respectively. Moreover, exhaustion and regeneration cycles increase clinoptilolite capacity up to 36%.

Castaldi et al. (2008) examined sorption processes and XRD analysis of a Sardinian type zeolite. In that study the Pb^{2+}, Cd^{2+}, and Zn^{2+} adsorption capacity of a natural zeolite was evaluated in batch operations at pH 5.5. Additionally, X-ray diffraction (XRD) method was used to determine the differneces of the zeolite structure caused by the exchange with cations of different ionic radius. Results showed that the zeolite adsorption capacity for the three cations was $Zn^{2+}>Pb^{2+}>Cd^{2+}$. Moreover, XRD pattern of zeolite, analyzed according to the Rietveld Method, showed that the main mineralogical phase involved in the adsorption process was clinoptilolite. Also, besides structure information showed that the incorporation of Pb^{2+}, Cd^{2+}, and Zn^{2+} into the zeolite frameworks changed slightly but appreciably the lattice parameters.

Medvidović et al. (2007) investigated effect of flow rate for removal of lead ions by fixed bed of clinoptilolite. Isothermal column experiments were performed under a constant inlet concentration and bed depth, and different flow rates. A solution of lead ions with the concentration of 1.024 mmol/L was prepared by dissolving $Pb(NO)_3$ in distilled water. Experiments were carried out in a glass column with the inner diameter of 12 mm and a height of 500 cm, filled with 2.9 g (4.5 cm^3) of the clinoptilolite sample to the bed depth of 40 mm. Isothermal experiments at 20°C were performed at the constant inlet concentration and bed depth with changes of flow rates through the fixed bed of 1, 2 and 3 mL/min. Results showed that capacities of the breakthrough and exhaustion points did not change significantly with the increase of the flow rate and its near 265 BV, while the time needed to reach breakthrough is significantly shorter 20.42, 10.04, and 6.58 hours, respectively.

Teutli-Sequeira et al. (2009) studied influence of Na^{+}, Ca^{2+}, Mg^{2+}, and NH_4^{+} on the sorption behavior of Cd^{2+} from aqueous solutions by a Mexican type zeolite. The effects of pH and contact time on the adsorption process were examined. Results showed that the adsorption was similar in the pH range from 4 to 6. Sorption equilibrium was reached in about 48 h and the rate of cadmium sorption by the zeolite was rapid in the first 5 h of the reaction time. Kinetic experiments were best described by the pseudo-second order model, batch adsorption experiments conducted at room temperature (25°C) showed that the adsorption pattern followed the Langmuir–Freundlich isotherm model; these results indicated chemisorption of cadmium on a heterogeneous material. Sodium, calcium, magnesium and ammonium interfere in the sorption of cadmium by the zeolitic material.

3.2 Multicomponent Ion Exchange Studies

Mier and Callejas et al. (2000) examined multicomponent heavy metal removal with Mexican type clinoptilolite by ion exchange process. Interactions of Pb^{2+}, Cd^{2+}, and Cr^{4+} competing for ion exchange sites in naturally occurring clinoptilolite were investigated. Results revealed that dissolved Pb^{2+} and Cd^{2+} were effectively removed within 18 h in batch reactors, with higher removal efficiencies (>95%) in the acidic pH range. The presence of Cr^{4+}, which can interact with these metals to form anionic complexes, significantly diminished the Pb^{2+} and Cd^{2+} removal efficiencies. A decrease in the efficiency of clinoptilolite to remove Pb^{2+} was also observed in the high (≥10) pH range. Pb^{2+} ion outcompeted Cd^{2+} ion for ion exchange sites in a flow through column packed with clinoptilolite. The preferential removal of Pb^{2+} in column, but not in batch reactors, reflects that competitive retention can be affected by contact time because diffusion kinetics may influence the removal efficiency to a greater extent than equilibrium partitioning. Altogether, these results show that natural zeolites hold great potential to remove cationic heavy metal species from industrial wastewater. Nevertheless, process efficiency can be hindered by the

presence of competitive ions with reduced accessibility and/or affinity for ion exchange.

Berber-Mendoza et al. (2002) studied competitive exchange of Pb^{2+} and Cd^{2+} from aqueous solution on clinoptilolite. Results showed that the single exchange isotherms for Pb^{2+} and Cd^{2+} were adjusted quite well by the Langmuir isotherm and the exchange capacity for the Pb^{2+} ion is about 2.3 times that for the Cd^{2+} ion. The results of the competitive exchange showed that the ion exchange isotherm for Pb^{2+} was not significantly dependent upon the Cd^{2+} concentration; this means that Pb^{2+} ion was exchanged more selectively than the Cd^{2+} ion. However, the exchange isotherm for Cd^{2+} was considerably affected by the presence of Pb^{2+} ions. The exchange capacity for Cd^{2+} diminished drastically increasing the concentration of Pb^{2+} ion. Therefore, both ions compete for the same cationic sites of the zeolite but the zeolite is much more selective for the Pb^{2+} ion than for the Cd^{2+} ion.

Petrus et al. (2005) investigated ternary and quaternary ion exchange equilibria between heavy metal solution (Pb^{2+}, Cd^{2+}, Cu^{2+}) and sodium form of clinoptilolite. The value of the ion exchange equilibrium constant was estimated using the Langmuir, Competitive Langmuir, and thermodynamic sorption models. Results demonstrated that ion exchange capacity for a given heavy metal ion is not constant and differs in single or multicomponent systems.

Bayraktaroğlu (2006) studied binary and ternary ion exchange property of sodium form of Gördes (Manisa) clinoptilolite for ammonium, cadmium, and sodium ions. $NH_4^+ - Na^+$, $Cd^{2+} - Na^+$ binary systems and $NH_4^+ - Cd^{2+} - Na^+$ multicomponent system were investigated both in batch and column systems at 25°C. Results showed that Gördes clinoptilolite has affinity for both NH_4^+ and Cd^{2+} ions. The selectivity sequence was determined as $NH_4^+ > Cd^{2+} > Na^+$ in simultaneous multicomponent batch and column systems. Moreover, it was concluded that the increase of flow rate decreases breakthrough capacities and

column efficiencies of Gördes clinoptilolite in binary and multicomponent column operations.

Aşiroğlu (2006) examined binary and multicomponent ion exchange property of sodium form of Gördes (Manisa) clinoptilolite for ammonium, lead, and sodium ions. NH_4^+ – Na^+, Pb^{2+} – Na^+ binary systems and NH_4^+ – Pb^{2+} – Na^+ multicomponent system were investigated both in batch and column systems at 25°C. Studies were done by using clinoptilolite having particle size 0.25 – 0.50 mm. Experimental parameters were selected regarding flow rate and solution concentration. As a result they concluded Gördes clinoptilolite has affinity for both NH_4^+ and Pb^{2+} ions and selectivity sequence of the zeolite in multicomponent equilibrium was determined as Pb^{2+}> NH_4^+>Na^+.

CHAPTER 4

MATERIALS AND METHODS

4.1 Preparation and Characterization of Clinoptilolite Samples

4.1.1 Clinoptilolite Samples

The clinoptilolite sample that is used throughout this study was originated from a sedimentary deposit in Gördes (Manisa) in Western Anatolia and obtained from Mineral Research and Exploration Institute that is located in Ankara. Original clinoptilolite sample was nearly 15 kg and consists of particles approximately 1 cm in diameter.

For the determination of optimum particle size and maximum ion exchange capacity small portion of clinoptilolite sample was crushed and sieved into ASTM E-11 standard size ranges of 5/6 (4.00 – 3.36 mm), 8/10 (2.38 – 2.00 mm), 14/18 (1.41 – 1.00 mm), 20/30 (0.841 – 0.595 mm), 35/60 (0.500 – 0.250 mm), and 70/140 (0.210 – 0.105 mm).

Once optimum particle size for experimental parameters was determined, the size of the zeolite reduced to optimum level by crushing and sieving processes.

4.1.2 Characterization of Clinoptilolite Samples

Clinoptilolite sample is from a batch which was used in different thesis studies, thus characterization of the clinoptilolite sample have already been done in those

previous studies. Therefore, X-ray diffraction pattern (XRD) and Scanning Electron Micrograph (SEM) analysis for characterization of original clinoptilolite sample before pretreatment process were determined previously (Tufan, 2002 and Bayraktaroğlu, 2006).

Chemical composition of the original clinoptilolite sample was determined with X-ray fluorescence (XRF) technique, performed at Mineral Research and Exploration Institute (MTA) laboratories and also was reported in previous studies. Based on chemical composition of the zeolite, theoretical cation exchange capacity and Si/Al ratio of Manisa (Gördes) clinoptilolite was estimated as 2.36 meq/g and 5.2, respectively (Bayraktaroğlu, 2006).

4.1.3 Preparation of Nearly Homoionic Sodium Form of Clinoptilolite

Untreated, original form of Gördes type clinoptilolite zeolite contains cations such as Na^+, K^+, Ca^{2+}, and Mg^{2+}. These cations are exchangeable and may be substituted with different type of cations when required conditions are satisfied. Practically, any pretreatment operation results in increase of one type of cations included in clinoptilolite structure. This form of zeolite called as homoionic form. In this study, it was attempted to replace these cations by Na^+ ions to prepare a nearly homoionic form of clinoptilolite and to improve effective ion exchange capacity and performance in ion exchange applications.

Near homoionic form of clinoptilolite was obtained by treating the zeolite with sodium chloride (NaCl) solution. Column specifications and flow conditions are given in Table 4.1. The pretreatment procedure is as follows: Clinoptilolite is washed with deionized water prior to pretreatment, in order to remove the surface dust. Since surface dust causes high pressure drop problems during the operation of packed bed columns, especially for smaller particle size zeolites, removal of the dust is important. For pretreatment operation, the 10 g of zeolite is packed in a column of 2.0 cm inside diameter and 12 cm in height, followed

by shaking of the bed to avoid channeling until the height of the bed remained unaltered. After the complete packing of the material, a high flow rate of deionized water is used in down flow mode to check if there is any flow or pressure drop problem.

After that, 1.5 N sodium chloride solution is pumped to pretreatment column from a feed tank at down flow mode. During operation samples are taken from effluent in every 30 minutes to check whether exchangeable cation concentrations decreased to sufficiently low values or not. Measurements of the cations are made by atomic absorption spectrophotometer (AAS) for Ca^{2+} and Mg^{2+} ions and flame photometer for Na^{+} and K^{+} ions.

Table 4.1 Pretreatment Operation Parameters and Conditions

Pretreatment Column Specifications	
Inside Diameter (cm)	2.0
Height (cm)	12
Packing Material (Clinoptilolite) Specifications	
Particle Size (ASTM E-11)	35/60
Weight of Zeolite (g)	10
Sodium Chloride (NaCl) Solution Specifications	
Total Normality (N)	1.5
Amount (BV)	150
Operation Specifications	
Flow Rate (BV/h)	25
Temperature (°C)	25 (±1)

When pretreatment operation finished, the pretreated clinoptilolite was washed with deionized water. Washing was continued till no more chloride ion detected in effluent washing water when a drop of 0.1 percent $AgNO_3$ was introduced in it. Then the clinoptilolite sample was dried at 75ºC for 24 hours and finally,

pretreated sodium form of clinoptilolite kept in vessel, containing saturated NaCl solution, for future use.

4.2 Reagents

All chemicals used in pretreatment, binary and multicomponent ion exchange experiments were analytical grade reagents. The aqueous solutions of related ions were prepared by dissolving NaCl (J.T. Baker), $Pb(NO_3)_2$, and $Cd(NO_3)_2.4H_2O$ (Acros) in deionized water which had a conductivity of 18.2 μS/cm.

4.3 Batch Studies for Determination of Maximum Ion Exchange Capacity

Fixed bed column operations may be damaged from flow nonidealities. These problems cause improper experimental results in ion exchange operations performed using packed bed columns. Theoretical exchange capacity (TEC) defined as the number of exchangeable ions per known amount of zeolites and because of structural conditions TEC is different from maximum ion exchange level (MEL); therefore determination of MEL under specified experimental conditions is important for evaluation of experimental data (Inglezakis, 2005).

Maximum exchange level (MEL) is depending on the equilibrium conditions of the particular ion exchange system and depends on the normality and the temperature of the solution (Inglezakis, 2005). Therefore, Maximum exchange level was determined simply by equilibrating batchwise a sample of an ion exchanger with a solution of an ion and calculating the capacity from the uptake value thus obtained.

Batch ion exchange experiments were conducted by contacting weighed amounts of near homoionic sodium form of clinoptilolite with known volumes and concentrations of solution mixtures of the cations of interest. $Pb(NO_3)_2$ salt were

used as cation source for Pb^{2+}. Total solution concentrations and total volumes of the mixtures were held constant at 0.01 N and 80 mL.

The solutions were then dispensed in polypropylene bottles and mixed with 0.250 grams of zeolite samples each having different particle sizes. Particle sizes were previously mentioned in section 4.1.1.

After that, mixtures were agitated in water bath for 48 hours at constant temperature. After the equilibrium was reached, the mixtures were separated by filtration then the solution parts were analyzed by using flame photometer (Jenway) for Na^{+} and K^{+} ions and atomic absorption spectrophotometer (Shimadzu) for Ca^{2+}, Mg^{2+}, and Pb^{2+} ions. Following the ion analysis and measuring final equilibrium concentrations, maximum ion exchange capacities were estimated.

4.4 Column Studies for Ion Exchange Process

4.4.1 Determination of Optimum Particle Size

Optimum particle size determination studies were made by using a column having 1.0 cm inside diameter and 15 cm height. During experiments all conditions and parameters were kept constant except particle size. Six different particle sizes examined to determine their ion exchange behavior, breakthrough and total ion exchange capacity.

The column was packed with 5.0 g of pretreated clinoptilolite followed by shaking of the bed, to avoid channeling, until the height of the bed remained unchanged. Determination of ion exchange behavior studies were made by Pb^{2+} ions removal for which clinoptilolite has higher selectivity than Cd^{2+} ion. The solutions used in the experiments were prepared by dissolving $Pb(NO_3)_2$ salt in deionized water. Sketch of the experimental setup is demonstrated in Figure 4.1.

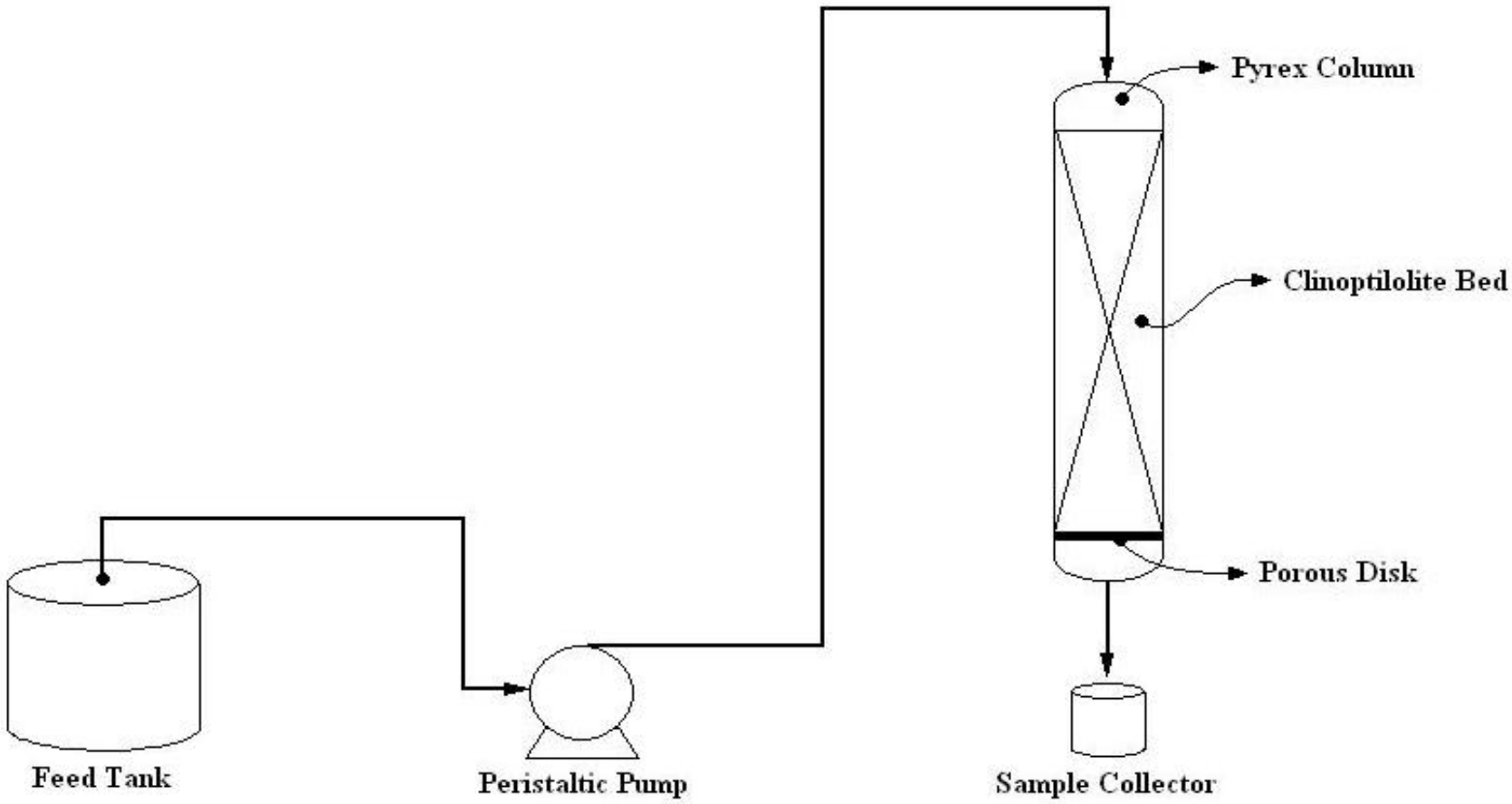

Figure 4.1 Schematic Representation of Experimental Setup

The solution was pumped from a tank to the top of the column, passed through clinoptilolite packing in down flow mode, and samples from effluent solution were taken at 50 mL intervals so as to determine the concentration of ions in the effluent. Constant flow was maintained by using peristaltic pump (Cole Parmer Masterflex L/S). The experimental parameters of determination of optimum particle size study are listed in Table 4.2.

Table 4.2 Experimental Parameters for Determination of Optimum Particle Size

Column Specifications	
Inside Diameter (cm)	1
Height (cm)	15
Packing Material (Clinoptilolite) Specifications	
Particle Size (ASTM E-11)	5/6, 8/10, 14/18, 20/30, 35/60, 70/140
Weight of Zeolite (g)	5
Pb^{2+} Solution Specifications	
Total Normality (N)	0.01
pH	4 – 6
Operation Specifications	
Flow Rate (mL/min)	10
Temperature (°C)	25 (±1)

The process was stopped when the ion concentration in the effluent became equal to the initial concentration in the influent. Collected samples were analyzed for determination of either Pb^{2+} or Cd^{2+} concentrations and the breakthrough curves were established. It should be noted that, during breakthrough analysis, the breakthrough point concentration was taken as 5% of the feed concentration.

4.4.2 Binary Column Studies

Column studies for Pb^{2+} – Na^{+} and Cd^{2+} – Na^{+} binary ion systems were conducted by using column having 1.0 cm inside diameter and 15 cm height. The column was packed with 5.0 g, 35/60 ASTM E-11 mesh size, and pretreated sodium form of clinoptilolite. To avoid flow nonidealities as a result of channeling in packing bed, clinoptilolite sample was neatly placed in column by applying tapping method, until the height of the bed remained unchanged. The packed bed height was approximately 8.0 cm.

Examination of Pb^{2+} and Cd^{2+} ions removal on clinoptilolite zeolite was carried out by using solutions which have predetermined initial concentrations. The influent solutions which used in the experiments were prepared by dissolving $Pb(NO_3)_2$ and $Cd(NO_3)_2.4H_2O$ salts in deionized water. When the salt completely dissolved, the concentration of the solution was checked by using atomic absorption spectrometer (AAS). If required, concentration was adjusted to the target value by adding either salt or water.

The experiments were carried out at isothermal conditions. Ambient room temperature was nearly 25 °C. The schematic representation of the experimental setup is shown in Figure 4.1. The solution was pumped from a tank to the top of the column, passed through clinoptilolite packing in down flow mode, and 5 mL samples from effluent were taken after every 50 mL solution left the column so as to determine the concentration of ions in the effluent. Constant flow was maintained by using Cole Parmer Masterflex L/S model peristaltic pump. The experimental parameters of binary ion exchange operation in column are listed in Table 4.3.

The process was stopped when the ion concentration in the effluent became equal to the initial concentration in the influent. Collected samples were analyzed for determination of either Pb^{2+} or Cd^{2+} concentrations and the breakthrough

curves were established. It should be noted that, during breakthrough analysis, the breakthrough point concentration was taken as 5% of the feed concentration.

Table 4.3 Experimental Parameters for Binary Ion Exchange in Column

Column Specifications	
Inside Diameter (cm)	1.0
Height (cm)	15
Packing Material (Clinoptilolite) Specifications	
Particle Size (ASTM E-11)	35/60
Weight of Zeolite (g)	5.0
Packed Bed Height (cm)	8
Pb^{2+} or Cd^{2+} Solution Specifications	
Total Normality (N)	0.005, 0.01, 0.02
pH	4 – 6
Operation Specifications	
Flow Rate (mL/min)	5, 10, 20
Temperature (°C)	25 (±1)

4.4.3 Ternary Column Studies

Ternary column experiments were carried out using same operation procedure as it was applied to binary column experiments. However, main difference between binary and ternary column experiments was that feed solution used in ternary system included two different ions (Pb^{2+} and Cd^{2+}) together. Solutions were prepared regarding to form mixture of 50% Pb^{2+} of total normality.

For ternary column ion exchange experiments same experimental setup which previously established for binary column studies was used as presented in Figure 4.1. The experimental parameters of ternary ion exchange process in column are listed in Table 4.4.

Table 4.4 Experimental Parameters for Ternary Ion Exchange in Column

Column Specifications	
Inside Diameter (cm)	1.0
Height (cm)	15
Packing Material (Clinoptilolite) Specifications	
Particle Size (ASTM E-11)	35/60
Weight of Zeolite (g)	5.0
Packed Bed Height (cm)	8
Pb^{2+} and Cd^{2+} Mix. Solution Specifications	
Total Normality (N)	0.005, 0.01, 0.02
Percentage of Pb^{2+} (eq./eq.%)	50
pH	4 – 6
Operation Specifications	
Flow Rate (mL/min)	5, 10, 20
Temperature (°C)	25 (±1)

4.5 Analysis of Samples

Concentrations of Na^{+} and K^{+} ions were determined using flame photometer (Jenway) and the concentrations of Ca^{2+}, Mg^{2+}, Pb^{2+}, and Cd^{2+} were analyzed using atomic absorption spectrophotometer (Shimadzu). Calibrations of equipments were made before every measurement. Measuring conditions of metal ions by using atomic absorption spectrophotometer are listed in Table 4.5.

Table 4.5 Measuring Conditions of Metal Ions

Type of Metal Ion	**Wavelength (nm)**
Ca^{2+}	422.7
Mg^{2+}	285.2
Pb^{2+}	283.3
Cd^{2+}	228.8

CHAPTER 5

RESULTS AND DISCUSSION

5.1 Characterization of Clinoptilolite Samples

5.1.1 Mineral Characterization

Previously, the clinoptilolite sample was used in different thesis studies. Hence, mineralogical characterization of the zeolite has already been done. X-ray diffraction (XRD) analysis was used to determine the mineralogical composition of Gördes type clinoptilolite samples. The results of XRD analysis are shown in Figure 5.1. Data were compared with International Center for Diffraction Data and the clinoptilolite peaks were identified (Tufan, 2002; Aşiroğlu, 2006).

X-ray pattern (Figure 5.1) showed that the zeolite mainly composed of clinoptilolite as a crystaline phase. The approximate percentages of impurities were determined by thin section analysis (Tufan, 2002; Gül, 2003) and it was determined that the sample contains 90±5% clinoptilolite; the rest is small amounts of quartz, feldspar, biotite, and rock fragments (3±1% quartz, 2±0.5% feldspar, 1±0.5% biotite and 0.3% rock fragments).

In addition to X-ray diffraction analysis, Scanning Electron Micrograph (SEM) analysis showed the morphology of the clinoptilolite sample. Typical coffin-shaped crystal structure was observed (Bayraktaroğlu, 2006). Scanning Electron Micrograph of as-received, Gördes type clinoptilolite is shown in Figure 5.2.

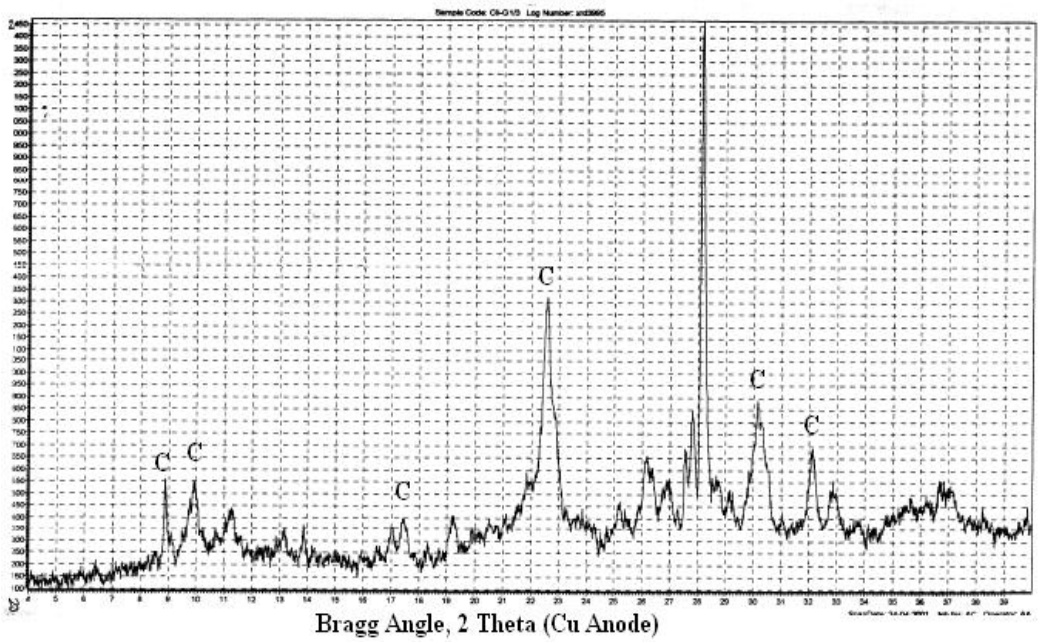

Figure 5.1 X-ray Diffraction Pattern of Gördes Type Clinoptilolite for 35/60 Mesh Sizes (Tufan, 2002)

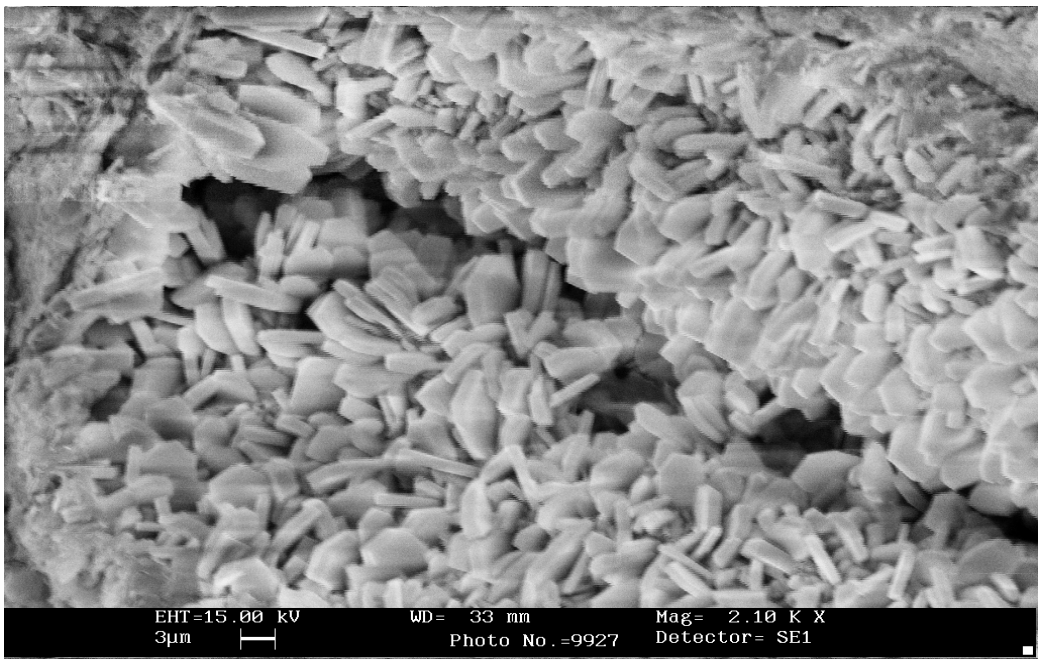

Figure 5.2 Scanning Electron Micrograph (SEM) Image of Gördes Clinoptilolite (Bayraktaroğlu, 2006)

5.1.2 Chemical Composition of Clinoptilolite Sample

Chemical composition of as-received and near homoionic Na form of clinoptilolite samples were determined using XRF analysis and are presented in Table 5.1. According to the Table 5.1, as-received clinoptilolite sample has low amounts of sodium and high amounts of potassium and calcium contents which is usually the case for Western Anatolian Zeolites (Yücel et al., 1995; Çulfaz and Yağız, 2004).

Si/Al ratio of original, as-received, sample and Na form of clinoptilolite sample were calculated as 5.37 and 5.51, respectively. The results indicate that, Si/Al ratios of both samples are in typical ranges 5 to 6 for clinoptilolite zeolite (Tsitsishvili et al., 1992).

Table 5.1 Chemical Composition of Original and Sodium Form of Clinoptilolite

	Original Clinoptilolite (Bayraktaroğlu, 2006) (w/w %)	**Na form of Clinoptilolite (w/w %)**
SiO_2	68.20	69.10
Al_2O_3	11.20	11.10
Fe_2O_3	2.40	2.10
MgO	1.00	0.80
CaO	2.10	0.50
Na_2O	0.60	3.20
K_2O	4.40	2.50
MnO	0.10	0.10
TiO_2	0.10	0.10
P_2O_5	0.10	0.10
LOI	9.80	10.40

Regarding the chemical composition of as-received and near homoionic Na form of clinoptilolite samples, theoretical exchange capacities were estimated and the results are presented in Table 5.2.

Table 5.2 Theoretical Exchange Capacities and Percentage of Exchangeable Cations

	Original Clinoptilolite		**Na form of Clinoptilolite**	
	(meq/g)	**(eq./eq.%)**	**(meq/g)**	**(eq./eq.%)**
Ca^{2+}	0.75	31.65	0.18	8.41
K^{+}	0.93	39.24	0.53	24.77
Mg^{2+}	0.50	21.09	0.40	18.69
Na^{+}	0.19	8.02	1.03	48.13
TEC	**2.37 meq/g**		**2.14 meq/g**	

Theoretical exchange capacity of as-received and near homoionic Na form of clinoptilolite samples were calculated as 2.37 and 2.14 meq/g, respectively. However, these values ignore the elements coming from impurities.

Bayraktaroğlu (2006) determined theoretical exchange capacity of near homoionic Na form of clinoptilolite sample as 2.28 meq/g by using batch type pretreatment method. In that study, the near homoionic form of clinoptilolite was obtained by treating each 50 g of original clinoptilolite sample with 500 mL of 1.0 N NaCl solution in a vessel with stirring by a wrist-action shaker at ambient temperature for 10 days. The exchange solutions were replaced with fresh NaCl solution every 24 hours which is called as batch pretreatment method.

The pretreated clinoptilolite has sodium content of 1.03 meq/g in continuous pretreatment method while this value raises up to 1.16 meq/g in batch pretreatment method (Aşiroğlu, 2006). Therefore, it has been concluded that,

batch type pretreatment method is better than continuous method to increase sodium content of clinoptilolite; however, time, amount of pretreatment chemicals, and amount of pretreatment solution required for batch method are much higher than continuous method.

5.2 Effect of Pretreatment

Previously in the materials and methods part (Chapter 4) it was stated that, pretreatment was applied to as-received form of clinoptilolite in order to improve ion exchange ability of natural clinoptilolite before performing ion exchange experiments.

Since the selectivity of clinoptilolite for Na^+ ion is lower than other exchangeable ions such as, Ca^{2+}, K^+, and Mg^{2+} (Semmens and Martin, 1988), clinoptilolite was conditioned with 1.5 N NaCl solution, nearly 6 hours by applying experimental conditions which were presented in Table 4.1.

The percentage content of exchangeable cations in as-received and pretreated clinoptilolite zeolites were calculated from chemical composition analysis' results and are presented in Table 5.2.

The results presented in Table 5.2 showed the increase of Na^+ content of the clinoptilolite by displacement of other exchangeable cations (K^+, Ca^{2+}, and Mg^{2+}) from zeolite structure. Moreover, results showed that, replacement of Ca^{2+} ion was easier than replacement of K^+ and Mg^{2+} ions applying pretreatment procedure which was represented in section 4.1.4 previously. This is because Mg^{2+} ions are strongly bonded to clinoptilolite structure. It is proposed that, K^+ is located at a specific site which is situated in an eight-membered ring and has the highest coordination (six framework oxygen and three water molecules) among all the cation sites in the unit cell (Jama, 1988). Because of this location and strong bonding to the zeolite structure, K^+ ion has low ion exchange ability.

5.3 Determination of Maximum Exchange Level

Maximum exchange level (MEL) is characteristic for ion exchange systems in which experimental parameters are already defined. Specified temperature and normality are the main experimental parameters. MEL depends on equilibrium conditions of the previously specified ion exchange system and as mentioned before it depends on temperature and normality of the solution (Inglezakis, 2005).

MEL is determined by conducting equilibrium studies and is expressed in terms of exchangeable ions per unit mass of the exchange material. This capacity definition is commonly used in determination of zeolite properties and is well identified (Inglezakis, 2005).

Since continuous column ion exchange operations may suffer from flow nonidealities like channeling, experiments sometimes results in erroneous results. Furthermore, theoretical capacity of zeolites is different from real ion exchange capacities because of chemical and porous structure properties. Hence, determination of MEL under experimental conditions is important for evaluation of experimental data of ion exchange processes. Maximum ion exchange level was simply determined by equilibrating batchwise a sample of an ion exchanger with a solution of an ion and calculating the capacity from the uptake value thus obtained.

Batch ion exchange experiments were conducted by contacting weighed amounts of near homoionic sodium form of clinoptilolite with known volumes of solution mixtures of the cations of interest. $Pb(NO_3)_2$ were used as cation source for Pb^{2+}. Total solution concentrations and total volumes of the mixtures were held constant at 1039 mg/L (≈0.01 N) and 80 mL, respectively. The solutions were then dispensed in polypropylene bottles and mixed with 0.250 grams of zeolite

samples each having different particle sizes. Particle sizes were previously mentioned in section 4.1.1.

Table 5.3 Exchangeable Ion Concentrations at Equilibrium

Mesh Size	Na^+ (mg/L)	K^+ (mg/L)	Pb^{2+} (mg/L)	Ca^{2+} (mg/L)	Mg^{2+} (mg/L)
5/6	80	13	672	3.72	0.97
8/10	45	7	674	3.77	0.80
14/18	65	3	679	2.84	0.54
20/30	75	1	681	2.31	0.61
35/60	80	0.6	706	3.07	0.66
70/140	75	0.5	712	2.98	0.62

After that, mixtures were agitated in water bath for 48 hours at constant temperature of 25 °C. After the equilibrium was reached, the mixtures were separated by filtration then the solution parts were analyzed by using flame photometer for Na^+ and K^+ ions and atomic absorption spectrometer for Ca^{2+}, Mg^{2+}, and Pb^{2+} ions. Measurement of final equilibrium concentrations are shown in Table 5.3 and maximum ion exchange capacities were estimated and results are represented in Table 5.4.

Table 5.4 Maximum Ion Exchange Capacities

Mesh Size	Mass Zeo. (g)	Vol. of Soln. (mL)	MEL (meq/g)
5/6	0.261	80	1.09
8/10	0.251	80	1.12
14/18	0.250	80	1.11
20/30	0.250	80	1.10
35/60	0.251	80	1.03
70/140	0.250	80	1.01

Although particle sizes are varying, maximum exchange levels, under these experimental conditions, do not show significant difference (Table 5.4) and it is nearly 1.08 meq/g. Therefore, it should be noted that, theoretical exchange capacity (2.14 meq/g) of sodium enriched form of clinoptilolite is significantly greater than the maximum exchange level (MEL) and in continuous column operations MEL is important to evaluation of experimental data.

5.4 Determination of Optimum Particle Size

In order to determine optimum particle size, clinoptilolite sample was crushed and sieved into size ranges 5/6 (4.00 – 3.36 mm), 8/10 (2.38 – 2.00 mm), 14/18 (1.41 – 1.00 mm), 20/30 (0.841 – 0.595 mm), 35/60 (0.500 – 0.250 mm), and 70/140 (0.210 – 0.105 mm) US mesh ranges (ASTM E-11).

After crushing the samples, one should be very careful when selecting the suitable particle size for ion exchange experiments. Very large particle sizes lead to lower ion exchange capacities in continuous column operations and very small particle sizes cause high flow resistance within the column. Moreover, channeling and high pressure drops may occur in column operations. On the contrary, smaller particle sizes result in higher removal performances.

In order to determine optimum particle size for column operations, 0.01 N Pb^{2+} solution was pumped to column in down flow mode at 10 mL/min flow rate. The concentration and flow rate values were chosen from Table 4.3. Both values are in the range of experimental parameters. Since selectivity of clinoptilolite is higher for Pb^{2+} ion than Cd^{2+} ion, (Langella et al., 2000 and Cincotti et al., 2001) lead ion was used for determination of optimum particle size. During experiments, all parameters were kept constant except particle sizes and the results are shown in Figure 5.3.

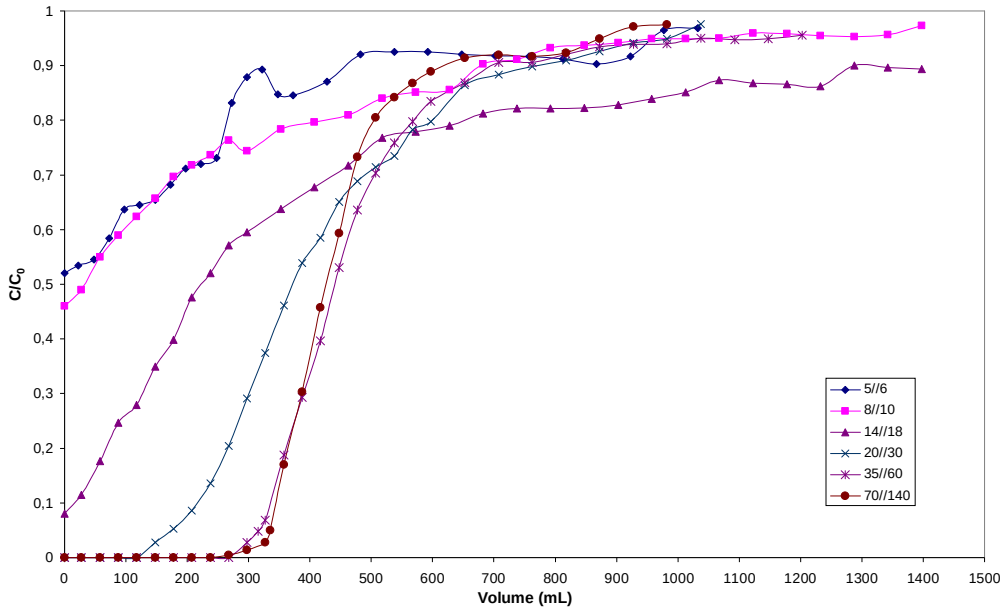

Figure 5.3 Breakthrough Curves for Determination of Optimum Particle Sizes

Results demonstrate that, mesh fractions between 5/6, 8/10, and 14/18 are not suitable for removal of ions for existing conditions. Because, there are no breakthrough point during the experiments which mean that at least some portion of lead ions which enters column leaves system without any exchange operation which is the evidence of mass transfer resistance in fixed bed.

Breakthrough plot of experimental data obtained from 20/30 mesh fraction experiment, forms breakthrough point and develops sigmoid shape breakthrough curve. However, the breakthrough capacity and volume of solution treated up to breakthrough point values are much lower than results which were obtained from 35/60 and 70/140 mesh fraction experiments.

35/60 and 70/140 mesh fraction experiments results in highest ion exchange levels among the others. They both have similar breakthrough capacities and similar exhaustion points. They both form typical sigmoid type breakthrough curve. However, as mentioned before, smaller particle sizes cause important flow problems during column operations and pressure drop problems. Therefore, since

breakthrough capacities and exhaustion points are closer to each other, to minimize flow resistance and pressure drop problems, 35/60 mesh fraction of Na form of clinoptilolite zeolite was chosen as optimum particle size.

Abusafa (1995) for ammonium and cesium exchange and Tufan (2002) for ammonium exchange on clinoptilolite also determined the most suitable particle size range as 0.25 – 0.50 mm, (35/60 mesh size ASTM E-11), for the column systems, specifications of which previously tablulated in Table 4.2.

5.5 Effect of pH

Since it can influence the metal speciation, pH has an important effect on heavy metal removal by zeolites. Furthermore, pH should be high enough to prevent competition of H^+ ions with metal ions for the same exchange and it should also be acidic, since metal bearing wastewaters are usually acidic. Because of all these reasons, in ion exchange processes, observation of pH is important. In literature, for heavy metal clinoptilolite interactions, pH was adjusted to range around 4 – 7 and high removal efficiencies were obtained. pH ranges of previous studies are shown in Table 5.5.

Table 5.5 Some Cd^{2+} and Pb^{2+} Removal Studies and pH Ranges

Researcher	Study	pH
Curkovic and Stefanovic (1997)	Cd^{2+} and Pb^{2+} removal	4.5 – 7
Ouki and Kavannagh (1999)	Cd^{2+} and Pb^{2+} removal	4 – 5
Panayotova (2002)	Cd^{2+} removal	5 – 7
Singh et al. (2000)	Cd^{2+} removal	4.5 – 6
Ponizovsky and Tsadilas (2003)	Pb^{2+} removal	3 – 5
Bektaş and Kara (2004)	Pb^{2+} removal	2 – 7
Present Study	**Pb^{2+} and Cd^{2+} removal**	**4 – 6**

Table 5.5 presents pH values of ion exchange experiments were observed pH ranges between 4 and 6. Between these pH ranges, high removal efficiencies for Pb^{2+} and Cd^{2+} ions were obtained. Moreover, there was no precipitation phenomena observed during experiments. Considering these observations and previous studies, for all ions tested, it can be concluded that pH adjustment was not necessary and metal removal is independent of solution pH at observed pH range.

5.6 Continuous Column Experiments

Zeolites may be used for heavy metal removal processes to remove ions from solutions. There are mainly two methods to achieve this phenomenon. First method, the zeolite may be mixed with solution containing heavy metal ions and when the system reaches equilibrium zeolite particles are separated by filtration or sedimentation. This method is called also as batchwise separation technique. Second method, the solution that contains heavy metal ions may be passed through packed bed column in which packing material is zeolite particles. This method is called also as continuous column technique. Using second method, one should be aware of potential mass transfer limitations. The design of ion exchange process must consider residence time and mass transfer limitations. Therefore, column operations using clinoptilolite as packing material were conducted for both Pb^{2+} – Na^{+} and Cd^{2+} – Na^{+} binary systems and Pb^{2+} – Cd^{2+} – Na^{+} ternary system with different operating conditions (Table 4.3 and Table 4.4) in order to determine performance of zeolite under different operating conditions.

5.6.1 Pb^{2+} – Na^{+} and Cd^{2+} – Na^{+} Binary Systems Column Experiments

In this study, performance of Na enriched form of Gördes clinoptilolite for the removal of cadmium and lead ions was tested. A number of column runs were conducted to investigate ion exchange features of Gördes clinoptilolite and the

results were demonstrated by using breakthrough curves. They are suitable in order to calculate the equilibrium capacity of packed bed and column efficiencies since column efficiency is the ratio of breakthrough capacity to total capacity.

A breakthrough curve represents the effluent concentration versus effluent volume. The effluent concentration was expressed as normalized to inlet concentration (C/C_0) which means the ratio of the effluent concentration in treated water to initial influent cadmium or lead ion concentration.

Experiments were performed by using Pb^{2+} and Cd^{2+} ions solutions to investigate lead and cadmium exchange characteristics of Gördes type clinoptilolite. A number of column experiments were conducted under different loading conditions.

5.6.1.1 Effect of Flow Rate on Ion Exchange Capacity

The effect of three different flow rates, i.e. 5, 10, and 20 mL/min on the performance of Na form of Gördes type clinoptilolite for removal of Pb^{2+} ion with 0.005 N, 0.01 N, and 0.02 N initial concentrations are presented in Figures 5.4 – 5.6, respectively. The breakthrough capacities for those flow rates under the condition of influent Pb^{2+} concentration of 0.005 N are 0.65, 0.62, 0.38 meq/g, respectively. Figure 5.5 and Figure 5.6 give the relationship between the loading flow rate and breakthrough capacity using influent Pb^{2+} concentrations of 0.01 N and 0.02 N. The breakthrough capacities corresponding to the conditions of influent concentrations 0.01 N and 0.02 N are 0.65, 0.63, 0.30 meq/g and 0.56, 0.42, 0.27 meq/g at the influent flow rates 5, 10, and 20 mL/min, respectively.

Table 5.6 shows that, there is relatively significant difference in breakthrough capacities when flow rate was decreased from 20 mL/min to 10 mL/min.

However, there is only a slight increase in the breakthrough capacity when flow rate was decreased from 10 mL/min to 5 mL/min.

Under these experimental conditions, as it can be seen from results, increasing flow rates from 10 mL/min to 20 mL/min decreases Pb^{2+} ion removal efficiency of Na form of Gördes clinoptilolite.

Medvidovic et al. (2006) has also studied the effect of flow rate on the ion exchange capacity of clinoptilolite by using lead ion and concluded that reduction of flow rate enhances the lead removal efficiency.

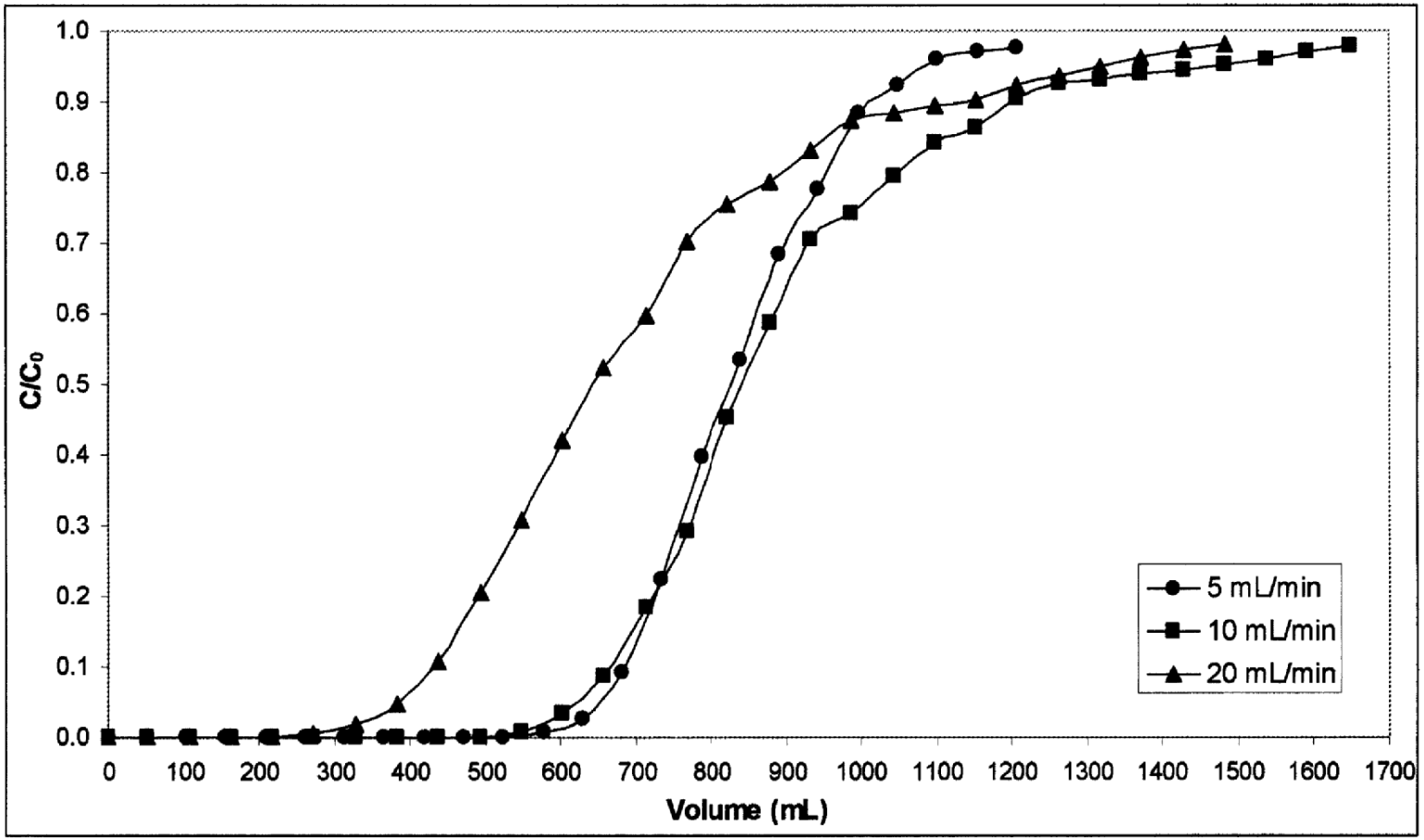

Figure 5.4 Effect of Flow Rate on the Column Performance of Na Formed Gördes Clinoptilolite, Particle Size 35/60 Mesh and Influent Pb^{2+} Concentration 0.005 N

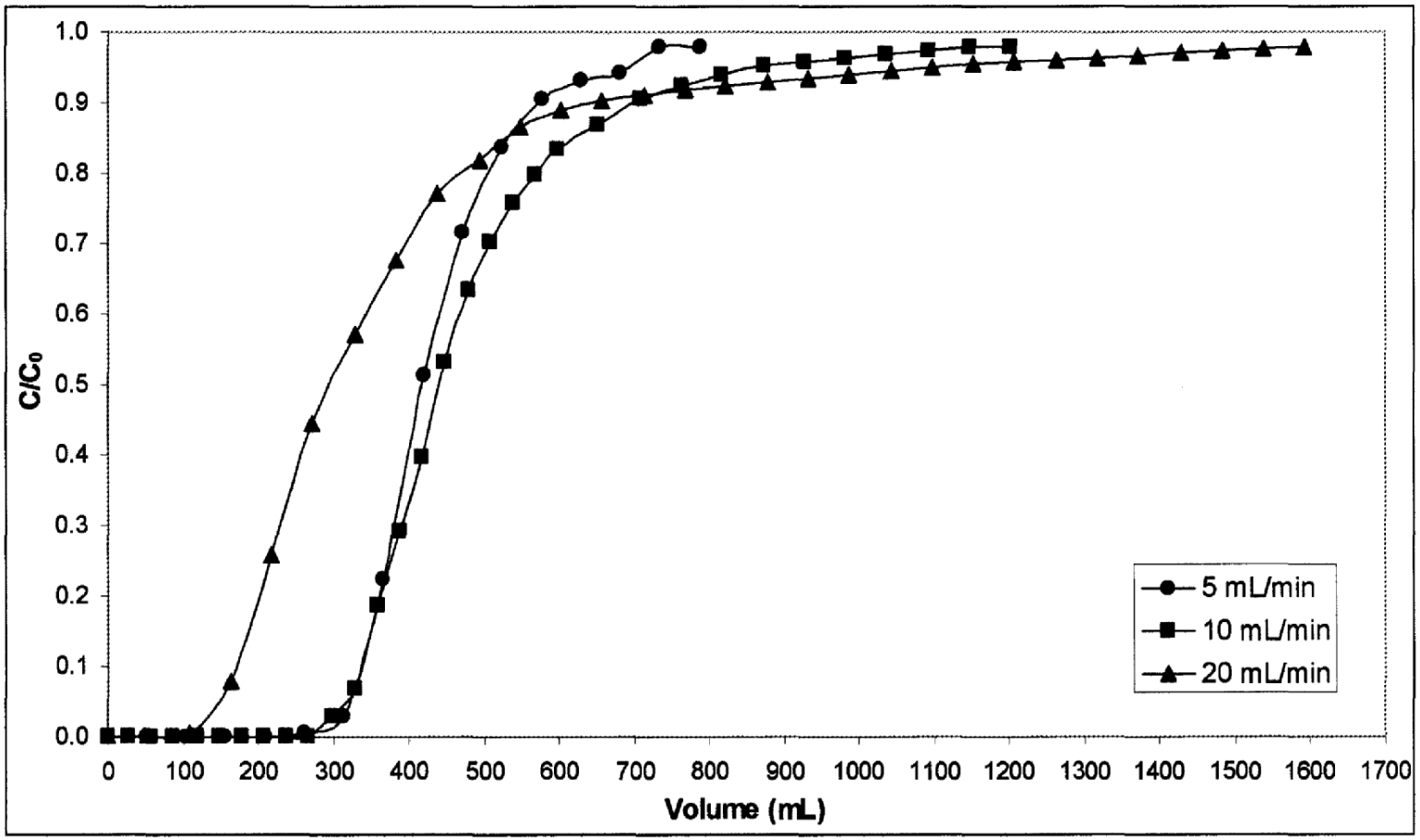

Figure 5.5 Effect of Flow Rate on the Column Performance of Na Formed Gördes Clinoptilolite, Particle Size 35/60 Mesh and Influent Pb^{2+} Concentration 0.01 N

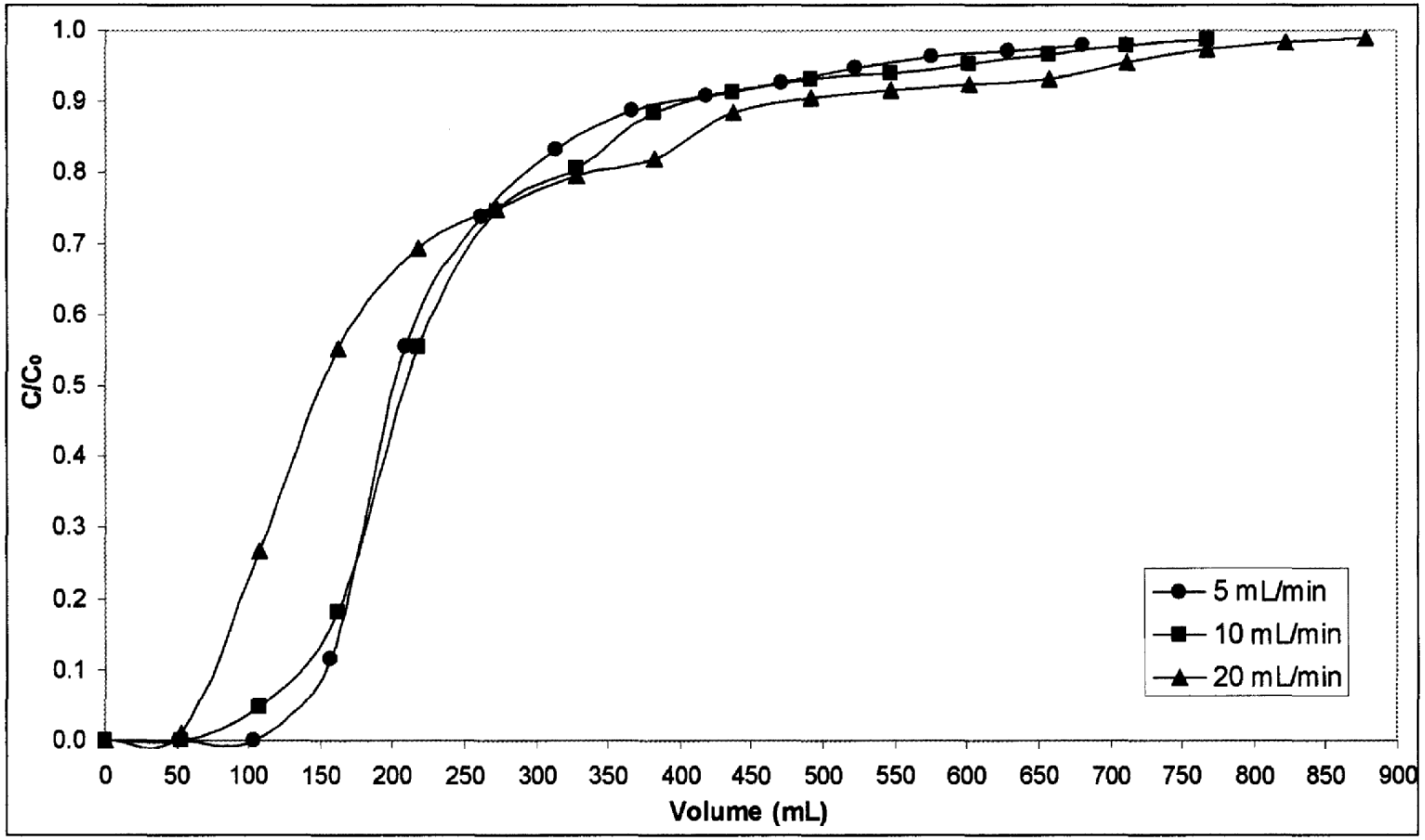

Figure 5.6 Effect of Flow Rate on the Column Performance of Na Formed Gördes Clinoptilolite, Particle Size 35/60 Mesh and Influent Pb^{2+} Concentration 0.02 N

In this study, also the effect of flow rate on cadmium ion removal performance was examined. For this purpose, three different flow rates, 5, 10, and 20 mL/min, were tested to treat 0.005 N, 0.01 N, and 0.02 N initial concentrations of Cd^{2+} ion solutions and the results are presented in Figures 5.7 – 5.9, respectively.

The breakthrough capacities for those flow rates, i.e., 5, 10, and 20 mL/min, under the condition of influent Cd^{2+} concentration 0.005 N are 0.28, 0.09, and 0.07 meq/g. At higher initial concentration levels, as it can be seen from Table 5.7, Figure 5.8, and Figure 5.9, heavy metal removal by continuous column operation is not applicable under the experimental conditions. Furthermore, there is higher difference in breakthrough capacities with changing flow rates.

Comparing Cd^{2+} and Pb^{2+} removal performances it may be seen that under the experimental conditions, Na form of Gördes type clinoptilolite has much higher removal rates for Pb^{2+} ion than Cd^{2+} ion.

Semmens and Seyfarth (1978) worked also on properties of near homoionic form of sodium clinoptilolite by lead and cadmium. And they concluded that near homoionic form of sodium clinoptilolite has affinity for both Pb^{2+} and Cd^{2+} ions.

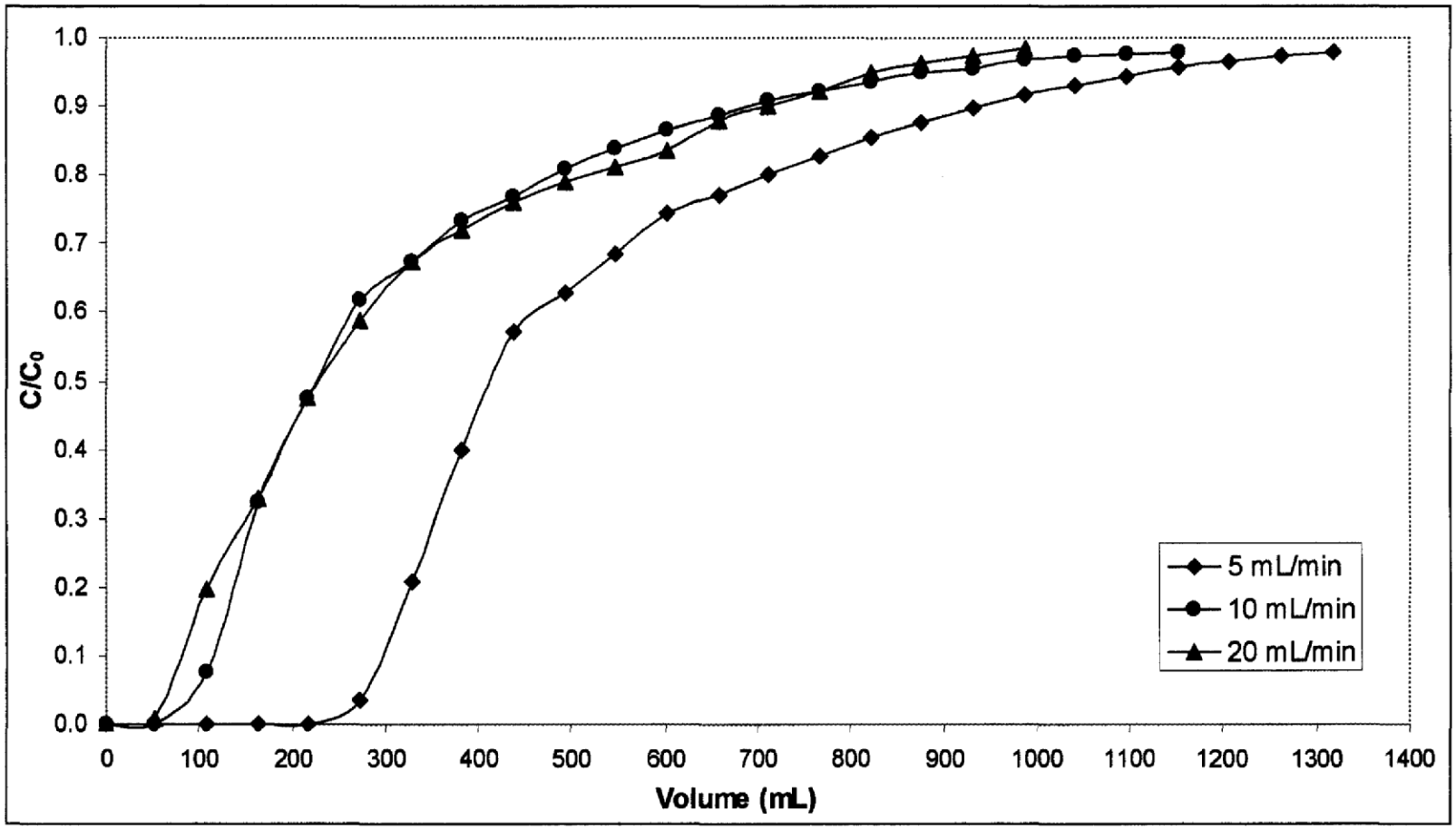

Figure 5.7 Effect of Flow Rate on the Column Performance of Na Formed Gördes Clinoptilolite, Particle Size 35/60 Mesh and Influent Cd^{2+} Concentration 0.005 N

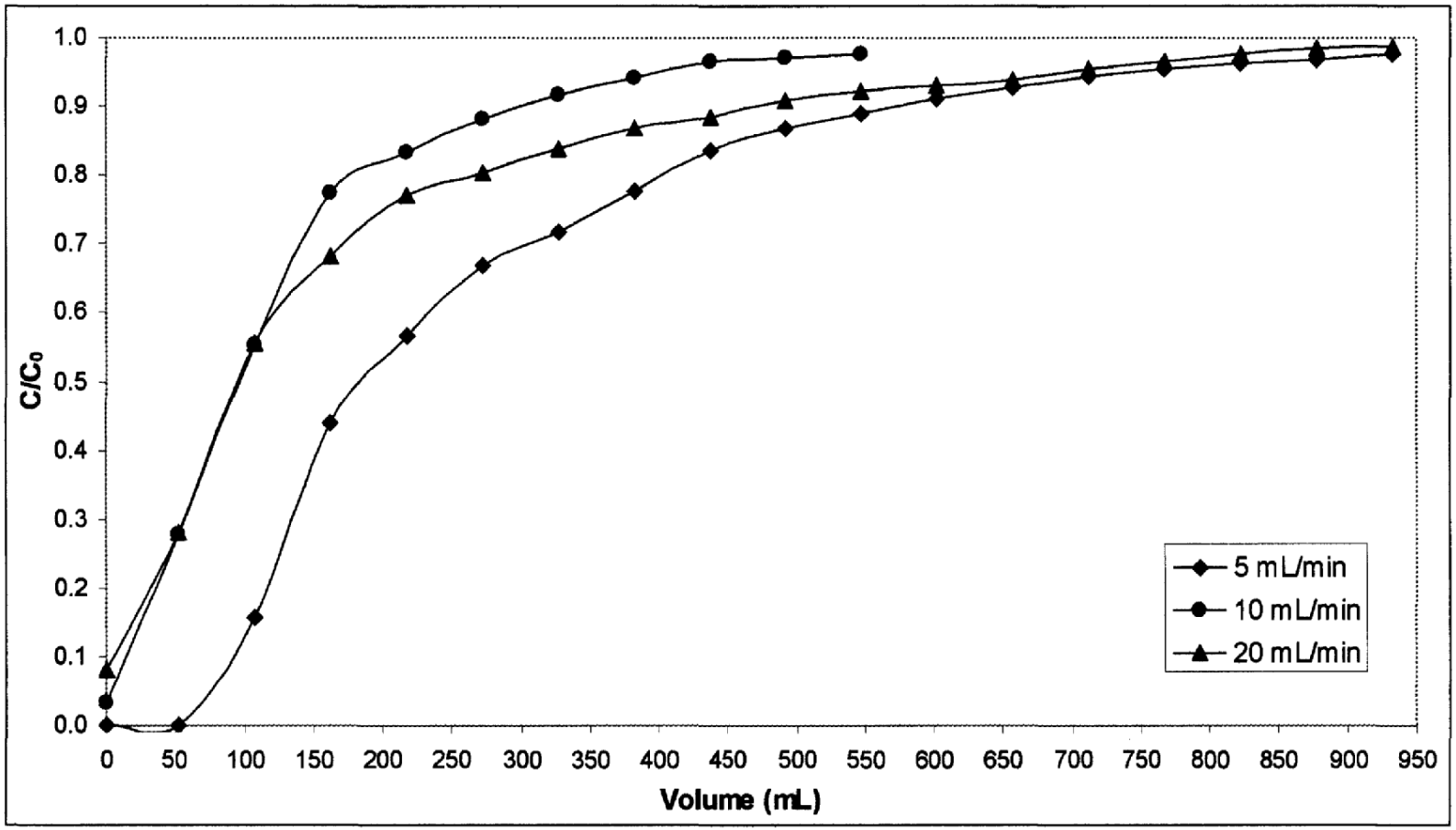

Figure 5.8 Effect of Flow Rate on the Column Performance of Na Formed Gördes Clinoptilolite, Particle Size 35/60 Mesh and Influent Cd^{2+} Concentration 0.01 N

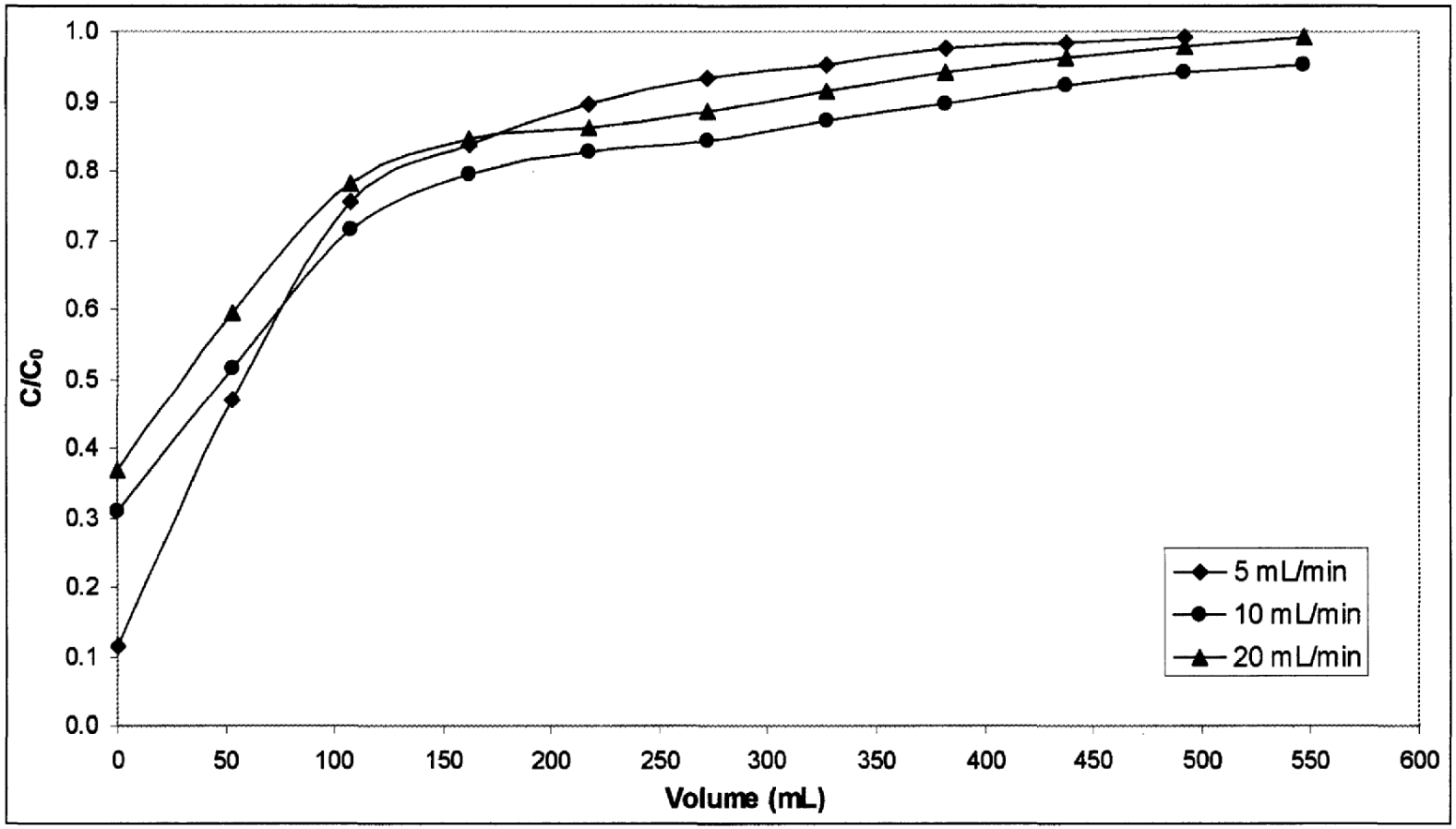

Figure 5.9 Effect of Flow Rate on the Column Performance of Na Formed Gördes Clinoptilolite, Particle Size 35/60 Mesh and Influent Cd^{2+} Concentration 0.02 N

5.6.1.2 Effect of Cd^{2+} and Pb^{2+} Concentrations on the Breakthrough Capacity

Breakthrough experiments with influent Cd^{2+} and Pb^{2+} concentrations varying between 0.005 N to 0.02 N were carried out to demonstrate the effect of the feed concentration on the breakthrough capacity. Breakthrough curves at flow rates 5, 10, and 20 mL/min are given in Figures 5.10 – 5.12 for lead (Pb^{2+}) ion and in Figures 5.13 – 5.15 for cadmium (Cd^{2+}) ion, respectively.

For lead (Pb^{2+}) ion, the shapes of breakthrough curves are sigmoid. With decreasing concentrations the curves shifted to higher treated solution volume values at breakthrough point as expected. Table 5.6 indicates that, at flow rate 5 mL/min, volume of solution that was treated up to breakthrough for 0.005 N, 0.01 N, and 0.02 N solutions are 646, 320, and 128 mL, respectively. At flow rate 10 mL/min, volume of solution that was treated up to breakthrough for 0.005 N, 0.01 N, and 0.02 N solutions are 607, 313, and 108 mL, respectively. Finally, at flow rate 20 mL/min, volume of solution that was treated up to breakthrough for 0.005 N, 0.01 N, and 0.02 N solutions are 383, 142, and 61 mL, respectively. Moreover, for the Pb^{2+} ion removal operation, breakthrough capacity of the clinoptilolite decreases with increasing influent concentration.

For cadmium ion, only at lower concentration levels, such as 0.005 N, the experimental data that obtained from column operation, form sigmoid shape breakthrough curve although the breakthrough capacity is low. At higher concentration levels, sigmoid shape breakthrough curve formations have not been observed. Table 5.7 shows that, for 0.005 N Cd^{2+} ion concentration, volume of solution that was treated up to breakthrough point for 5, 10, and 20 mL/min flow rates are 276, 87, and 64 mL, respectively.

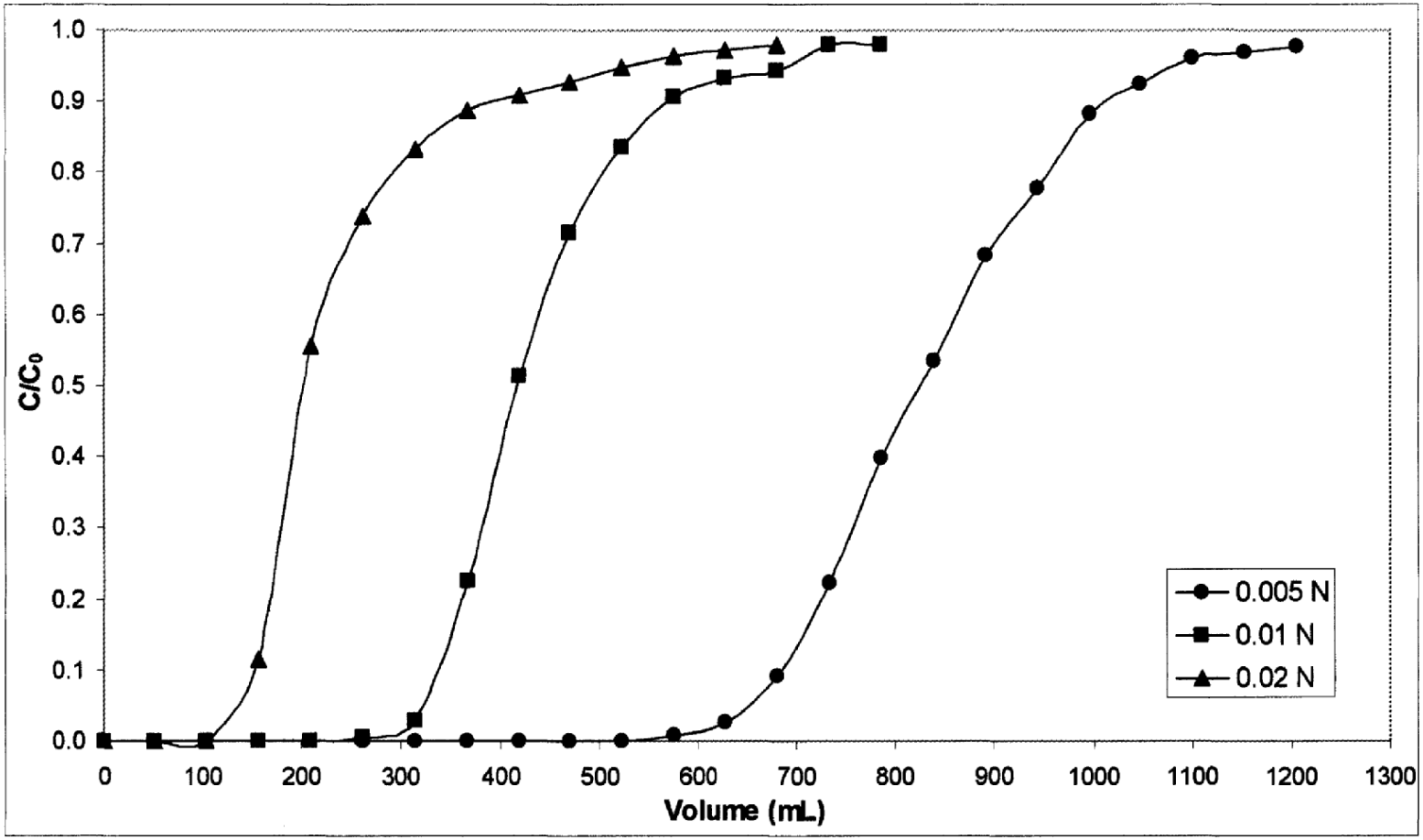

Figure 5.10 Effect of Influent Pb^{2+} Concentration on Breakthrough Curve, Particle Size 35/60 Mesh and Flow Rate 5 mL/min

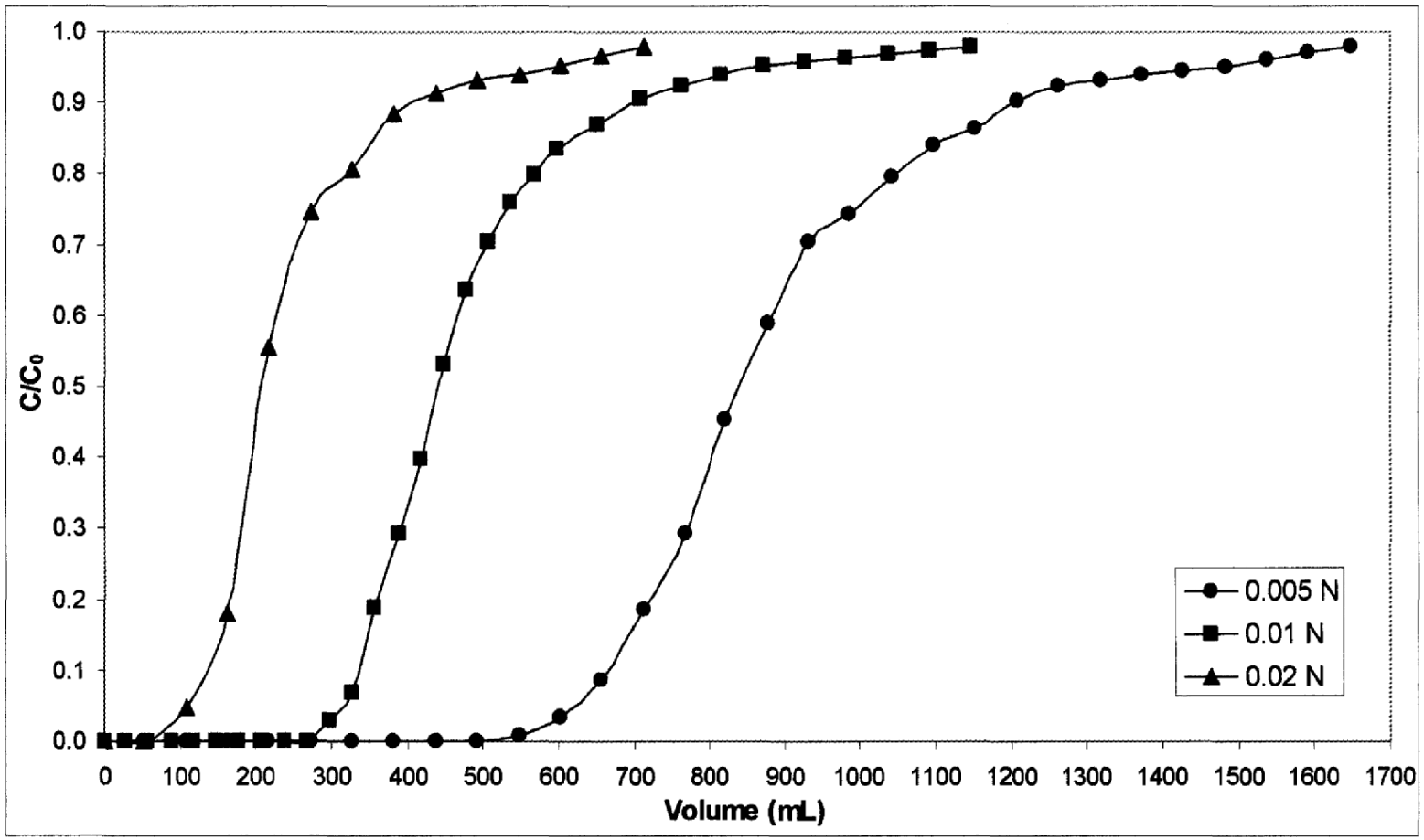

Figure 5.11 Effect of Influent Pb^{2+} Concentration on Breakthrough Curve, Particle Size 35/60 Mesh and Flow Rate 10 mL/min

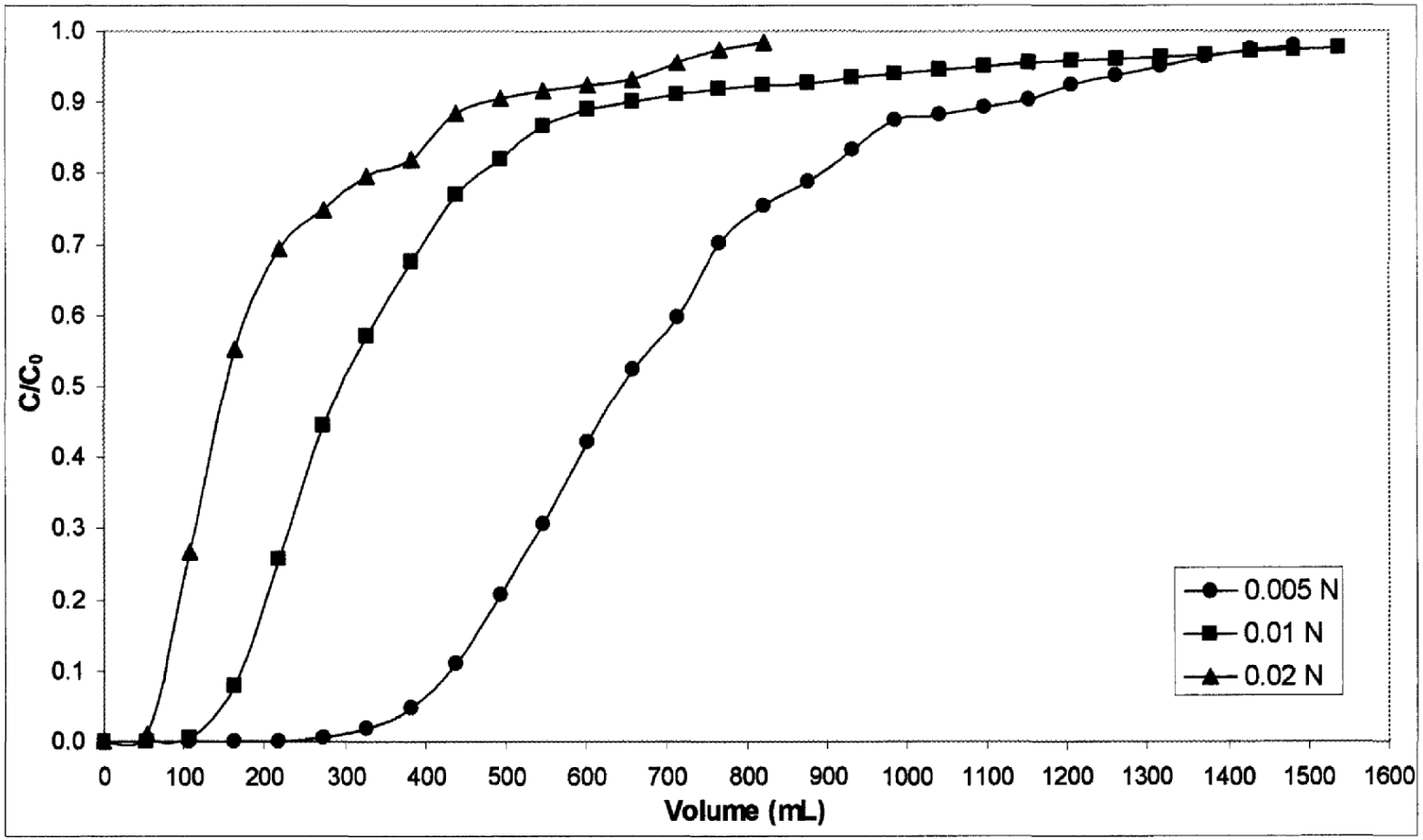

Figure 5.12 Effect of Influent Pb^{2+} Concentration on Breakthrough Curve, Particle Size 35/60 Mesh and Flow Rate 20 mL/min

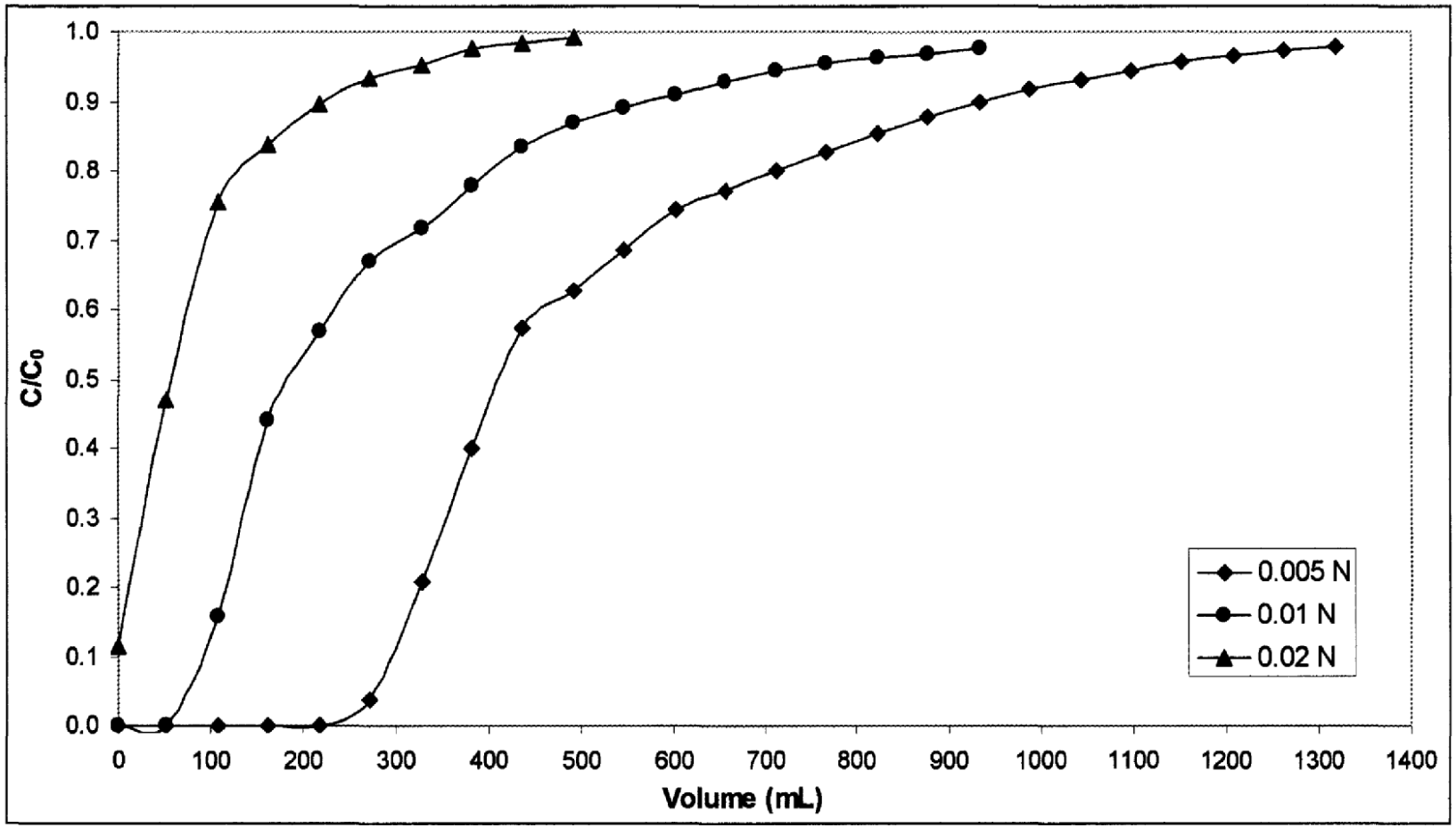

Figure 5.13 Effect of Influent Cd^{2+} Concentration on Breakthrough Curve, Particle Size 35/60 Mesh and Flow Rate 5 mL/min

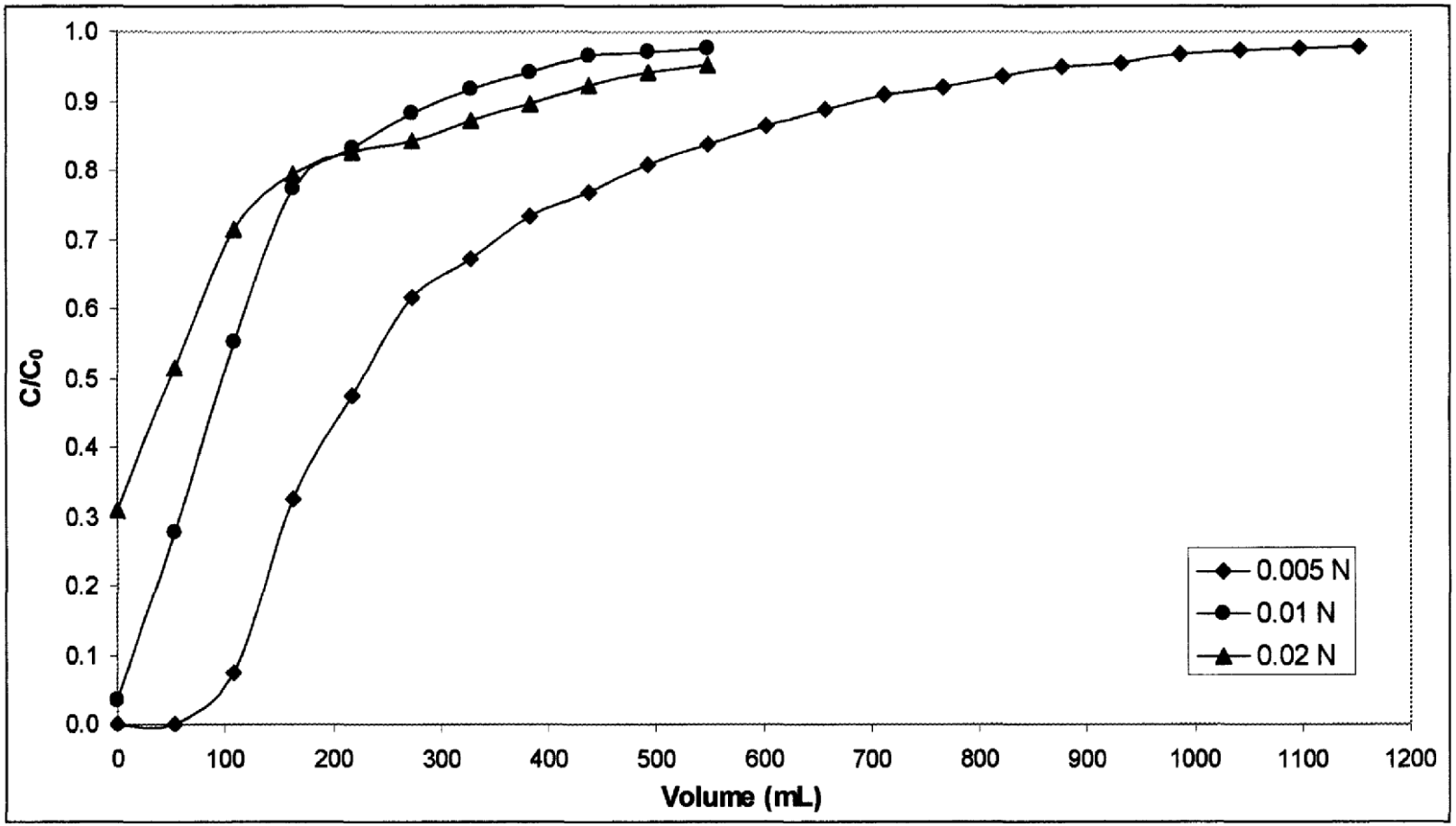

Figure 5.14 Effect of Influent Cd^{2+} Concentration on Breakthrough Curve, Particle Size 35/60 Mesh and Flow Rate 10 mL/min

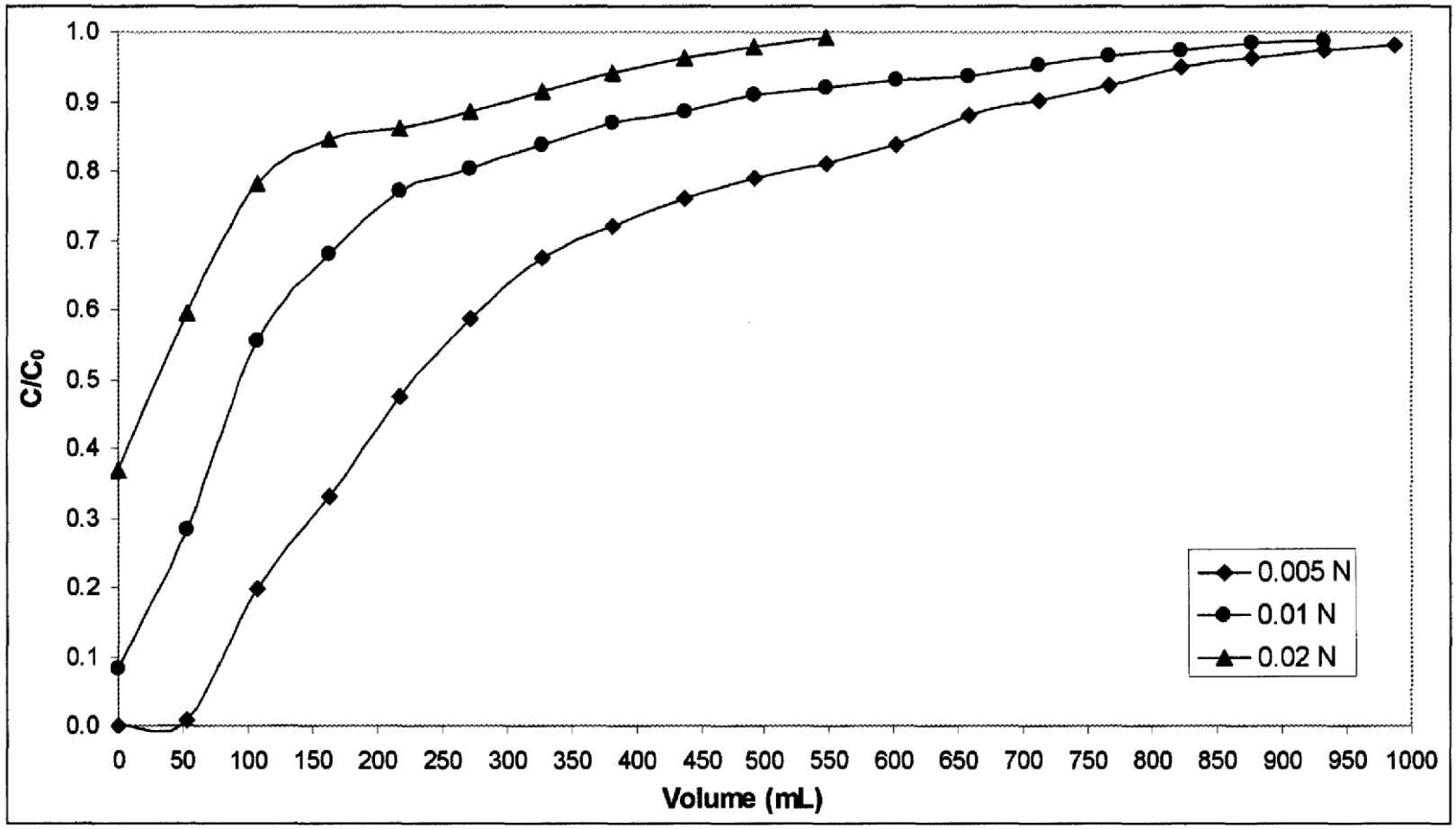

Figure 5.15 Effect of Influent Cd^{2+} Concentration on Breakthrough Curve, Particle Size 35/60 Mesh and Flow Rate 20 mL/min

Table 5.6 Pb^{2+} Ion Removal Performance of Na Form of Gördes Clinoptilolite

Exp. No	Process	Influent Pb^{2+} Conc. (N)	Influent Flow Rate (mL/min)	Particle Size (ASTM E-11)	Vol. of Effluent Treated at Breakthrough (mL)	Breakthrough Capacity (meq/g)	Total Capacity (meq/g)	Column Efficiency (%)
1	$Pb^{2+} - Na^{+}$ Exchange	0.005	5	35/60	646	0.65	0.84	77.4
2	$Pb^{2+} - Na^{+}$ Exchange	0.005	10	35/60	621	0.62	0.90	68.9
3	$Pb^{2+} - Na^{+}$ Exchange	0.005	20	35/60	383	0.38	0.71	53.5
4	$Pb^{2+} - Na^{+}$ Exchange	0.01	5	35/60	320	0.65	0.88	73.9
5	$Pb^{2+} - Na^{+}$ Exchange	0.01	10	35/60	313	0.63	0.98	64.3
6	$Pb^{2+} - Na^{+}$ Exchange	0.01	20	35/60	142	0.30	0.77	39.0
7	$Pb^{2+} - Na^{+}$ Exchange	0.02	5	35/60	128	0.56	0.97	57.7
8	$Pb^{2+} - Na^{+}$ Exchange	0.02	10	35/60	108	0.42	1.00	42.0
9	$Pb^{2+} - Na^{+}$ Exchange	0.02	20	35/60	61	0.27	0.90	30.0

Table 5.7 Cd^{2+} Ion Removal Performance of Na Form of Gördes Clinoptilolite

Exp. No	Process	Influent Pb^{2+} Conc. (N)	Influent Flow Rate (mL/min)	Particle Size (ASTM E-11)	Vol. of Effluent Treated at Breakthrough (mL)	Breakthrough Capacity (meq/g)	Total Capacity (meq/g)	Column Efficiency (%)
1	$Cd^{2+} - Na^{+}$ Exchange	0.005	5	35/60	276	0.28	0.52	53.8
2	$Cd^{2+} - Na^{+}$ Exchange	0.005	10	35/60	87	0.09	0.32	28.1
3	$Cd^{2+} - Na^{+}$ Exchange	0.005	20	35/60	64	0.07	0.31	22.6
4	$Cd^{2+} - Na^{+}$ Exchange	0.01	5	35/60	70	0.16	0.54	29.6
5	$Cd^{2+} - Na^{+}$ Exchange	0.01	10	35/60	4	0.01	0.26	3.8
6	$Cd^{2+} - Na^{+}$ Exchange	0.01	20	35/60	NA*	NA	0.33	NA
7	$Cd^{2+} - Na^{+}$ Exchange	0.02	5	35/60	NA	NA	0.34	NA
8	$Cd^{2+} - Na^{+}$ Exchange	0.02	10	35/60	NA	NA	0.44	NA
9	$Cd^{2+} - Na^{+}$ Exchange	0.02	20	35/60	NA	NA	0.55	NA

(*) NA: not applicable

5.6.2 Simultaneous Multicomponent Ion Exchange Column Experiments on Pb^{2+} – Cd^{2+} – Na^{+} Ternary System

Heavy metals are well known toxic materials and their disposals are significant industrial waste problem. Their amount in the environment not only increases day by day, but also since not biodegradable, they tend to accumulate in living organisms (Petrus et al., 2003). The probability of presence of cadmium and lead ions together are high. Therefore, determination of simultaneous removal of these ions from wastewaters is important. In industry simultaneous removal of heavy metals is very common application and ion exchange process is the one of them even if it may be difficult to perform and process maintenance is expensive. Hence, in order to reduce process costs, due to having higher selectivities for heavy metals, natural zeolites such as clinoptilolite hold great potential to remove heavy metal ions such as cadmium and lead from wastewaters.

To determine simultaneous removal of cadmium and lead performance of sodium form of Gördes clinoptilolite ternary column experiments were carried out. Main difference between binary and ternary column experiments was that, feed solution used in ternary system included two different ions Pb^{2+} and Cd^{2+} together. Solutions were prepared to form mixture of 50% Pb^{2+} – 50% Cd^{2+} of total normality. The experimental parameters of ternary ion exchange process in column were listed in Table 4.4 previously.

Breakthrough capacity and breakthrough point were determined with respect to ion that firstly emerged from column.

Since ions are exchanged with different strength, breakthrough curves become more complicated if several components which have to be removed simultaneously. Ion that zeolite has more affinity will be captured stronger than other ion. Therefore, at the outlet stream the weaker ion will breakthrough first.

Experiments were performed by using Pb^{2+} and Cd^{2+} mixture solutions to investigate simultaneous lead and cadmium exchange characteristics of Gördes type clinoptilolite. The loading conditions and ion removal performances, i.e. breakthrough capacities, total capacities, and column efficiencies, are presented in Table 5.8 and change of breakthrough property with respect to flow rate (5, 10, and 20 mL/min) demonstrated in Figures 5.16 – 5.18 for 50% Pb^{2+} – 50% Cd^{2+} of total normality mixture.

As it can be observed from the lead, cadmium, and sodium ternary system in Figures 5.16 – 5.18, cadmium ion was first detected in the effluent; so breakthrough capacity and breakthrough point were calculated with respect to Cd^{2+} ion. As apparent from the data, there was relatively significant difference between the behaviors in the breakthrough capacity when flow rate was increased.

Breakthrough curve results clearly show that the removal of ions is dependent on flow rate. Lower flow rate experiments yielded higher ion exchange capacities. At higher flow rates, the retention time was insufficient for the ion exchange to take place completely between zeolite and ions.

Breakthrough properties of each single ion, i.e., lead or cadmium, in multicomponent system decreased compared to the binary ion exchange experiment results. This phenomenon is evident to competition between lead and cadmium for ion exchange sites and this competition is in favor for lead ion. With this observation, it was concluded that the affinity of zeolite for lead ion is higher than that for cadmium ion in lead, cadmium, and sodium multicomponent column system and therefore selectivity sequence of clinoptilolite was determined as $Pb^{2+}>Cd^{2+}>Na^{+}$.

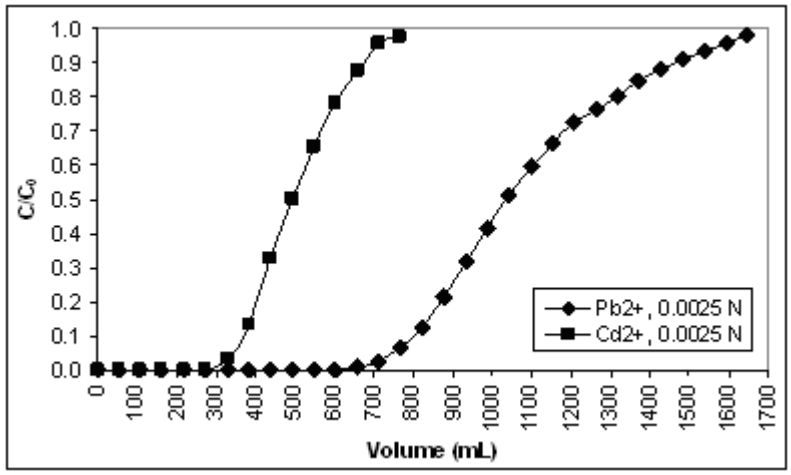

(a)

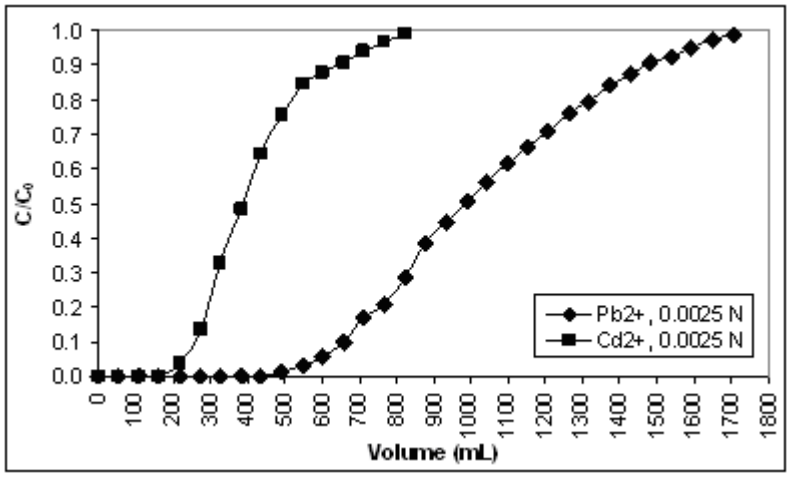

(b)

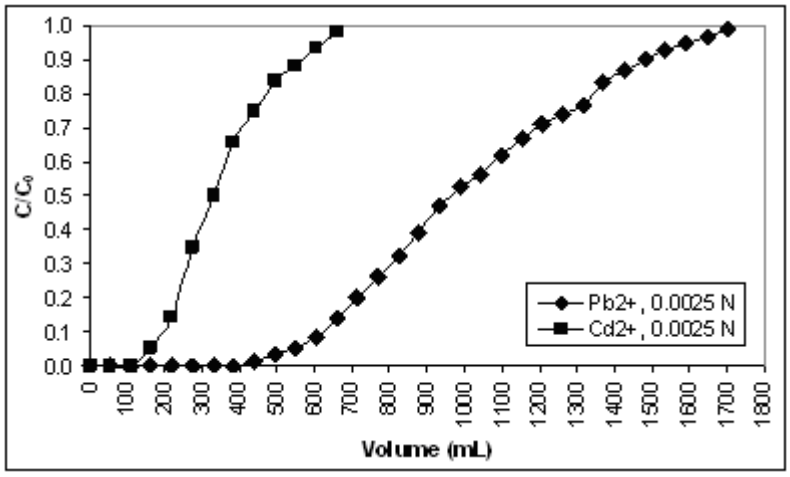

(c)

Figure 5.16 Breakthrough Curves for Simultaneous Removal of Lead and Cadmium for Total Concentration of 0.005 N (a) at 5 mL/min, (b) at 10 mL/min, and (c) at 20 mL/min

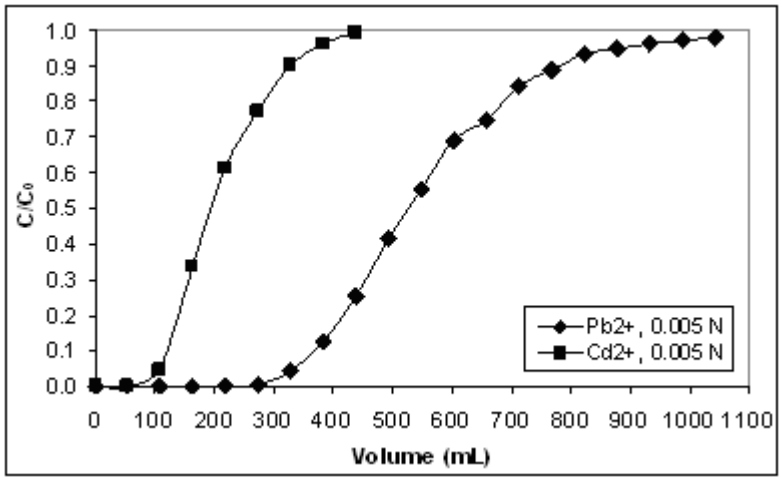

(a)

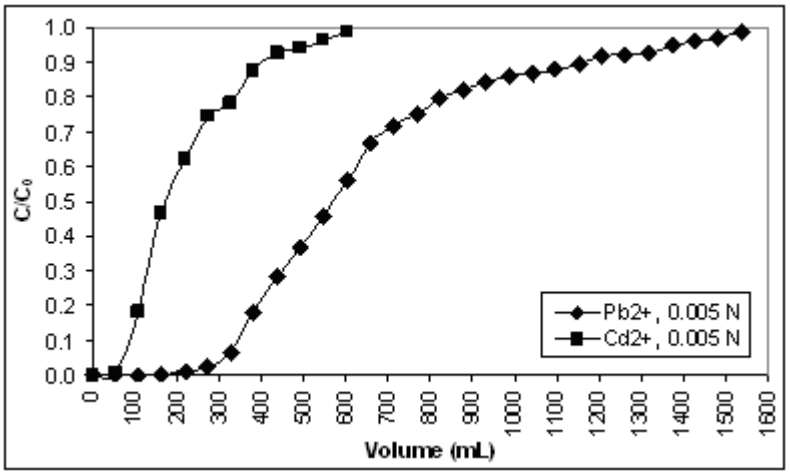

(b)

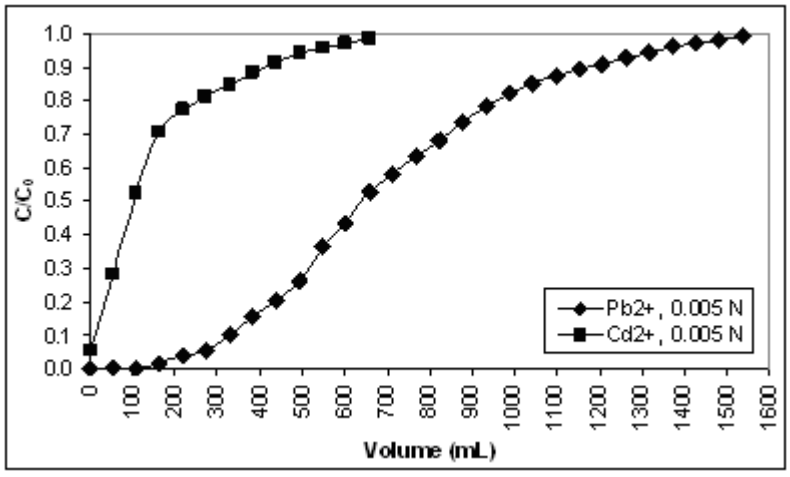

(c)

Figure 5.17 Breakthrough Curves for Simultaneous Removal of Lead and Cadmium for Total Concentration of 0.01 N (a) at 5 mL/min, (b) at 10 mL/min, and (c) at 20 mL/min

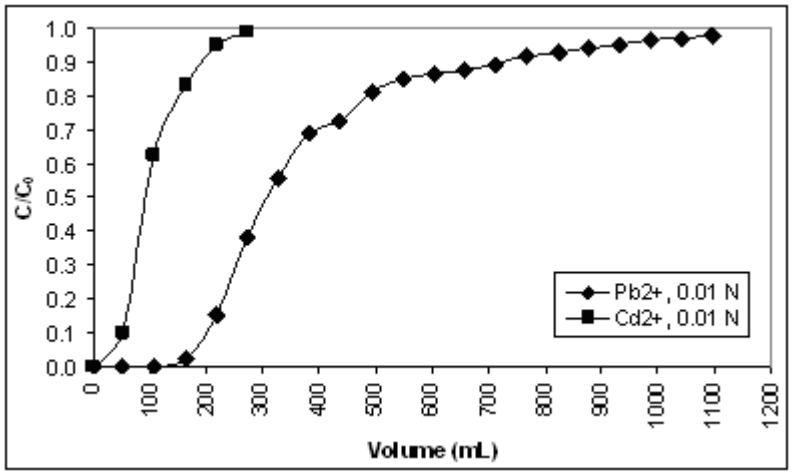

(a)

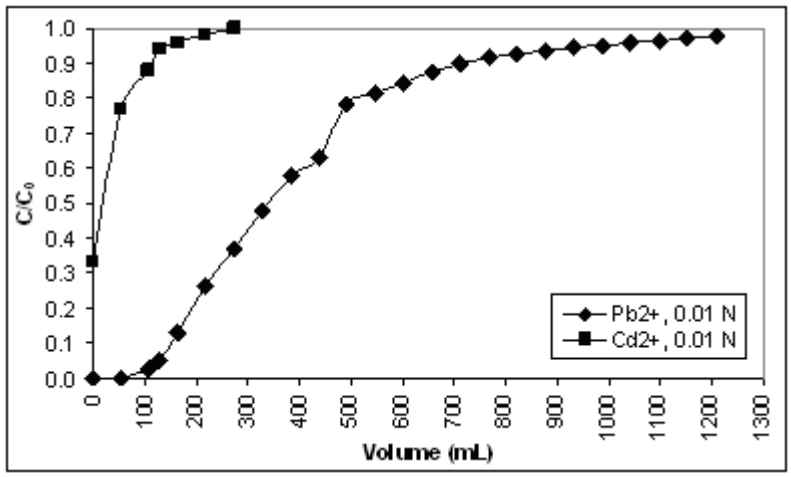

(b)

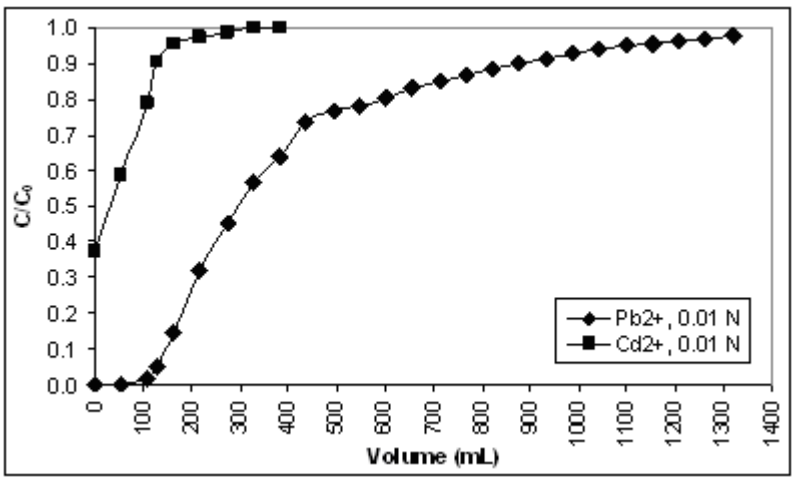

(c)

Figure 5.18 Breakthrough Curves for Simultaneous Removal of Lead and Cadmium for Total Concentration of 0.02 N (a) at 5 mL/min, (b) at 10 mL/min, and (c) at 20 mL/min

Table 5.8 Simultaneous Ion Exchange Performance of Na Form of Gördes Clinoptilolite

Exp. No	System	Total Normality (N)*	Influent Flow Rate (mL/min)	Particle Size (ASTM e-11)	Break. Cap. (meq/g)		Total Cap. (meq/g)	
					Pb^{2+}	Cd^{2+}	Pb^{2+}	Cd^{2+}
1	$Pb^{2+} - Cd^{2+} - Na^{+}$ Ternary System	0.005	5	35/60	0.37	0.18	0.54	0.25
2	$Pb^{2+} - Cd^{2+} - Na^{+}$ Ternary System	0.005	10	35/60	0.30	0.11	0.51	0.21
3	$Pb^{2+} - Cd^{2+} - Na^{+}$ Ternary System	0.005	20	35/60	0.27	0.08	0.51	0.18
4	$Pb^{2+} - Cd^{2+} - Na^{+}$ Ternary System	0.01	5	35/60	0.35	0.11	0.56	0.21
5	$Pb^{2+} - Cd^{2+} - Na^{+}$ Ternary System	0.01	10	35/60	0.32	0.07	0.65	0.22
6	$Pb^{2+} - Cd^{2+} - Na^{+}$ Ternary System	0.01	20	35/60	0.27	NA**	0.70	0.17
7	$Pb^{2+} - Cd^{2+} - Na^{+}$ Ternary System	0.02	5	35/60	0.37	0.07	0.77	0.21
8	$Pb^{2+} - Cd^{2+} - Na^{+}$ Ternary System	0.02	10	35/60	0.26	NA	0.79	0.08
9	$Pb^{2+} - Cd^{2+} - Na^{+}$ Ternary System	0.02	20	35/60	0.25	NA	0.80	0.12

(*) 50% of total normality consists of Pb^{2+} ions and the remaining is Cd^{2+} ions.
(**) NA: Not Applicable

Moreover, from Table 5.8 and Figures 5.16 – 5.18 it can be seen that increasing total ion concentration leads to decrease in breakthrough capacity and even not formation of breakthrough point for cadmium ion. However, for lead ion there is no such kind of properties. Breakthrough capacities for lead ion only slightly changes with increasing total normality which also proves selectivity of Na form of Gördes clinoptilolite for lead ion is higher than cadmium ion.

CHAPTER 6

CONCLUSIONS

This study demonstrated some important properties of pretreated, Na enriched form of Gördes type clinoptilolite for the lead and cadmium removal by applying binary and ternary ion exchange column operations. Based on the results of this study, the following conclusions were drawn:

- Maximum exchange level (MEL) of Na form of Gördes clinoptilolite, under the experimental conditions, was determined as nearly 1.08 meq/g. Although theoretical exchange capacity is much higher (2.14 meq/g).

- The particle size of clinoptilolite has significant effect on the breakthrough capacity and optimum particle size under experimental conditions was found as 35/60 US mesh.

- Breakthrough capacities of sodium enriched form of Gördes clinoptilolite for removal of lead and cadmium ions decreased with increasing flow rate from 5 mL/min to 20 mL/min both in binary and multicomponent column operations.

- Increasing influent concentration from 0.005 N to 0.02 N significantly decreases breakthrough capacity of Na enriched form of Gördes clinoptilolite for removal of lead and cadmium ions both in binary and multicomponent column operations.

- Clinoptilolite had more affinity to Pb^{2+} ion than Cd^{2+} ion when they were present together in multicomponent column systems. Hence, selectivity sequence for ternary system is the same as binary system, i.e., $Pb^{2+}>Cd^{2+}>Na^{+}$.

- Column studies indicate that sodium form of Gördes clinoptilolite is effective for simultaneous removal of lead and cadmium ions especially at low influent concentrations and flow rates. However, early breakthrough of Cd^{2+} significantly reduces the dynamic capacity of the clinoptilolite bed.

CHAPTER 7

RECOMMENDATIONS

For the further investigation the following studies can be recommended:

- Exhausted clinoptilolite can be regenerated so that performance of the regenerated clinoptilolite may be tested.

- Determination and optimization of regeneration conditions may be studied to improve ion exchange property of zeolite.

- Exchange behavior of both pretreated and as-received form of Gördes clinoptilolite can be examined for removal of heavy metals from an industrial wastewater.

- Continuous column pretreatment procedure may be enhanced and optimized to improve ion exchange property of the clinoptilolite zeolite.

REFERENCES

Aşiroğlu S., "Lead (II) and Ammonium Exchange on Na Form of Gördes Clinoptilolite", *MS Thesis*, METU, Ankara, (2006)

Bailey S.E., Olinb T.J., Brickab R.M., Adrian D.D., "A review of potentially low-cost sorbents for heavy metals", *Water Research*, 33, (1999), pp. 2469 – 2479

Bayraktaroğlu K., "Multicomponent Ion Exchange on Clinoptilolite", *MS Thesis*, METU, Ankara, (2006)

Bektaş N., Kara S., "Removal of Lead from Aqueous Solutions by Natural Clinoptilolite: Equilibrium and Kinetic Studies", *Separation and Purification Technology*, 39, (2004), pp. 189 – 200

Berber-Mendoza S., Leyva-Ramos R., Mendoza-Barron J., Guerrero-Coronado R.M., "Competitive exchange of lead (II) and cadmium (II) from aqueous solution on clinoptilolite", *Studies in Surface Science and Catalysis*, 142, (2002), pp. 1849 – 1856

Bhatia S., "Zeolite Catalysis; Principles and Applications", *CRC Press Inc.*, United States, (1990)

Blanchard G., Maunaye M., Martin G., "Removal of Heavy Metals from Waters by means of Natural Zeolites" *Water Research*, 18(12), (1984), pp. 1501 – 1507

Breck T.W., "Zeolites Molecular Sieves: Structure, Chemistry and Use", *John Wiley and Sons*, New York, (1974)

Castaldi P., Santona L., Enzo S., Melisa P., "Sorption processes and XRD analysis of a natural zeolite exchanged with Pb^{2+}, Cd^{2+} and Zn^{2+} cations", *Journal of Hazardous Materials*, 156, (2008), pp. 428 – 434

Cincotti A., Lai N., Orrù R., Cao G., "Sardinian Natural Clinoptilolites for Heavy Metals and Ammonium Removal: Experimental and Modeling", *Chemical Engineering Journal*, 84, (2001), pp. 275 – 282

Ćurković L., Cerjan - Stefanović Š., Filipan T., "Metal Ion Exchange by Natural and Modified Zeolites", *Water Res.*, 31(6), (1997), pp. 1379 – 1382

Çulfaz M., Yağız M., "Ion Exchange Properties of Natural Clinoptilolite: Lead – Sodium and Cadmium – Sodium Equilibria", *Separation and Purification Technology*, 37(2), (2004), pp. 93 – 105

Devlet Planlama Teskilatı (DPT), "Madencilik Özel İhtisas Komisyonu Endüstriyel Hammaddeler Alt Komisyonu - Diğer Endüstri Mineralleri Çalışma Grubu Raporu", (1996), http://ekutup.dpt.gov.tr/madencil/sanayiha/oik480c1.pdf (Accessed date: April 05, 2010)

El Akrami H.A., "Column Studies of Ammonium Ion Exchange on Clinoptilolite", *MS Thesis*, METU, Ankara, (1991)

Faghihian H., Marageh M.G., Kazemian H. "The Use of Clinoptilolite and Its Sodium Form for Removal of Cesium and Strontium from Nuclear Wastewater and Pb^{2+}, Ni^{2+}, Cd^{2+}, Ba^{2+} from Municipal Wastewater", *Applied Radiation and Isotopes*, 50, (1999), pp. 655 – 660

Gedik K., "Cadmium Removal Using Clinoptilolite: Influence of Conditioning and Regeneration", *MS Thesis*, METU, Ankara, (2006)

Gül Ö., "Exchanges of Strontium on Clinoptilolite Zeolite", *MS Thesis*, METU, Ankara, (2003)

Güray Ş., "Removal of Lead from Water by Natural Clinoptilolite", *MS Thesis*, METU, Ankara, (1997)

Haralambous A., Maliou E., Malamis M., "The Use of Zeolite for Ammonium Uptake", *Water Science Tech.*, (1992), pp. 139 – 145

Inglezakis V.J., Loizidou M.D., Grigoropoulou H.P., "Ion exchange of Pb^{2+}, Cu^{2+}, Fe^{3+}, and Cr^{3+} on natural clinoptilolite: selectivity determination and influence of acidity on metal uptake", *Journal of Colloid and Interface Science,* 261, (2003), pp. 49 – 54

Inglezakis V.J., Loizidou M.D., Grigoropoulou H.P., "Ion Exchange Studies on Natural and Modified Zeolites and the Concept of Exchange Site Accessibility", *Journal of Colloid and Interface Science,* 275, (2004), 570 – 576

Inglezakis V.J., "The concept of capacity in zeolite ion exchange systems", *Journal of Colloid and Interface Science,* 281, (2005), pp. 68 – 79

Jama M.A., "Equilibrium study of ammonium ion exchange by clinoptilolite", *MS Thesis,* METU, Ankara, (1988)

Koyama K., Takeuchi Y., "Clinoptilolite: The Distribution of Potassium Atoms and Its Role in Thermal Stability", *Zeitschrift Fur Kristallographie,* Vol. 145, (1977), pp. 216 – 249

Langella A., Pansini M., Cappelletti P., Gennaro B., Gennaro M., Colella C., "NH_4^+, Cu^{2+}, Zn^{2+}, Cd^{2+} and Pb^{2+} Exchange for Na^+ in a Sedimentary Clinoptilolite, North Sardinia, Italy", *Microporous and Mesoporous Materials,* 37, (2000), pp. 337 – 343

Loizidou M., Townsend R.P., *Zeolites,* 7, (1987), p153

Malliou E., Loizidou M., Spyrellis N., "Uptake of Lead and Cadmium by Clinoptilolite", *The Science of the Total Environment,* 149, (1994), 139 – 144

Malliou E., Malamis M., Sakellarides P.O., "Lead and Cadmium Removal by Ion Exchange", *Water Science Tech.,* (1992), pp. 133 – 138

Medvidovic N., Peric J., Trgo M.J., "Column performance in lead removal from aqueous solutions by fixed bed of natural zeolite clinoptilolite", *Separation and Purification Technology,* 49, (2006), pp. 237 – 244

Medvidović N.V., Perić J., Trgo M., Mužeka M.N., "Removal of lead ions by fixed bed of clinoptilolite – The effect of flow rate", *Microporous and Mesoporous Materials*, 105, (2007), pp. 298 – 304

Merkle A.B., Slaughter M., "Determination and Refinement of the Structure of Heulandite" *Am. Min.*, 53, (1968), pp.1120 – 1138

Mier M.V., Callejasa R.L., Gehr R., Cisneros B.E.J., Alvarez P.J.J., "Heavy metal removal with Mexican clinoptilolite: multi-component ionic exchange", *Water Research*, 35, (2001), pp. 373 – 378

Mumpton F.A., "Clinoptilolite Redefined", *Am. Min.*, 47, (1960), pp. 351 – 369

O'Connor J.F., Townsend R.P., "Exchange of lead (II) ions in synthetic faujasitic zeolites: The effect of framework charge", *Zeolites*, 5, (1985), pp. 158 – 164

Oren A.H., Kaya A., "Factors affecting adsorption characteristics of Zn^{2+} on two natural zeolites", *Journal of Hazardous Materials*, 131, (2006), pp. 59 – 65

Ouki S.K., Kavannagh M., "Treatment of Metals Contaminated Wastewaters by Use of Natural Zeolites", *Water Science and Technology*, 39, (1999), pp. 115 – 122

Panayotova M., Velikov B., "Kinetics of Heavy Metal Ions Removal by Use of Natural Zeolite" *Journal of Env. Sci. and Health*, A37(2), (2002), pp. 139 – 147

Panday K.K., Prasada G., Singha V.N., "Copper (II) removal from aqueous solutions by fly ash", *Water Research*, 19, (1985), pp. 869 – 873

Petrus R., Warchol J., "Heavy metal removal by clinoptilolite. An equilibrium study in multi-component systems", *Water Research*, 39, (2005), pp. 819 – 830

Petrus R., Warchol J., "Ion exchange equilibria between clinoptilolite and aqueous solutions of Na^{+}/Cu^{2+}, Na^{+}/Cd^{2+}, and Na^{+}/Pb^{2+}", *Microporous and Mesoporous Materials*, 61, (2003), pp. 137 – 146

Ponizovsky A.A., Tsadilas C.D., "Lead (II) Retention by Alfisol and Clinoptilolite: Cation Balance and pH effect", Geoderma, 115, (2002), pp. 303 – 312

Sand L.B., Mumpton F.A., "Natural Zeolites: Occurrence, Properties, Use", *Pergamon Press*, Oxford, UK, (1978), pp. 135 – 350

Schlenker J.L., 9th International Zeolite Conference, I, (1993), 3

Semmens M.J., Seyfarth M., "Natural Zeolites, Occurence, Properties and Use", *Pergamon Press*, New York, (1978)

Semmens M.J., Martin W.P., "The influence of pretreatment on the capacity and selectivity of clinoptilolite for metal ions", *Water Research*, 22, (1988), pp. 537 – 542

Teutli-Sequeira A., Solache-Ríos M., Olguín M.T., "Influence of Na^+, Ca^{2+}, Mg^{2+}, and NH_4^+ on the sorption behavior of Cd^{2+} from aqueous solutions by a Mexican zeolitic material", *Hydrometallurgy*, 97, (2009), pp. 46 – 52

Townsend R.P., Bekkum H., Flanigen, E.M., and Jansen, J.C., "Ion Exchange in Zeolites", *Introduction to Zeolite Science and Practice*, 15, pp. 359 – 390

Tsitsishvili G.V., Andronikashvili T.G, Kirov G.N., Filizova L.D., "Natural Zeolites", *Ellis Horwood Limited*, London, (1992)

Tufan E.Ö., "Ion Exchange Properties of Gördes Clinoptilolite: Ammonium Exchange", *MS Thesis*, METU, Ankara, (2002)

Yücel H., Çulfaz A., Ural A.T., Abusafa A., "Türkiye'nin doğal zeolit kaynaklarının teknolojik değerlendirmesi", METU, Ankara, (1995)

APPENDIX A

SAMPLE CALCULATION FOR DETERMINATION OF BREAKTHROUGH CAPACITY AND COLUMN EFFICIENCY BY USING BREAKTHROUGH CURVE

Experimental Parameters

Influent Pb^{2+} Concentration: 0.005 N
Flow Rate: 10 mL/min
Particle Size: 35/60 US Mesh
Packing Material: Sodium Form of Gördes Type Clinoptilolite
Amount of Zeolite: 5.0 g

Sampling

Samples were taken after every 50 mL of effluent of the column. Every sample was 5 mL, which was divided by 2 and measured data point assumed to read at that point.

Calculation Procedure

1. Experimental breakthrough curve (Figure A.1) was obtained by plotting normalized lead ion concentration (C/C_0) versus effluent volume where the data were taken from Table A.1.

2. For estimation of breakthrough and total capacity of clinoptilolite, numerical integration was performed by using combination of Simpson's 1/3 and 3/8 Rule.

Table A.1 Data Obtained from Lead Removal under the Experimental Conditions

Eff. Volume (mL)	**C (mg/L)**	**C/C_0**
0	0.00	0.00
52.5	0.00	0.00
107.5	0.00	0.00
162.5	0.00	0.00
217.5	0.00	0.00
272.5	0.00	0.00
327.5	0.00	0.00
382.5	0.00	0.00
437.5	0.00	0.00
492.5	0.00	0.00
547.5	4.52	0.01
602.5	18.13	0.03
657.5	45.69	0.09
712.5	96.81	0.18
767.5	153.54	0.29
822.5	237.40	0.45
877.5	308.35	0.59
932.5	369.98	0.71
987.5	389.78	0.74
1042.5	417.54	0.80
1097.5	441.25	0.84
1152.5	452.82	0.86
1207.5	474.22	0.90
1262.5	485.20	0.93
1317.5	489.25	0.93
1372.5	492.39	0.94
1427.5	495.04	0.94
1482.5	499.12	0.95
1537.5	504.24	0.96
1592.5	509.73	0.97
1647.5	512.96	0.98
1702.5	515.42	0.98
1757.5	518.06	0.99
1812.5	520.69	0.99
1867.5	519.34	0.99
1922.5	521.76	0.99

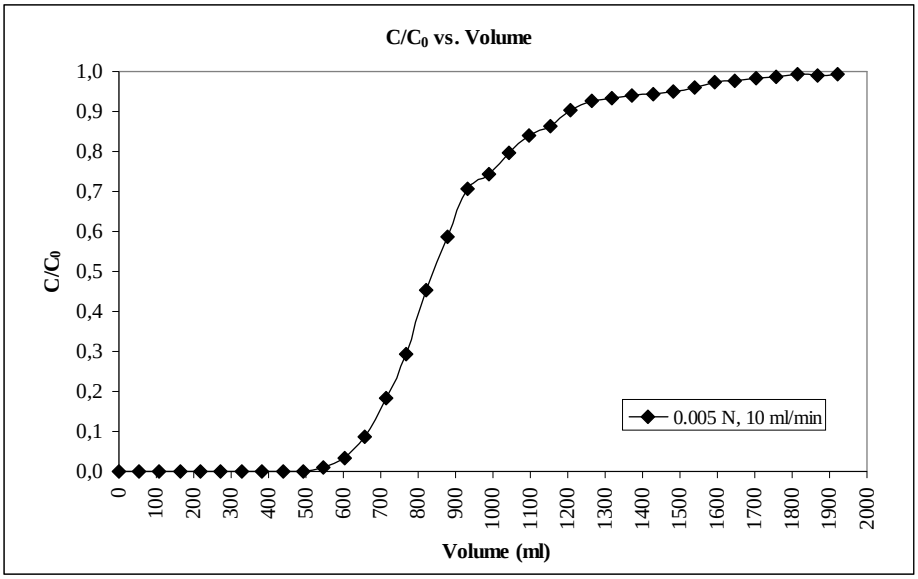

Figure A.1 Breakthrough Curve for Influent Pb^{2+} Concentration of 0.005 N and Flow Rate 10 mL/min

Breakthrough Capacity (Q_B)

Total Area = 620.83 mL

Area under the Curve = 1.97 mL (from Simpson's Rule)

Area above Curve = 620.83 – 1.97 = 618.86 mL

$$Q_B = (618.86mL)\times\left(\frac{5meq}{L}\right)\times\left(\frac{1L}{1000mL}\right)\times\left(\frac{1}{5g_{zeolite}}\right) = 0.62\,meq/g_{zeolite}$$

Total Capacity (Q_T)

Total Area = 1647.50 mL

Area under the Curve = 747.17 mL (from Simpson's Rule)

Area above Curve = 1647.50 – 747.17 = 900.33 mL

$$Q_T = (900.33mL)\times\left(\frac{5meq}{L}\right)\times\left(\frac{1L}{1000mL}\right)\times\left(\frac{1}{5g_{zeolite}}\right) = 0.90\,meq/g_{zeolite}$$

Column Efficiency

$$\eta_c = \frac{0.62}{0.90} = 0.689 \rightarrow 68.9\%$$

APPENDIX B

EXPERIMENTAL DATA FOR Pb^{2+} – Na^{+} BINARY SYSTEM

Table B.1 Experimental Data for Influent Pb^{2+} Concentration of 0.005 N and Flow Rate of 5 mL/min at 25 °C

Eff. Volume (mL)	C (mg/L)	C/C_0
0.00	0.00	0.00
51.25	0.00	0.00
103.75	0.00	0.00
156.25	0.00	0.00
208.75	0.00	0.00
261.25	0.00	0.00
313.75	0.00	0.00
366.25	0.00	0.00
418.75	0.00	0.00
471.25	0.00	0.00
523.75	0.00	0.00
576.25	4.02	0.01
628.75	14.62	0.03
681.25	48.79	0.09
733.75	118.61	0.22
786.25	211.37	0.40
838.75	284.80	0.54
891.25	363.98	0.68
943.75	413.15	0.78
996.25	469.99	0.88
1048.75	491.06	0.92
1101.25	510.86	0.96
1153.75	515.96	0.97
1206.25	519.16	0.98
1258.75	527.46	0.99

Table B.2 Experimental Data for Influent Pb^{2+} Concentration of 0.005 N and Flow Rate of 10 mL/min at 25 °C

Eff. Volume (mL)	**C (mg/L)**	**C/C_0**
0.0	0.00	0.00
52.5	0.00	0.00
107.5	0.00	0.00
162.5	0.00	0.00
217.5	0.00	0.00
272.5	0.00	0.00
327.5	0.00	0.00
382.5	0.00	0.00
437.5	0.00	0.00
492.5	0.00	0.00
547.5	4.52	0.01
602.5	18.13	0.03
657.5	45.69	0.09
712.5	96.81	0.18
767.5	153.54	0.29
822.5	237.40	0.45
877.5	308.35	0.59
932.5	369.98	0.71
987.5	389.78	0.74
1042.5	417.54	0.80
1097.5	441.25	0.84
1152.5	452.82	0.86
1207.5	474.22	0.90
1262.5	485.20	0.93
1317.5	489.25	0.93
1372.5	492.39	0.94
1427.5	495.04	0.94
1482.5	499.12	0.95
1537.5	504.24	0.96
1592.5	509.73	0.97
1647.5	512.96	0.98
1702.5	515.42	0.98
1757.5	518.06	0.99
1812.5	520.69	0.99
1867.5	519.34	0.99
1922.5	521.76	0.99

Table B.3 Experimental Data for Influent Pb^{2+} Concentration of 0.005 N and Flow Rate of 20 mL/min at 25 °C

Eff. Volume (mL)	**C (mg/L)**	**C/C_0**
0.0	0.00	0.00
52.5	0.00	0.00
107.5	0.00	0.00
162.5	0.00	0.00
217.5	0.00	0.00
272.5	2.12	0.00
327.5	9.11	0.02
382.5	24.01	0.05
437.5	54.78	0.11
492.5	103.66	0.21
547.5	154.95	0.31
602.5	212.51	0.42
657.5	263.94	0.52
712.5	301.17	0.60
767.5	353.96	0.70
822.5	380.15	0.75
877.5	396.65	0.79
932.5	419.57	0.83
987.5	440.30	0.87
1042.5	445.21	0.88
1097.5	450.49	0.89
1152.5	454.98	0.90
1207.5	465.50	0.92
1262.5	472.13	0.94
1317.5	479.04	0.95
1372.5	486.08	0.96
1427.5	490.50	0.97
1482.5	494.23	0.98
1537.5	498.56	0.99
1592.5	502.77	1.00

Table B.4 Experimental Data for Influent Pb^{2+} Concentration of 0.01 N and Flow Rate of 5 mL/min at 25 °C

Eff. Volume (mL)	**C (mg/L)**	**C/C_0**
0.00	0.00	0.00
51.25	0.00	0.00
103.75	0.00	0.00
156.25	0.00	0.00
208.75	0.00	0.00
261.25	6.83	0.01
313.75	30.37	0.03
366.25	241.35	0.22
418.75	551.35	0.51
471.25	767.08	0.71
523.75	897.09	0.84
576.25	971.11	0.90
628.75	999.83	0.93
681.25	1012.23	0.94
733.75	1050.19	0.98
786.25	1051.77	0.98
838.75	1050.19	0.98

Table B.5 Experimental Data for Influent Pb^{2+} Concentration of 0.01 N and Flow Rate of 10 mL/min at 25 ℃

Eff. Volume (mL)	**C (mg/L)**	**C/C_0**
0.0	0.00	0.00
27.5	0.00	0.00
57.5	0.00	0.00
87.5	0.00	0.00
117.5	0.00	0.00
147.5	0.00	0.00
177.5	0.00	0.00
207.5	0.00	0.00
237.5	0.00	0.00
267.5	0.00	0.00
297.5	29.71	0.03
327.5	72.40	0.07
357.5	198.02	0.19
387.5	309.47	0.29
417.5	418.79	0.40
447.5	560.07	0.53
477.5	670.51	0.64
507.5	741.71	0.70
537.5	800.58	0.76
567.5	842.06	0.80
597.5	880.19	0.83
652.5	917.19	0.87
707.5	955.31	0.91
762.5	975.87	0.92
817.5	991.01	0.94
872.5	1006.15	0.95
927.5	1011.19	0.96
982.5	1016.75	0.96
1037.5	1022.97	0.97
1092.5	1027.60	0.97
1147.5	1032.28	0.98
1202.5	1034.01	0.98

Table B.6 Experimental Data for Influent Pb^{2+} Concentration of 0.01 N and Flow Rate of 20 mL/min at 25 °C

Eff. Volume (mL)	**C (mg/L)**	**C/C_0**
0.0	0.00	0.00
52.5	0.00	0.00
107.5	4.90	0.00
162.5	77.93	0.08
217.5	256.27	0.26
272.5	443.89	0.44
327.5	569.73	0.57
382.5	674.66	0.68
437.5	769.78	0.77
492.5	817.17	0.82
547.5	865.55	0.87
602.5	887.78	0.89
657.5	900.18	0.90
712.5	909.73	0.91
767.5	916.91	0.92
822.5	922.17	0.92
877.5	926.66	0.93
932.5	932.56	0.93
987.5	939.45	0.94
1042.5	943.14	0.94
1097.5	949.85	0.95
1152.5	953.43	0.95
1207.5	956.09	0.96
1262.5	959.72	0.96
1317.5	962.64	0.96
1372.5	965.31	0.97
1427.5	968.74	0.97
1482.5	972.03	0.97
1537.5	975.32	0.98
1592.5	977.67	0.98
1647.5	980.31	0.98
1702.5	982.75	0.98
1757.5	983.44	0.98

Table B.7 Experimental Data for Influent Pb^{2+} Concentration of 0.02 N and Flow Rate of 5 mL/min at 25 °C

Eff. Volume (mL)	C (mg/L)	C/C_0
0.00	0.00	0.00
51.25	0.00	0.00
103.75	0.00	0.00
156.25	232.29	0.11
208.75	1126.77	0.56
261.25	1496.49	0.74
313.75	1691.13	0.83
366.25	1799.62	0.89
418.75	1841.53	0.91
471.25	1879.39	0.93
523.75	1924.06	0.95
576.25	1952.78	0.96
628.75	1968.73	0.97
681.25	1987.59	0.98
733.75	2022.97	1.00

Table B.8 Experimental Data for Influent Pb^{2+} Concentration of 0.02 N and Flow Rate of 10 mL/min at 25 °C

Eff. Volume (mL)	C (mg/L)	C/C_0
0.0	0.00	0.00
52.5	2.23	0.00
107.5	94.52	0.05
162.5	361.91	0.18
217.5	1110.83	0.55
272.5	1493.57	0.75
327.5	1613.59	0.81
382.5	1769.75	0.88
437.5	1830.99	0.91
492.5	1864.67	0.93
547.5	1883.04	0.94
602.5	1908.17	0.95
657.5	1933.41	0.97
712.5	1962.65	0.98
767.5	1976.61	0.99

Table B.9 Experimental Data for Influent Pb^{2+} Concentration of 0.02 N and Flow Rate of 20 mL/min at 25 °C

Eff. Volume (mL)	**C (mg/L)**	**C/C_0**
0.0	0.00	0.00
52.5	21.39	0.01
107.5	537.86	0.27
162.5	1110.88	0.55
217.5	1392.35	0.69
272.5	1502.18	0.75
327.5	1596.22	0.79
382.5	1646.34	0.82
437.5	1780.18	0.89
492.5	1821.39	0.91
547.5	1840.29	0.92
602.5	1854.16	0.92
657.5	1872.65	0.93
712.5	1921.20	0.96
767.5	1954.63	0.97
822.5	1976.69	0.98
877.5	1989.21	0.99

APPENDIX C

EXPERIMENTAL DATA FOR Cd^{2+} – Na^{+} BINARY SYSTEM

Table C.1 Experimental Data for Influent Cd^{2+} Concentration of 0.005 N and Flow Rate of 5 mL/min at 25 °C

Eff. Volume (mL)	C (mg/L)	C/C_0
0.0	0.00	0.00
52.5	0.00	0.00
107.5	0.00	0.00
162.5	0.00	0.00
217.5	0.00	0.00
272.5	10.29	0.04
327.5	59.01	0.21
382.5	113.16	0.40
437.5	162.27	0.57
492.5	177.69	0.63
547.5	194.18	0.69
602.5	210.63	0.74
657.5	218.19	0.77
712.5	226.63	0.80
767.5	234.63	0.83
822.5	241.75	0.85
877.5	248.43	0.88
932.5	254.68	0.90
987.5	259.88	0.92
1042.5	263.72	0.93
1097.5	267.54	0.94
1152.5	271.41	0.96
1207.5	273.60	0.97
1262.5	275.64	0.97
1317.5	277.17	0.98

Table C.2 Experimental Data for Influent Cd^{2+} Concentration of 0.005 N and Flow Rate of 10 mL/min at 25 °C

Eff. Volume (mL)	**C (mg/L)**	**C/C_0**
0.0	0.00	0.00
52.5	0.00	0.00
107.5	22.05	0.08
162.5	94.88	0.32
217.5	138.42	0.47
272.5	180.08	0.62
327.5	196.57	0.67
382.5	214.24	0.73
437.5	224.39	0.77
492.5	236.25	0.81
547.5	244.63	0.84
602.5	252.71	0.86
657.5	259.43	0.89
712.5	265.41	0.91
767.5	269.25	0.92
822.5	273.16	0.93
877.5	277.32	0.95
932.5	279.15	0.96
987.5	282.63	0.97
1042.5	284.47	0.97
1097.5	285.31	0.98
1152.5	285.74	0.98

Table C.3 Experimental Data for Influent Cd^{2+} Concentration of 0.005 N and Flow Rate of 20 mL/min at 25 °C

Eff. Volume (mL)	**C (mg/L)**	**C/C_0**
0.0	0.0	0.00
52.5	2.56	0.01
107.5	56.57	0.20
162.5	94.28	0.33
217.5	135.95	0.48
272.5	167.88	0.59
327.5	192.82	0.67
382.5	206.23	0.72
437.5	217.23	0.76
492.5	225.64	0.79
547.5	232.13	0.81
602.5	239.34	0.84
657.5	251.64	0.88
712.5	257.55	0.90
767.5	263.81	0.92
822.5	271.49	0.95
877.5	275.62	0.96
932.5	278.71	0.97
987.5	281.03	0.98

Table C.4 Experimental Data for Influent Cd^{2+} Concentration of 0.01 N and Flow Rate of 5 mL/min at 25 °C

Eff. Volume (mL)	**C (mg/L)**	**C/C_0**
0.0	0.0	0.00
52.5	0.0	0.00
107.5	87.01	0.16
162.5	244.46	0.44
217.5	314.93	0.57
272.5	371.62	0.67
327.5	398.84	0.72
382.5	431.73	0.78
437.5	463.36	0.83
492.5	482.51	0.87
547.5	494.15	0.89
602.5	505.67	0.91
657.5	515.03	0.93
712.5	523.76	0.94
767.5	529.71	0.95
822.5	534.91	0.96
877.5	537.12	0.97
932.5	541.53	0.98

Table C.5 Experimental Data for Influent Cd^{2+} Concentration of 0.01 N and Flow Rate of 10 mL/min at 25 °C

Eff. Volume (mL)	C (mg/L)	C/C_0
0.0	18.41	0.03
52.5	152.07	0.28
107.5	302.21	0.55
162.5	423.44	0.77
217.5	455.82	0.83
272.5	482.44	0.88
327.5	501.87	0.92
382.5	515.42	0.94
437.5	528.05	0.97
492.5	531.44	0.97
547.5	534.17	0.98

Table C.6 Experimental Data for Influent Cd^{2+} Concentration of 0.01 N and Flow Rate of 20 mL/min at 25 °C

Eff. Volume (mL)	C (mg/L)	C/C_0
0.0	41.34	0.08
52.5	141.96	0.28
107.5	279.97	0.56
162.5	343.19	0.68
217.5	388.63	0.77
272.5	405.09	0.80
327.5	422.31	0.84
382.5	438.21	0.87
437.5	446.29	0.89
492.5	458.10	0.91
547.5	464.20	0.92
602.5	469.32	0.93
657.5	472.43	0.94
712.5	480.54	0.95
767.5	486.23	0.96
822.5	491.42	0.97
877.5	495.73	0.98
932.5	497.71	0.99

Table C.7 Experimental Data for Influent Cd^{2+} Concentration of 0.02 N and Flow Rate of 5 mL/min at 25 °C

Eff. Volume (mL)	C (mg/L)	C/C_0
0.0	121.31	0.11
52.5	498.24	0.47
107.5	801.64	0.75
162.5	890.28	0.84
217.5	952.12	0.89
272.5	994.39	0.93
327.5	1012.72	0.95
382.5	1037.85	0.98
437.5	1045.51	0.98
492.5	1055.46	0.99

Table C.8 Experimental Data for Influent Cd^{2+} Concentration of 0.02 N and Flow Rate of 10 mL/min at 25 °C

Eff. Volume (mL)	C (mg/L)	C/C_0
0.0	352.32	0.31
52.5	588.62	0.52
107.5	816.98	0.72
162.5	907.98	0.80
217.5	945.01	0.83
272.5	962.17	0.84
327.5	996.68	0.87
382.5	1024.33	0.90
437.5	1053.10	0.92
492.5	1074.61	0.94
547.5	1086.17	0.95

Table C.9 Experimental Data for Influent Cd^{2+} Concentration of 0.02 N and Flow Rate of 20 mL/min at 25 °C

Eff. Volume (mL)	**C (mg/L)**	**C/C_0**
0.0	423.42	0.37
52.5	684.81	0.60
107.5	899.96	0.78
162.5	971.54	0.84
217.5	992.12	0.86
272.5	1017.53	0.88
327.5	1052.71	0.92
382.5	1081.32	0.94
437.5	1106.04	0.96
492.5	1124.68	0.98
547.5	1141.03	0.99

APPENDIX D

EXPERIMENTAL DATA FOR Pb^{2+} – Cd^{2+} – Na^{+} TERNARY SYSTEM

Table D.1 Experimental Data for Influent Pb^{2+} and Cd^{2+} Ions Mixture Total Conc. of 0.005 N and Flow Rate of 5 mL/min at 25 °C

Eff. Volume (mL)	Pb^{2+}		Cd^{2+}	
	C (mg/L)	C/C_0	C (mg/L)	C/C_0
0.0	0.00	0.00	0.00	0.00
52.5	0.00	0.00	0.00	0.00
107.5	0.00	0.00	0.00	0.00
162.5	0.00	0.00	0.00	0.00
217.5	0.00	0.00	0.00	0.00
272.5	0.00	0.00	0.00	0.00
327.5	0.00	0.00	4.72	0.03
382.5	0.00	0.00	18.48	0.13
437.5	0.00	0.00	44.67	0.33
492.5	0.00	0.00	68.94	0.50
547.5	0.00	0.00	89.98	0.65
602.5	0.00	0.00	107.57	0.78
657.5	2.21	0.01	120.68	0.88
712.5	6.99	0.03	131.76	0.96
767.5	18.42	0.07	134.20	0.98
822.5	34.25	0.12	137.39	1.00
877.5	59.10	0.21		
932.5	87.90	0.32		
987.5	114.98	0.42		
1042.5	141.56	0.51		
1097.5	165.05	0.60		
1152.5	183.91	0.66		
1207.5	201.23	0.73		
1262.5	211.83	0.76		
1317.5	222.39	0.80		
1372.5	235.02	0.85		
1427.5	244.57	0.88		
1482.5	252.63	0.91		
1537.5	258.41	0.93		
1592.5	264.72	0.96		
1647.5	271.12	0.98		

Table D.2 Experimental Data for Influent Pb^{2+} and Cd^{2+} Ions Mixture Total Conc. of 0.005 N and Flow Rate of 10 mL/min at 25 °C

Eff. Volume (mL)	Pb^{2+}		Cd^{2+}	
	C (mg/L)	C/C_0	C (mg/L)	C/C_0
0.0	0.00	0.00	0.00	0.00
52.5	0.00	0.00	0.00	0.00
107.5	0.00	0.00	0.00	0.00
162.5	0.00	0.00	0.00	0.00
217.5	0.00	0.00	5.42	0.04
272.5	0.00	0.00	19.26	0.14
327.5	0.00	0.00	45.83	0.33
382.5	0.00	0.00	67.18	0.48
437.5	0.00	0.00	89.67	0.64
492.5	3.51	0.01	105.33	0.75
547.5	8.62	0.03	117.82	0.84
602.5	16.34	0.06	122.57	0.88
657.5	28.17	0.10	126.37	0.91
712.5	46.68	0.17	131.23	0.94
767.5	58.34	0.21	135.14	0.97
822.5	79.91	0.29	138.20	0.99
877.5	107.30	0.38		
932.5	124.44	0.45		
987.5	141.11	0.50		
1042.5	157.27	0.56		
1097.5	171.64	0.61		
1152.5	184.48	0.66		
1207.5	197.85	0.71		
1262.5	212.64	0.76		
1317.5	221.76	0.79		
1372.5	235.06	0.84		
1427.5	244.67	0.88		
1482.5	253.15	0.91		
1537.5	258.64	0.93		
1592.5	265.40	0.95		
1647.5	271.26	0.97		
1702.5	275.25	0.98		
1757.5	277.69	0.99		

Table D.3 Experimental Data for Influent Pb^{2+} and Cd^{2+} Ions Mixture Total Conc. of 0.005 N and Flow Rate of 20 mL/min at 25 °C

Eff. Volume (mL)	Pb^{2+}		Cd^{2+}	
	C (mg/L)	C/C_0	C (mg/L)	C/C_0
0	0.00	0.00	0.00	0.00
52.5	0.00	0.00	0.00	0.00
107.5	0.00	0.00	0.00	0.00
162.5	0.00	0.00	7.41	0.05
217.5	0.00	0.00	19.57	0.14
272.5	0.00	0.00	47.81	0.35
327.5	0.00	0.00	68.63	0.50
382.5	0.00	0.00	90.33	0.66
437.5	4.37	0.02	103.12	0.75
492.5	9.15	0.03	115.68	0.84
547.5	14.44	0.05	121.27	0.88
602.5	24.97	0.09	128.53	0.93
657.5	40.14	0.14	135.42	0.98
712.5	56.81	0.20	137.63	1.00
767.5	75.35	0.26		
822.5	92.68	0.32		
877.5	112.39	0.39		
932.5	134.57	0.47		
987.5	149.92	0.52		
1042.5	161.79	0.56		
1097.5	177.00	0.62		
1152.5	191.36	0.67		
1207.5	203.48	0.71		
1262.5	211.24	0.74		
1317.5	220.33	0.77		
1372.5	238.75	0.83		
1427.5	248.47	0.87		
1482.5	257.84	0.90		
1537.5	266.21	0.93		
1592.5	272.34	0.95		
1647.5	277.69	0.97		
1702.5	283.41	0.99		
1757.5	285.71	1.00		

Table D.4 Experimental Data for Influent Pb^{2+} and Cd^{2+} Ions Mixture Total Conc. of 0.01 N and Flow Rate of 5 mL/min at 25 °C

Eff. Volume (mL)	Pb^{2+}		Cd^{2+}	
	C (mg/L)	C/C_0	C (mg/L)	C/C_0
0	0.00	0.00	0.00	0.00
52.5	0.00	0.00	0.00	0.00
107.5	0.00	0.00	12.50	0.04
162.5	0.00	0.00	95.48	0.34
217.5	0.00	0.00	173.57	0.61
272.5	2.66	0.01	219.87	0.77
327.5	21.89	0.04	256.04	0.90
382.5	63.51	0.12	273.52	0.96
437.5	130.11	0.25	282.47	0.99
492.5	213.67	0.42	284.05	1.00
547.5	284.79	0.55	284.11	1.00
602.5	355.19	0.69		
657.5	384.79	0.75		
712.5	434.12	0.84		
767.5	456.94	0.89		
822.5	480.37	0.93		
877.5	489.06	0.95		
932.5	495.71	0.96		
987.5	499.27	0.97		
1042.5	504.31	0.98		

Table D.5 Experimental Data for Influent Pb^{2+} and Cd^{2+} Ions Mixture Total Conc. of 0.01 N and Flow Rate of 10 mL/min at 25 °C

Eff. Volume (mL)	Pb^{2+}		Cd^{2+}	
	C (mg/L)	C/C_0	C (mg/L)	C/C_0
0	0.00	0.00	0.00	0.00
52.5	0.00	0.00	1.41	0.00
107.5	0.00	0.00	53.43	0.18
162.5	0.00	0.00	136.93	0.47
217.5	4.75	0.01	181.58	0.62
272.5	12.46	0.02	219.31	0.75
327.5	31.33	0.06	230.28	0.78
382.5	90.41	0.18	256.73	0.87
437.5	140.47	0.28	271.66	0.92
492.5	183.01	0.37	276.47	0.94
547.5	227.52	0.46	282.74	0.96
602.5	279.46	0.56	290.42	0.99
657.5	331.22	0.66		
712.5	358.32	0.72		
767.5	374.25	0.75		
822.5	396.78	0.80		
877.5	409.31	0.82		
932.5	419.80	0.84		
987.5	428.42	0.86		
1042.5	432.38	0.87		
1097.5	437.73	0.88		
1152.5	445.52	0.89		
1207.5	456.04	0.91		
1262.5	459.33	0.92		
1317.5	462.42	0.93		
1372.5	472.18	0.95		
1427.5	477.17	0.96		
1482.5	481.39	0.97		
1537.5	490.72	0.98		
1592.5	496.47	1.00		
1647.5	498.12	1.00		
1702.5	498.04	1.00		

Table D.6 Experimental Data for Influent Pb^{2+} and Cd^{2+} Ions Mixture Total Conc. of 0.01 N and Flow Rate of 20 mL/min at 25 °C

Eff. Volume (mL)	Pb^{2+}		Cd^{2+}	
	C (mg/L)	C/C_0	C (mg/L)	C/C_0
0	0.00	0.00	15.12	0.05
52.5	0.00	0.00	80.98	0.28
107.5	0.00	0.00	152.65	0.52
162.5	8.34	0.02	204.87	0.70
217.5	18.45	0.04	224.51	0.77
272.5	27.63	0.05	236.21	0.81
327.5	52.64	0.10	245.64	0.84
382.5	78.31	0.15	257.12	0.88
437.5	102.46	0.20	265.31	0.91
492.5	132.47	0.26	274.26	0.94
547.5	182.68	0.36	279.19	0.96
602.5	221.67	0.44	283.26	0.97
657.5	267.25	0.53	287.34	0.99
712.5	294.25	0.58	289.42	0.99
767.5	322.14	0.63		
822.5	345.69	0.68		
877.5	371.64	0.73		
932.5	396.47	0.78		
987.5	416.72	0.82		
1042.5	431.24	0.85		
1097.5	443.11	0.87		
1152.5	452.64	0.89		
1207.5	461.79	0.91		
1262.5	469.43	0.93		
1317.5	477.12	0.94		
1372.5	486.75	0.96		
1427.5	493.41	0.97		
1482.5	498.18	0.98		
1537.5	502.43	0.99		
1592.5	503.55	0.99		

Table D.7 Experimental Data for Influent Pb^{2+} and Cd^{2+} Ions Mixture Total Conc. of 0.02 N and Flow Rate of 5 mL/min at 25 °C

Eff. Volume (mL)	Pb^{2+}		Cd^{2+}	
	C (mg/L)	C/C_0	C (mg/L)	C/C_0
0	0.00	0.00	0.00	0.00
52.5	0.00	0.00	57.39	0.10
107.5	0.00	0.00	361.54	0.63
162.5	26.18	0.03	479.37	0.83
217.5	151.02	0.15	549.78	0.95
272.5	381.20	0.38	571.23	0.99
327.5	560.84	0.56	575.84	1.00
382.5	689.64	0.69		
437.5	727.70	0.73		
492.5	812.95	0.81		
547.5	852.53	0.85		
602.5	864.71	0.87		
657.5	875.37	0.88		
712.5	892.38	0.89		
767.5	916.47	0.92		
822.5	927.91	0.93		
877.5	942.35	0.94		
932.5	952.12	0.95		
987.5	963.62	0.97		
1042.5	972.07	0.97		
1097.5	980.20	0.98		
1152.5	989.63	0.99		
1207.5	995.42	1.00		
1262.5	997.76	1.00		

Table D.8 Experimental Data for Influent Pb^{2+} and Cd^{2+} Ions Mixture Total Conc. of 0.02 N and Flow Rate of 10 mL/min at 25 °C

Eff. Volume (mL)	Pb^{2+}		Cd^{2+}	
	C (mg/L)	C/C_0	C (mg/L)	C/C_0
0	0.00	0.00	192.85	0.33
52.5	0.00	0.00	447.01	0.77
107.5	30.54	0.03	510.09	0.88
130.0	53.00	0.05	547.39	0.94
162.5	131.62	0.13	557.61	0.96
217.5	268.80	0.26	571.48	0.98
272.5	374.11	0.37	580.33	1.00
327.5	484.59	0.48	581.05	1.00
382.5	585.87	0.58	580.46	1.00
437.5	637.92	0.63		
492.5	796.42	0.78		
547.5	826.59	0.81		
602.5	857.19	0.84		
657.5	889.94	0.88		
712.5	912.41	0.90		
767.5	930.17	0.92		
822.5	941.02	0.93		
877.5	951.62	0.94		
932.5	959.72	0.95		
987.5	965.12	0.95		
1042.5	973.43	0.96		
1097.5	980.06	0.97		
1152.5	988.59	0.97		
1207.5	993.47	0.98		
1262.5	997.62	0.98		
1317.5	1004.08	0.99		
1372.5	1009.27	0.99		

Table D.9 Experimental Data for Influent Pb^{2+} and Cd^{2+} Ions Mixture Total Conc. of 0.02 N and Flow Rate of 20 mL/min at 25 °C

Eff. Volume (mL)	Pb^{2+}		Cd^{2+}	
	C (mg/L)	C/C_0	C (mg/L)	C/C_0
0	0.00	0.00	214.32	0.38
52.5	0.00	0.00	334.64	0.59
107.5	20.85	0.02	450.08	0.79
128	50.00	0.05	516.11	0.91
162.5	149.32	0.15	543.54	0.95
217.5	325.27	0.32	554.57	0.97
272.5	460.82	0.45	562.13	0.99
327.5	576.31	0.57	568.66	1.00
382.5	651.96	0.64	569.41	1.00
437.5	747.49	0.74		
492.5	777.77	0.77		
547.5	792.02	0.78		
602.5	815.24	0.80		
657.5	843.84	0.83		
712.5	862.52	0.85		
767.5	884.02	0.87		
822.5	901.29	0.89		
877.5	916.13	0.90		
932.5	928.61	0.91		
987.5	942.14	0.93		
1042.5	956.58	0.94		
1097.5	963.67	0.95		
1152.5	971.18	0.96		
1207.5	978.56	0.96		
1262.5	984.22	0.97		
1317.5	991.73	0.98		
1372.5	997.92	0.98		
1427.5	1002.08	0.99		
1482.5	1006.40	0.99		
1537.5	1011.28	0.99		

APPENDIX E

REPRODUCIBILITY EXPERIMENTS

In order to determine whether the experimental results are reliable or not, two experiments were performed under same conditions, i.e. same influent concentration, same flow rate, same amounts of zeolites at same mesh sizes for packed bed, and same pretreatment procedure was applied to original clinoptilolite. The breakthrough curves for these experiments are demonstrated in Figure E.1. The results show that, there is only a negligible difference in ion exchange property for removal of heavy metals, i.e., Pb^{2+} and Cd^{2+} ions, by using Na form of Gördes type clinoptilolite. Therefore, the experiments are reproducible.

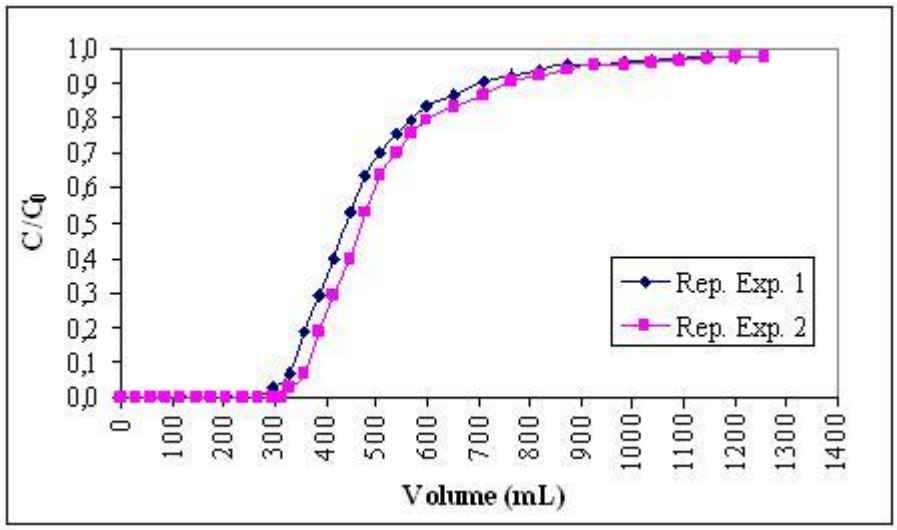

Figure E.1 Reproducibility Experiments